

“ELECTRONIC STRUCTURE OF Cr-AI ALLOYS”

THESIS

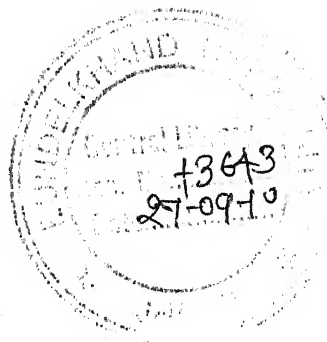
Submitted To

BUNDELKHAND UNIVERSITY, JHANSI

For the award of the degree of
DOCTOR OF PHILOSOPHY

in

PHYSICS



By

SURENDRA KUMAR VERMA

Department of Physics, Bundelkhand University
Jhansi (U.P.)

Under the Supervision of

Dr. S. S. RAJPUT

Bundelkhand Institute of Engineering & Technology,
Jhansi (U.P.)

2006

CERTIFICATE

This is to certify that *Mr. Surendra Kumar Verma* a candidate for the degree of *Doctor of Philosophy* in Physics under the Faculty of Science of Bundelkhand University, Jhansi (U.P.) has worked under my supervision for the period required by the University ordinance and that the accompanying thesis on "*Electronic Structure of Cr-Al Alloys*" which he is submitting, is his own work.

Date: 03-02-2006

Place: Jhansi



Dr. S.S. Rajput

(Supervisor)

DECLARATION

I hereby declare that except the guidance and suggestions from my supervisor, The present work which I submitting for the degree of *Doctor of Philosophy* in Physics is my own work.

Date: 03-02-2006

Place: Jhansi



Surendra Kumar Verma

Forwarded



Dr. S.S. Rajput

(Supervisor)

What I am,
What I hope to be,
I owe to my
Angel Parents

ACKNOWLEDGEMENTS

The pursuit of scientific and technical knowledge is long arduous and at time an obscure path but the presence of leadership, inspiration and close cooperation along the way makes it an easier achievement.

I owe highest degree of gratitude to my revered supervisor and guide Dr. S.S. Rajput, B.I.E.T., Jhansi whose ever energetic and scintillating personality has been a constant source of energy and commitment. His foresight has been valuable at every stage of my research. In the moments of despair no words will do justice in expressing my reverence for him.

With great pleasure and deep sense of gratitude I express my hearty thanks to our Vice Chancellor Prof. R.P. Agarwal, Bundelkhand University, Jhansi and Dean, Faculty of Science for his invaluable guidance and timely suggestions. His constructive criticism was helpful and insightful. I owe a great deal to him for his sightedness and support in the process of my research work.

I especially wish to thank Prof. Ramesh Chandra, Former Vice Chancellor, Bundelkhand University, Jhansi for wholehearted support and constant encouragement during course of my study. I must mention here that I have learned so much from him during our interactions throughout my research and other administrative assignments.

I would be failing in my duty if I do not express my sincere thanks to Dr. A.K. Singh, Head, Department of Physics, Bundelkhand University, Jhansi who inspired me to carry out my work with positive determination. I also thank Dr. Singh for providing necessary facilities in the department of Physics to carry out my research work. I will always cherish his informal

and open discussions and I am deeply indebted to him for his very helpful and special attitude towards me.

This acknowledgement would not be completed without mentioning the help of my colleagues and friends, Dr. Rajeev Singh, Dr. S.K. Shrivastava, Man Singh, Dr. D.K. Sahu and Dr. B.S. Bhadoria for their whole-hearted co-operation during the research work.

It gives me immense pleasure to thank my Jija ji Mr. A.K. Lagarkha for his generous help and assistance in various forms during the course of work.

I could not find appropriate words in the lexicon to accentuate my profound regard to my beloved Parents for their immaculate and impeccable affection. Overflow with gratitude to my younger sister Rekha, brother Sandeep, my wife Pravesh and my son Vinay for their affection, encouragement and moral support to make this dream materialized.

Place: Jhansi

Date: 03/02/2006



Surendra Kumar Verma

CONTENTS

	Page
LIST OF TABLES AND CHARTS	VII
LIST OF FIGURES	VIII-X
SYNOPSIS	XI-XVI
CHAPTER 1: INTRODUCTION	1-8
CHAPTER 2: CHARGE SELF-CONSISTENT KKR-CPA	9-17
2.1. Introduction	9
2.2. Koringa-Kohn-Rostoker Coherent-Potential- Approximation (KKR-CPA)	10
2.3. Charge Self-Consistent KKR-CPA	16
2.4. Conclusions	17
CHAPTER 3: APPLICATION OF CHARGE SELF-CONSISTENT KKR- CPA TO Cr-Al ALLOYS	18-40
3.1. Introduction	18
3.2. Computational details	19
3.3. Results and discussion	26
3.4. Conclusions	40

CHAPTER 4: APPLICATION OF KORINGA-KOHN-ROSTOKER

COHERENT - POTENTIAL - APPROXIMATION TO

S-PHASE SHIFT DOUBLE PEAK SEMICIRCULAR

MODEL 41-102

4.1. Introduction 41

4.2. The S-phase shift semi circular model 42

4.3. Double peak semi circular model 57

4.4. Density of states 67

4.5. The CPA equation and computational details 77

4.6. Results and discussion 82

4.7. Conclusions 102

CHAPTER 5: SUMMARY AND CONCLUSIONS 103-104

REFERENCES: 105-108

LIST OF TABLES AND CHART

	Page
TABLE 3.1: - LATTICE CONSTANTS OF Cr-Al ALLOYS.	19
TABLE 3.2: - DENSITY OF STATES (DOS) AT FERMI ENERGY (E_F) FOR Cr-Al ALLOYS.	25
CHART 3.1: - FLOW CHART OF CHARGE SELF-CONSISTENT KKR- CPA.	21

LIST OF FIGURES

<i>Figure No.</i>	<i>Caption</i>	<i>Page</i>
Figure 3.1.	The average density of states by using charge self-consistent KKR-CPA method (solid curve) and density of states obtained by Cr-based rigid band model (broken curve) for $Cr_{0.95}Al_{0.05}$.	27
Figure 3.2.	The average density of states by using charge self-consistent KKR-CPA method (solid curve) and density of states obtained by Cr-based rigid band model (broken curve) for $Cr_{0.85}Al_{0.15}$.	29
Figure 3.3.	The average density of states by using charge self-consistent KKR-CPA method (solid curve) and density of states obtained by Cr-based rigid band model (broken curve) for $Cr_{0.75}Al_{0.25}$.	30
Figure 3.4.	The component density of states of Cr (solid curve) and Al (broken curve) in $Cr_{0.95}Al_{0.05}$.	31
Figure 3.5.	The component density of states of Cr (solid curve) and Al (broken curve) in $Cr_{0.85}Al_{0.15}$.	32
Figure 3.6.	The component density of states of Cr (solid curve) and Al (broken curve) in $Cr_{0.75}Al_{0.25}$.	33
Figure 3.7.	The average density of states by using charge self-consistent KKR-CPA method (solid curve) and experimental X-ray photo spectra results (broken curve) for $Cr_{0.95}Al_{0.05}$.	36
Figure 3.8.	The average density of states by using charge self-consistent KKR-CPA method (solid curve) and experimental X-ray photo spectra results (broken curve) for $Cr_{0.85}Al_{0.15}$.	37

<i>Figure No.</i>	<i>Caption</i>	<i>Page</i>
Figure 3.9.	The average density of states by using charge self-consistent KKR-CPA method (solid curve) and experimental X-ray photo spectra results (broken curve) for $Cr_{0.75}Al_{0.25}$.	38
Figure 3.10.	Density of states at Fermi energy Verses concentration of Al in Cr_xAl_y .	39
Figure 4.1.	Change in density of state for $\Gamma_A = 1.0, \Gamma_B = 1.0, E_A = -2.0$ and $E_B = 2.0$ for concentration $X=0.0$.	83
Figure 4.2.	Change in density of state for $\Gamma_A = 1.0, \Gamma_B = 1.0, E_A = -2.0$ and $E_B = 2.0$ for concentration $X=0.10$.	84
Figure 4.3.	Change in density of state for $\Gamma_A = 1.0, \Gamma_B = 1.0, E_A = -2.0$ and $E_B = 2.0$ for concentration $X=0.20$.	87
Figure 4.4.	Change in density of state for $\Gamma_A = 1.0, \Gamma_B = 1.0, E_A = -2.0$ and $E_B = 2.0$ for concentration $X=0.30$.	88
Figure 4.5.	Change in density of state for $\Gamma_A = 1.0, \Gamma_B = 1.0, E_A = -2.0$ and $E_B = 2.0$ for concentration $X=0.35$.	89
Figure 4.6.	Change in density of state for $\Gamma_A = 1.0, \Gamma_B = 1.0, E_A = -2.0$ and $E_B = 2.0$ for concentration $X=0.40$.	90
Figure 4.7.	Change in density of state for $\Gamma_A = 1.0, \Gamma_B = 1.0, E_A = -2.0$ and $E_B = 2.0$ for concentration $X=0.50$.	91
Figure 4.8.	Change in density of state for $\Gamma_A = 1.0, \Gamma_B = 1.0, E_A = -2.0$ and $E_B = 2.0$ for concentration $X=0.90$.	94
Figure 4.9.	Change in density of state for $\Gamma_A = 1.0, \Gamma_B = 1.0, E_A = -2.0$ and $E_B = 2.0$ for concentration $X=1.0$.	95
Figure 4.10.	Change in density of state for $\Gamma_A = 1.0, \Gamma_B = 2.0, E_A = -2.0$ and $E_B = 2.0$ for concentration $X=0.0$.	96

<i>Figure No.</i>	<i>Caption</i>	<i>Page</i>
Figure 4.11.	Change in density of state for $\Gamma_A = 1.0, \Gamma_B = 2.0, E_A = -2.0$ and $E_B = 2.0$ for concentration $X=0.10$.	97
Figure 4.12.	Change in density of state for $\Gamma_A = 1.0, \Gamma_B = 2.0, E_A = -2.0$ and $E_B = 2.0$ for concentration $X=0.40$.	98
Figure 4.13.	Change in density of state for $\Gamma_A = 1.0, \Gamma_B = 2.0, E_A = -2.0$ and $E_B = 2.0$ for concentration $X=0.50$.	99
Figure 4.14.	Change in density of state for $\Gamma_A = 1.0, \Gamma_B = 2.0, E_A = -2.0$ and $E_B = 2.0$ for concentration $X=0.90$.	100
Figure 4.15.	Change in density of state for $\Gamma_A = 1.0, \Gamma_B = 2.0, E_A = -2.0$ and $E_B = 2.0$ for concentration $X=1.0$.	101

SYNOPSIS

ELECTRONIC STRUCTURE OF Cr-Al ALLOYS

By

SURENDRA KUMAR VERMA

Department of Physics, Institute of Basic Sciences,
Bundelkhand University, Jhansi (India)

The aim of this work is to study the electronic structure of disordered Cr-Al alloys. The electronic structure of this system cannot be studied by using standard method of band theory because disordered system lacks the translational invariance. During the past decades, Coherent Potential Approximation (CPA) theory has been very successful in understanding the electronic structure of disordered alloys. The CPA is a mean field approximation in which the disordered alloy is replaced by an effective medium, which is determined by a self-consistent condition. This theory when applied to muffin-tin potential of disordered alloy is known as Korringa-Kohn-Rostoker Coherent Potential Approximation (KKR-CPA)^{RI-R5}. Within the local density approximation of the density functional theory, it can be made fully charged self-consistent. Thus, the charged self-consistent KKR-CPA provides a first principles parameter-free theory of electronic structure calculation of disordered alloys.

We have chosen $\text{Cr}_X \text{Al}_{1-X}$ alloys because it is important Body Centered Cubic (bcc) alloy system. The system forms solid solution for $0.745 \leq X \leq 1$ in a bcc paramagnetic phase^{R6}. To my knowledge, no such calculation has been reported for these systems till now, although some experimental results are available on Cr-Al alloys^{R7}. We shall focus on the results of Density Of States (DOS), as this is the basic quantity needed to explain the various experimental results.

We shall apply the charged self-consistent KKR-CPA method for calculation of DOS of Cr-Al system. Here, we shall outline some important equations involved in the method. Let us consider a binary alloy $\text{A}_X \text{B}_Y$ where X and Y are atomic concentrations. The basic quantity of interest is the ensemble-averaged Green's function of the alloy. The Green's function for a particular configuration of the alloy can be written as^{R1}

$$G(E, \vec{r}, \vec{r}') = \sum_{LL'} Z_L^n(E, \vec{r}_n) T_{LL'}^{nm}(\chi) Z_L^m(E, \vec{r}_m) - \delta_{nm} \sum_L Z_L^n(E, \vec{r}_n) J_L^n(E, \vec{r}_n) \quad (1)$$

Here, \vec{r}_n and \vec{r}_m are within n^{th} and m^{th} muffin-tin spheres and the wave functions $Z_L^n(E, \vec{r}_n)$ and $J_L^n(E, \vec{r}_n)$ are respectively the regular and irregular solutions of the Schrodinger equation for the single muffin-tin potential centered at \vec{r}_n , and the T^{nm} are path operators. The ensemble-averages of equation (1) are related to the ensemble average of the path operators, which is determined by invoking the CPA. The CPA condition, that the average scattering from each site must be zero, can be expressed

$$[t_C^{-1}]_{LL'} = [X \cdot t_A^{-1} + Y \cdot t_B^{-1} + (t_C^{-1} - t_A^{-1}) T_C^{00} (t_C^{-1} - t_B^{-1})]_{LL'} \quad (2)$$

Here $t_{A(B)}$ denotes on-the-energy-shell matrix element of the t-matrix of an isolated $A(B)$ atom and C is used to label quantities for the CPA medium. The path operator matrix is given by

$$[T_C^{00}]_{LL'} = \Omega / (2\pi)^3 \int [\{t_C^{-1}(\chi) - B_{\vec{K}}(\chi)\}^{-1}]_{LL'} d\vec{K} \quad (3)$$

Here, $B_{\vec{K}}$ are the KKR structure constants and Ω is the unit cell volume. For full charged self-consistency, the charge densities in A and B cells are needed. These can be obtained from the restricted site averages of the Green's function $\langle G(E, \vec{r}, \vec{r}') \rangle_{A(B)}$ as

$$\rho_{A(B)}(\vec{r}) = -(1/\pi) \int_{-\infty}^{E_F} \text{Im} \langle G(E, \vec{r}, \vec{r}') \rangle_{A(B)} dE \quad (4)$$

where $\rho_A(\vec{r})$ and $\rho_B(\vec{r})$ denote the charge densities associated with A and B cells respectively.

The component DOS for the A and B atoms are expressed as

$$\rho_{A(B)}(E) = -(1/\pi) \text{Im} \int \langle G(E, \vec{r}, \vec{r}') \rangle_{A(B)} d\vec{r} \quad (5)$$

The average density of states for the alloy is calculated as

$$\rho(E) = X \cdot \rho_A(E) + Y \cdot \rho_B(E) \quad (6)$$

For the computational details^{R4} of charged self-consistent KKR-CPA, we will start with atomic charge densities $(\rho_A^{in}, \rho_B^{in})$ for A and B and will calculate the potentials (V_A^{in}, V_B^{in}) using the local density approximation. The $t_A^{-1}(\chi)$ and $t_B^{-1}(\chi)$ will then be computed for the input potentials (V_A^{in}, V_B^{in}) . We will use the tetrahedron method for the calculation of path operator (T_C^{00}) . After solving the KKR-CPA equation (2) iteratively, the new charge densities $(\rho_A^{out}, \rho_B^{out})$ will be obtained from equation (4). The new potentials (V_A^{out}, V_B^{out}) in the alloy will then be calculated. The whole calculation is repeated, until the difference of old and new charge densities is within a certain tolerance (integrated Root Mean Square (rms) difference between input and output charge densities (0.0001 electrons)). Fermi energy will be calculated by generalized Lloyd's formula^{R8}, which does not give unphysical jumps in the integrated density of states.

We shall calculate the DOS of $\text{Cr}_x\text{Al}_{1-x}$ for various concentrations ($x = 1.0, 0.95, 0.85$ and 0.75) of Cr in the alloys. We shall compare our results of DOS with Cr-based rigid band model. We shall also study the DOS at Fermi energy (E_F) verses Cr concentration in alloys. We shall also compare our results of DOS with available experimental results^{R7}.

Since the KKR-CPA calculation takes a lot of computer time, therefore, we shall propose new scheme based on double peak semicircular model for the alloys. This proposed model would be modified form of earlier multi-peak model^{R9}. In the earlier multi-peak model cotangent of phase shifts of either constituents was modeled with the help of step functions and it was assumed that their derivatives are zero at boundaries. But in the

proposed scheme steps functions will not be used. We shall provide band-centers and bandwidths of constituents of alloys, and then we shall predict DOS of the alloy. The proposed model will also be the aim of the thesis.

References: -

- R1. J.S. Faulkner in progress in material sciences, ed. by T. Mossalski (Pergamon, New york, 1982) Vol. 27; J.S. Faulkner and G.M. Stocks, Phys. Rev. B21, 3222 (1980).
- R2. A. Bansil, Electronic Band Structure and Its applications. ed. M.Yussouff, (Springer-verlag, Berlin, 1987), p 273.
- R3. R. Prasad, Ind. J. Pure and Appl. Phys. 29, 255 (1991).
- R4. S.S. Rajput, Ph.D. Thesis, IIT, Kanpur India (1991).
- R5. S.S. Rajput , R.M. Singru and R. Prasad, Solid State Comm. 90, 339 (1994).
- R6. Handbook of Lattice Spacing and Structures of Metals and alloys, ed. W.B. Pearson (Pergamon Press; 1985).
- R7. K. Lawniczak - Jablonska, E. Minni, J. Pelka, E. Suoninen and J. Avleytner, Physica, Stat. Solid (b), 123, 627 (1984).
- R8. S. Kaprzyk and A. Bansil, Phys. Rev. B42, 7358(1990).
- R9. V.S. Yadav, Ph.D. Thesis, Bundelkhand University Jhansi, India (1999).

CHAPTER-1

INTRODUCTION:

There are a rich variety of disordered alloys having diverse electrical, magnetic, transport, optical and super conducting properties in nature; these properties make them very useful for technological applications. For understanding these properties knowledge of their electronic structure is essential. In disordered alloys due to the lackness of translational invariance, which is a characteristic of ordered solids, Bloch's theorem, which greatly simplifies the electronic structure calculation of ordered solids, is inapplicable to these systems. In other words, the standard band theory method developed for ordered solids cannot be applied to disordered alloys.

The main subject of this thesis is the calculations of electronic structure of substitutional random binary alloys which are the simplest kind of disordered systems. In such alloys there exists a lattice structure but each lattice point can be occupied by either of the constituent atoms. Examples of such systems are α -brass Cu-Zn, Cu-Ge, Cu-Pd, Cu-Ni, Cu-Au, Ag-Pd, Nb-Mo, Cr-V and Cr-Mo etc. Such an alloy will be denoted by $A_X B_Y$, Where X and Y are concentrations of A and B types of atoms in the alloy, respectively.

A great progress has been made in understanding the electronic structure of the disordered alloys during last three decades, by the application of Coherent Potential Approximation (CPA)¹⁻³. The CPA is a mean field approximation, which for the sake of configurational averaging replaces a disordered alloy ($A_X B_Y$) by an ordered solid of effective atoms. These effective atoms are determined by using the self-consistent condition

that if an A (B) atom is embedded in this effective medium, the average scattering with respect to the medium is zero i.e.

$$x.t_A^{CPA} + y.t_B^{CPA} = 0 \quad (1.1)$$

where $t_{A(B)}^{CPA}$ is atomic scattering operator for an A or B atom embedded in the effective medium. A simpler approximation is average t-matrix approximation (ATA)¹ in which the t-matrix corresponding to the effective atom is

$$t^{ATA} = x.t_A + y.t_B \quad (1.2)$$

where $t_{A(B)}$ is atomic scattering operator for an isolated A(B) atom. Another simple approximation is virtual crystal approximation (VCA)⁴ in which the potential corresponding to the effective atoms is assumed to be

$$V^{VCA} = x.V_A + y.V_B \quad (1.3)$$

where $V_{A(B)}$ is the potential of A(B) atom. This approximation is good only when the difference between the two constituents potential is small. Note that all these approximations (CPA, ATA, VCA) are single-site approximations; i.e. they neglect correlated scattering from clusters of atoms. The CPA has been found to be the best single-site approximation for calculation of electronic structure of disordered alloys.

A frequently quoted model in alloy theory is the rigid band model⁵. In this model the potentials of the constituent atoms are assumed to be the

same. However, Fermi energy (E_F) is adjusted to give the required number of valence electrons (N^V) per atom in the alloy as

$$N^V = \int_{-\infty}^{E_F} \rho(E) dE \quad (1.4)$$

where $\rho(E)$ is the density of states (DOS) per atom of the host system. The rigid band model is a crude approximation and does not explain many experimental results. Because of its simplicity, it is frequently used as a first step to get an idea of the electronic structure of the alloy.

There is very large number of interacting electrons ($\approx 10^{23}$) interacting with nuclear potentials in a solid. Therefore, the calculation of energy levels of such a system is a many-body problem, which cannot be solved exactly. However, this problem can be solved to a great degree of accuracy by using the one electron approximation. In this approximation, the many-body problem is reduced to a problem of one electron moving in some effective potential which is determined self-consistently. Muffin-tin approximation is further used to simplify the calculation of this potential. In this approximation the potential is assumed to be spherically symmetric within a sphere and Wigner-Seitz cell as

$$V(\vec{r}) = \begin{cases} V_{A(B)}(r) & , \quad \text{for } r < r_m \\ V_{A(B)}^I & , \quad \text{for } r > r_m \end{cases} \quad (1.5)$$

The V^I is a constant interstitial potential as⁶

$$V_{A(B)}^I = 3 \int_{r_m}^{r_{ws}} V(r) r^2 dr / (r_{ws}^3 - r_m^3) \quad (1.6)$$

where $V(r)$ is a spherically symmetric potential, which, it is hoped, will be slowly varying in the region between the muffin-tin sphere and the Wigner-Seitz sphere of radius r_{WS} . For a pure A(B) solid, $V_{A(B)}^I$ defines muffin-tin zero, i.e. this constant is subtracted from the potential (1.5) making interstitial potential zero. For the alloy, this is calculated as

$$V_{ALLOY}^I = x.V_A^I + y.V_B^I \quad (1.7)$$

Note that muffin-tin potentials are non-overlapping. The muffin-tin approximation is a reasonably good approximation for the potential as can be seen by referring to the book by Moruzzi et al⁷. Using this approximation, they have calculated various properties such as cohesive energy, bulk modulus, density of states and Fermi energy. They got very good agreements with experimental results and were able to explain general trends. Recent experience with alloys show that the muffin-tin approximation is also a good approximation for metallic alloys^{1-3, 8-14}. The muffin-tin potentials for the constituent atoms are constructed by using the local density approximation (LDA) of the density functional theory¹⁵. The potential can be written as³

$$V_{A(B)}(\vec{r}) = V_{COUL}^{A(B)}(\vec{r}) + V_{NUC}^{A(B)}(\vec{r}) + V_{XC}^{A(B)}(\vec{r}) \quad (1.8)$$

where coulomb, nuclear and exchange-correlation contributions are

$$V_{COUL}^{A(B)}(\vec{r}) = \int_{\Omega} d\vec{r}' \frac{\rho_{A(B)}(\vec{r}')}{|\vec{r} - \vec{r}'|} \quad (1.9)$$

$$V_{NUC}^{A(B)}(\vec{r}) = -e^2 Z_{A(B)} / r \quad (1.10)$$

$$V_{XC}^{A(B)}(\vec{r}) = \frac{\delta E_{XC}[\rho_{A(B)}(\vec{r})]}{\delta \rho_{A(B)}(\vec{r})} \quad (1.11)$$

where $\rho_{A(B)}$ is the electron charge density in A(B) cell, Z is the atomic number and Ω denotes the integral over the Wigner-Seitz unit cell. Here, E_{XC} is the exchange-correlation energy functional, which in the local density approximation is given by¹⁵

$$E_{XC}\{\rho\} \approx \int \rho(r) \varepsilon_{XC}(\rho(\vec{r})) d\vec{r} \quad (1.12)$$

where $\varepsilon_{XC}(\rho)$ is the contribution of exchange and correlation to the total energy (per electron) in a homogeneous but interacting electron gas of density ρ . For paramagnetic case, von Barth-Hedin form of ε_{XC} is¹⁶

$$\varepsilon_{XC}^B(r_s) = -\frac{0.91633}{r_s} - 0.045F\left(\frac{r_s}{21}\right) \quad (1.13)$$

where r_s is given by

$$\frac{4\pi}{3}(r_s)^3 = \left(\frac{1}{\rho}\right) \quad (1.14)$$

and function

$$F(x) = (1+x^3)\ln(1+1/x) - x^2 + x/2 - 1/3 \quad (1.15)$$

Gunnarsson and Lundqvist form of ε_{XC} for paramagnetic case is¹⁷

$$\varepsilon_{XC}^G(r_s) = -\frac{0.458}{r_s} - 0.0333F\left(\frac{r_s}{11.4}\right) \quad (1.16)$$

Vosko et.al. form of ε_{XC} for paramagnetic case is¹⁸

$$\varepsilon_{xc}^V(r_s) = \frac{-0.91633}{r_s} + A \left[\ln \left[\frac{x^2}{X(x)} \right] + \frac{2b}{Q} \tan^{-1} \left[\frac{Q}{2x+b} \right] - \frac{bx_0}{X(x_0)} \left[\ln \left[\frac{(x-x_0)^2}{X(x)} \right] + \frac{2(b+2x_0)}{Q} \tan^{-1} \left[\frac{Q}{2x+b} \right] \right] \right]$$

where

$$X(x) = x^2 + bx + c, \quad Q = (4c - b^2)^{1/2} \quad \text{and} \quad x = (r_s)^{1/2} \quad (1.17)$$

Here, $A = 0.0621814$, $x_0 = -0.10498$, $b = 3.72744$ and $c = 12.9352$

It has been seen that use of different exchange-correlation does not give large differences in the calculation of various properties¹⁵. For example differences in cohesive energies in Li, Na, K and Rb were found to be less than 8 mRy¹⁸. Because Moruzzi et al⁷, have found good agreement between theory and experiment for several metals including Cr and Al, using von Barth-Hedin form of the exchange-correlation potential. Therefore, We have used this form in our calculations for above reason as will be discussed in detail in Chapter 3.

The CPA theory has been very successful as a single-site approximation to calculate the electronic structure of random substitutional disordered alloys during last thirty years. This theory when applied to muffin-tin model of disordered alloys, is known as Korringa-Kohn-Rostoker-CPA (KKR-CPA) theory¹. In the perfect crystal limit, the KKR-CPA theory reduced to the standard KKR band theory¹. In earlier stage of application, potentials V_A and V_B were not determined self-consistently. In the most sophisticated application of the KKR-CPA, within the framework of the local density approximation V_A and V_B are determined self-consistently described in Chapter 2. This fully charge-self-consistent

KKR-CPA theory is a first principle parameter-free theory of the electronic structure of random alloys.

The outline of the thesis is as follows. In Chapter 2, we will present the brief formulation of charge self-consistent KKR-CPA. Section 2.1 presents the introduction of the chapter. In section 2.2, we derive the KKR-CPA equation in multiple scattering formalism. In section 2.3, we present the charge self-consistent KKR-CPA method.

In Chapter 3, we will apply the charge self-consistent KKR-CPA method in calculation of electronic structure of Cr-Al alloy. Section 3.1 present the introduction of the chapter, we will give the computational details of our calculation in section 3.2. The Green's function method is used to calculate charge densities of constituent atoms in the alloy. The flow chart of charge self-consistent KKR-CPA is also given in this section. The mixing scheme for CPA and charge self-consistency loop are discussed. The study of charge self-consistent potentials, charge densities and the density of states as a function of Cr concentration in the Cr_xAl_y for $x=0.95, 0.85$ and 0.75 are given in section 3.3. In this section we also compare the results of charge self-consistent KKR-CPA density of states with the density of states using Cr-based rigid band model. We have chosen von Barth-Hedin exchange correlation potential to calculate the new crystal potentials of constituent atoms in the alloy. For Cr-Al alloy, we compare the results of density of states calculated by using the charge self-consistent KKR-CPA method with the X-ray photo spectra experimental results. We find that there is a very good agreement between our results and experimental results for different concentration of alloy. It is also found that Cr-based rigid band model fails

in the calculation of electronic structure of Cr-Al alloys. In the final section 3.4 we summarize our main conclusions.

In Chapter 4, we apply the KKR-CPA to the s-phase shift double peak semicircular model. Section 4.1 provides an introduction of this chapter. In section 4.2 we discuss the s-phase shift semicircular model in the KKR framework. In section 4.3, the path operators and t-matrices for the s-phase shift double peak semicircular model is derived. In section 4.4, formula for the KKR-CPA density of states to the s-phase shift double peak semicircular model is derived. In section 4.5, we present the CPA equation and computational details for this model with programme. In section 4.6, we discuss our results for s-phase shift double peak semicircular model. In section 4.7, we summarize our main conclusions.

Finally, in Chapter 5, we give the summary of the achievements of the present work. Some suggestions for further improvements are also given and some possible remaining problems are mentioned.

CHAPTER – 2

CHARGE SELF-CONSISTENT KKR-CPA

2.1 INTRODUCTION

To understanding the electronic structure of disordered alloys, the Korringa-Kohn-Rostoker Coherent Potential Approximation (KKR-CPA) theory has been very successful in last three decades as was mentioned in chapter-1. It is basically an application of the coherent potential approximation (CPA)¹⁻³ to muffin-tin potential of the disordered alloys. In the CPA, one replaces a disordered alloy by an ordered array of effective atoms which are determined by a self-consistent condition. The muffin-tin approximation of the potential plays an important role in simplifying the theory. Because the constituent muffin-tin potentials are spherically symmetric within a certain radius r_m , various quantities such as t-matrices can be expressed in simple forms in the angular momentum space. The non-overlapping nature of the constituent potentials further simplifies the multiple scattering equations to tractable forms.

The KKR-CPA reduced to standard KKR band theory in the perfect crystal limit. Within the local density approximation of the density-functional theory (DFT)¹⁵⁻¹⁸, it can be made fully charge self-consistent. Thus charge self-consistent KKR-CPA provides a first principles parameter-free theory of electronic structure of disordered alloys. The theory rests on the same theoretical footing as the band theory of pure metals.

The outline of this chapter is as follows. In section 2.2, the formulation of the KKR-CPA will be briefly discussed. In section 2.3, we present a brief formulation of the charge self-consistent KKR-CPA. The final section 2.4 gives conclusions.

2.2 KORRINGA-KOHN-ROSTOKER COHERENT-POTENTIAL-APPROXIMATION (KKR-CPA)

Consider a disordered substitutional binary alloy $A_X B_Y$ of A and B atoms with concentrations X and Y respectively. The one electron potential in the alloy can be written as¹⁻³

$$V(\vec{r}) = \sum_{i=1}^N V_{\alpha}(\vec{r}_i) \quad (2.1)$$

where the vectors \vec{r}_i are defined by $\vec{r}_i = \vec{r} - \vec{R}_i$, \vec{R}_i are the location of the lattice points and N is the total number of sites in the solid. $V_{\alpha}(\vec{r})$ ($\alpha=A,B$) is the potential due to A or B atom and is assumed to be the muffin-tin form and does not overlap with each other;

$$\begin{aligned} V_{\alpha}(\vec{r}_i) &= V_{\alpha}(r_i) , & r_i < r_m \\ V_{\alpha}(\vec{r}_i) &= \text{Constant}, & r_i > r_m \end{aligned} \quad (2.2)$$

where r_m is the muffin-tin radius.

The Hamiltonian for a certain configuration of the alloy in atomic mass unit is

$$H = -\nabla^2 + V(\vec{r}) \quad (2.3)$$

The Green's function in operator notation for a system of scatterers is defined as

$$G = (EI - H)^{-1} \quad (2.4)$$

where E and I are energy and identity matrix. The equation (2.4) can be expanded using the Dyson's equation¹ as

$$G = G_0 + G_0 \mathbf{T} G_0 \quad (2.5)$$

where G_0 is the free electron Green's function and

$$\mathbf{T} = V + V G_0 \mathbf{T} \quad (2.6)$$

is the total scattering operator. \mathbf{T} may be written as

$$\mathbf{T} = \sum_{i,j}^N T_{i,j} \quad (2.7)$$

where the operators $T_{i,j}$ are called path operators and satisfy the following multiple scattering equation

$$T_{i,j} = t_i \delta_{i,j} + t_i G_0 \sum_{k \neq i} T_{kj} \quad (2.8)$$

Here,

$$t_i = V_i (1 + G_0 t_i) \quad (2.9)$$

is the t-matrix that describes the scattering from an isolated potential on the i -th site. Equation (2.9) in angular momentum space has on-the-energy-shell matrix elements as

$$t_{A(B)}^l(\chi) = -(\chi)^{-1} \exp(i\delta_l) \sin(\delta_l) \quad (2.10)$$

where l is the angular momentum index, $\chi = (E)^{1/2}$ and δ_l are phase shifts.

The free electron Green's function G_0 in real space can be expressed as²

$$G_0(\vec{r}, \vec{r}') = -i\chi \sum_L J_L(\chi.r_<) h_L(\chi.r_>) Y_L(\hat{r}_n) Y_L(\hat{r}'_m) \delta_{nm} \\ + \sum_{LL'} Y_L(\hat{r}_n) J_L(\chi.r_n) B_{nm}^{LL'} J_{L'}(\chi.r'_m) Y_{L'}(\hat{r}'_m) \quad (2.11)$$

where $\vec{r} = \vec{r}_n + \vec{R}_n$, $\vec{r}' = \vec{r}'_m + \vec{R}_m$ and $r_<(r_>)$ is the smaller (greater) of the variable r_n and r'_m . Also $L = (l, m)$ is a composite index, $Y_L(\hat{x})$ is the real spherical harmonic and J_L and h_L are the spherical Bessel and Hankel functions respectively. The matrix B is defined as

$$B_{nm}^{LL'}(\chi) = - \left[4\pi i \chi \sum_{L_1} i^{L-L'-L_1} C_{LL'L_1} Y_{L_1}(\vec{R}_m - \vec{R}_n) * h_{L_1}^+(\chi |\vec{R}_n - \vec{R}_m|) \right] (1 - \delta_{nm}) \quad (2.12)$$

where

$$C_{LL'L_1} = \int d\Omega_x Y_{L'}(\hat{x}) Y_{L_1}(\hat{x}) \quad (2.13)$$

and $h_{L_1}^+$ denotes the outgoing Hankel function.

Starting from equation (2.8) and after some algebraic manipulations, on the energy-shell matrix elements of the path operator can finally be expressed as

$$T_{nm}^{LL'}(\chi) = \left[\{t^{-1}(\chi) - B(\chi)\}^{-1} \right]_{nm}^{LL'} \quad (2.14)$$

The Fourier transform of equation (2.12)

$$[B_{\vec{k}}(\chi)]_{LL'} = (1/N) \sum_{nm} \exp[-i\vec{k}(\vec{R}_n - \vec{R}_m)] B_{nm}^{LL'}(\chi) \quad (2.15)$$

is related to the well-known KKR structure functions¹⁹. Equations (2.10) and (2.15) are very important in the KKR theory; $t(\chi)$ depends only on the potential while $B_{\vec{k}}(\chi)$ depends only on the lattice structure. These two matrices play a central role in the KKR-CPA theory.

Now the Green's function G can be written as²

$$G(E, \vec{r}, \vec{r}') = \sum_{LL'} Z_L^n(E, \vec{r}_n) T_{nm}^{LL'}(\chi) Z_{L'}^m(E, \vec{r}_m) - \delta_{nm} \sum_L Z_L^n(E, \vec{r}_n) J_L^n(E, \vec{r}_n) \quad (2.16)$$

where \vec{r} and \vec{r}' are within n^{th} and m^{th} muffin-tin spheres and the wave functions $Z_L^{n(m)}(E, \vec{r}_{n(m)})$ and $J_L^{n(m)}(E, \vec{r}_{n(m)})$ are respectively the regular and irregular solutions of the differential equation.

$$[-\nabla^2 + V_{n(m)}(\vec{r}_{n(m)}) - E] Z_L^{n(m)}(E, \vec{r}_{n(m)}) = 0 \quad (2.17a)$$

For spherically symmetric potentials one can write

$$\left. \begin{aligned} Z_L^{A(B)}(E, \vec{r}) &= Y_L(\hat{r}) Z_L^{A(B)}(E, r) \\ J_L^{A(B)}(E, \vec{r}) &= Y_L(\hat{r}) \alpha_L^{A(B)}(E, r) \end{aligned} \right\} \quad (2.17b)$$

where $Z_L^{A(B)}$ and $\alpha_L^{A(B)}$ are radial wave functions and are normalized such that for $r \geq r_m$ they join smoothly to

$$Z_L^{A(B)}(\chi, \vec{r}) = J_L(\chi, r) [t_{A(B)}^L]^{-1} - i \chi h_L(\chi, r) \quad (2.17c)$$

$$\alpha^{A(B)}(\chi, r) = J_L(\chi, r)$$

The regular wave function $Z_L^{A(B)}$ can be written as²⁰

$$Z_L^{A(B)} = \phi_L^{A(B)}(E) \psi_L^{A(B)}(r, E) \quad (2.17d)$$

where $\phi_L^{A(B)}(E)$ is an energy dependent renormalization factor independent of r such that $\psi_L^{A(B)} \rightarrow r^L$ for $r \rightarrow 0$ ²⁰.

Equations (2.16) and (2.14) are exact within the muffin-tin approximation and can be used to obtain the Green's function for a cluster of atoms²¹. However, here we are interested in an infinite system and would like to obtain ensemble average of $G(E, \vec{r}, \vec{r}')$. The ensemble averages of equation (2.16) are related to the ensemble averages of the path operators, which will be determined by invoking the CPA. The CPA condition that the average scattering from each site must be zero, can be expressed in terms of Green's function operator as

$$x. \langle G \rangle_A + y. \langle G \rangle_B = G \quad (2.18)$$

where $\langle G \rangle_{A(B)}$ denotes the restricted site average of G when zeroth site is occupied by an A (B) atom. Equivalently this condition can be written in terms of path operators as

$$x. \langle T_{nn} \rangle_{n=A} + y. \langle T_{nn} \rangle_{n=B} = T_{nn}^C \quad (2.19)$$

where $\langle T_{nn} \rangle_{n=A}$ and $\langle T_{nn} \rangle_{n=B}$ are the restricted site averages of T_{nn} where n^{th} site is occupied by an A (B) atom and T_{nn}^C is the nn path operator for the CPA medium. After solving equation (2.19), we get the KKR-CPA condition as

$$x.[D_A]_{LL'} + y.[D_B]_{LL'} = I_{LL'} \quad (2.20)$$

where

$$[D_{A(B)}]_{LL'} = [I + T_{00}^C (t_{A(B)}^{-1} - t_C^{-1})]_{LL'}^{-1} \quad (2.21)$$

and C is used to label quantities for the CPA medium. The path operator matrix is given by

$$[T_{00}^C]_{LL'} = \frac{\Omega}{(2\pi)^3} \int [t_C^{-1}(\chi) - B_{\vec{K}}(\chi)]_{LL'}^{-1} d\vec{K} \quad (2.22)$$

where Ω is the unit cell volume. We note that T_{00}^C involves a complicated Brillouin zone integration. Though $B_{\vec{K}}(\chi)$ is an off-diagonal matrix, for cubic symmetry the integral reduces to a diagonal matrix³ for $1 \leq 2$. By simple manipulations, one can reduce the KKR-CPA equation (2.20) with the help of equation (2.21) to a computationally simpler form as

$$[t_C^{-1}]_{LL'} = [x.t_A^{-1} + y.t_B^{-1} + (t_C^{-1} - t_A^{-1})T_{00}^C(t_C^{-1} - t_B^{-1})]_{LL'} \quad (2.23)$$

This equation can be solved only by a numerical iterative method. The input for iterating this equation is t_A^{-1} , t_B^{-1} via equation (2.10) and $B_{\vec{K}}(\chi)$ via equation (2.15).

2.3 CHARGE SELF-CONSISTENT KKR-CPA

For full charge self-consistency, the charge densities in A and B cells are needed. These can be obtained², once the restricted site averages of the Green's function $\langle G(E, \vec{r}, \vec{r}') \rangle_{A(B)}$ are known as

$$\rho_{A(B)}(\vec{r}) = -\left(\frac{1}{\pi}\right) \int_{-\infty}^{E_F} \text{Im} \langle G(E, \vec{r}, \vec{r}') \rangle_{A(B)} dE \quad (2.24)$$

where $\rho_{A(B)}$ denotes the charge density associated with an A (B) cell.

Equation (2.24) can be further rewritten as

$$\rho_{A(B)}(\vec{r}) = -\left(\frac{1}{\pi}\right) \int_{-\infty}^{E_F} \text{Im} \text{tr} [Z^{A(B)}(\vec{r}) Z^{A(B)}(\vec{r}') D_{A(B)} T_{00}^C]_{LL'} dE \quad (2.25)$$

For the charge self-consistent KKR-CPA, the KKR-CPA equation (2.23) is first solved for given potentials of A and B atoms. The new charge densities ρ_A and ρ_B are calculated from equation (2.25). New potentials are then calculated by using the local density approximation of the density-functional theory as has been described in Chapter 1. The new potentials are used to solve the KKR-CPA equation and again a new set of potentials is calculated. We iterate this process until the potentials and charge densities get converged.

To calculate the density of state and component density of states, we define the matrices F^A and F^B as²

$$F_{LL'}^{A(B)} = \int_{\Omega} Z_L^{A(B)}(\vec{r}) Z_{L'}^{A(B)}(\vec{r}) d\vec{r} \quad (2.26)$$

where Ω denotes the integral over the unit cell. Then the component density of states for the A and B atoms can be expressed as

$$\rho_{A(B)}(E) = -\left(\frac{1}{\pi}\right) \text{Im} \int_{\Omega} \langle G(E, \vec{r}, \vec{r}') \rangle_{A(B)} d\vec{r}$$

or

$$\rho_{A(B)}(E) = -\left(\frac{1}{\pi}\right) \text{Im} \text{tr} \left[F^{A(B)} D_{A(B)} T_{00}^C \right]_{LL}, \quad (2.27)$$

where tr denotes the trace in L-space. Since equation (2.27) is diagonal in L-space, it allows L decomposed symmetry components (s,p,t_{2g} and e_g) of $\rho_{A(B)}(E)$ in the alloy. The cubic symmetry reduces the number of distinct elements to four, i.e., s,p,t_{2g} and e_g. The average density of states for the alloy is calculated as

$$\rho(E) = -\left(\frac{1}{\pi}\right) \text{Im} \text{tr} \left[\{x.F^A D_A + y.F^B D_B\} T_{00}^C \right]_{LL}, \quad (2.28)$$

2.4 CONCLUSIONS:

In this chapter basically we have shown main equations of charge self-consistent KKR-CPA method. The detailed computational procedure and the flow chart will be given in Chapter 3.

CHAPTER- 3

APPLICATION OF CHARGE SELF- CONSISTANT

KKR-CPA TO Cr-AI ALLOYS

3.1 INTRODUCTION

In this chapter we will calculate the electronic structure of disordered paramagnetic Cr-Al alloys by the application of the charge self-consistent KKR-CPA²². We have chosen this system because it is very important bcc alloy system. Cr_XAl_Y alloy system form bcc solid solution for $1 \geq X \geq 74.5$ ²³. To our knowledge, no such calculations have been reported for this system till now, although some important experimental results of X-Ray photo spectra (XPS) and X-Ray emission spectra (XES) of the valence band on concentration $X=1.0, 0.95, 0.85$ and 0.75 are available on Cr-Al alloys²⁴. In experimental results, the shape and half width of XPS of valence band changes notably at $X=0.85$ and reported largest at this concentration. In this chapter we shall focus on the results for the density of states, as this is the basic quantity needed to explain various experimental results. We shall compare our calculated results of DOS with XPS of valence band of Cr_XAl_Y at $X=0.95, 0.85$ and 0.75 . We shall calculate the half width of DOS band and show its theoretical behavior.

The outline of this chapter is as follows. In section 3.2 we give computational details involved in the method with flow chart. In section 3.3, we present the results of electronic structure of Cr-Al alloys by using the charge self-consistent KKR-CPA method. We present our results of density of states as a function of Cr concentration in Cr-Al alloy. We have compared charge self-consistent KKR-CPA density of states (DOS) results with the rigid band model density of states results. We have compared the density of states with the available experimental data for Cr-Al alloy and have found

very good agreement between the two. The final section 3.4 gives conclusions.

3.2 COMPUTATIONAL DETAILS

We have applied the charge self-consistent KKR-CPA method to the Cr_XAl_Y alloy for different concentrations of Cr ($X = 1.0, 0.95, 0.85 \text{ and } 0.75$). This alloy has bcc structure and their lattice constants are presented²³ in table 3.1.

TABLE 3.1

Lattice constants of Cr_XAl_Y alloys

S.No.	Cr concentration (X)	Lattice constants (a.u.)
1	1.00	5.453
2	0.95	5.484
3	0.85	5.508
4	0.75	5.553

For the charge self-consistent KKR-CPA, we start with atomic charge densities (ρ_A^m, ρ_B^m) for Cr and Al, and calculate the potentials (V_A^m, V_B^m) from equation (1.8) as explained in Chapter 1. The $t_A^{-1}(x)$ and $t_B^{-1}(x)$ are then

computed for the input potentials (V_A^m, V_B^m) . The KKR-CPA equation is solved iteratively within a tolerance of 0.0001, to calculate the t_C^{-1} . Note that in each KKR-CPA iteration T_{00}^C has to be calculated using equation (2.22), which involves a complicated Brillouin Zone integration. In the initial stages of implementation of the KKR-CPA theory, this was a major problem, which was eventually solved by using special direction technique²⁵. Although this technique is quite simple, it does not give as accurate results as tetrahedron technique which has been developed by Kaprzyk et al²⁶, for disordered alloys. Since, higher accuracy is essential for full charge self-consistency, we have used the tetrahedron method using 858 \vec{K} points in the irreducible part of the Brillouin Zone. We have observed that it is difficult to achieve convergence if we use less number of \vec{K} points in the tetrahedron. The new charge densities $(\rho_A^{out}, \rho_B^{out})$ are obtained by equation (2.25). The new potentials (V_A^{out}, V_B^{out}) in the alloy are then calculated using equation (1.8) of Chapter 1. Again, these new potentials are taken as input to repeat the whole process, until the difference of old and new charge densities is within a certain tolerance (ϵ_{CHARGE}). This tolerance has been defined as

$$\epsilon_{CHARGE}^{A(B)} = \int_0^{r_m} (\rho_{A(B)}^{out} - \rho_{A(B)}^{in}) r^2 dr \quad (3.1)$$

This tolerance is taken to be 0.0001. The flow chart of the charge self-consistent KKR-CPA has been given below.

FLOW CHART OF CHARGE SELF-CONSISTENT

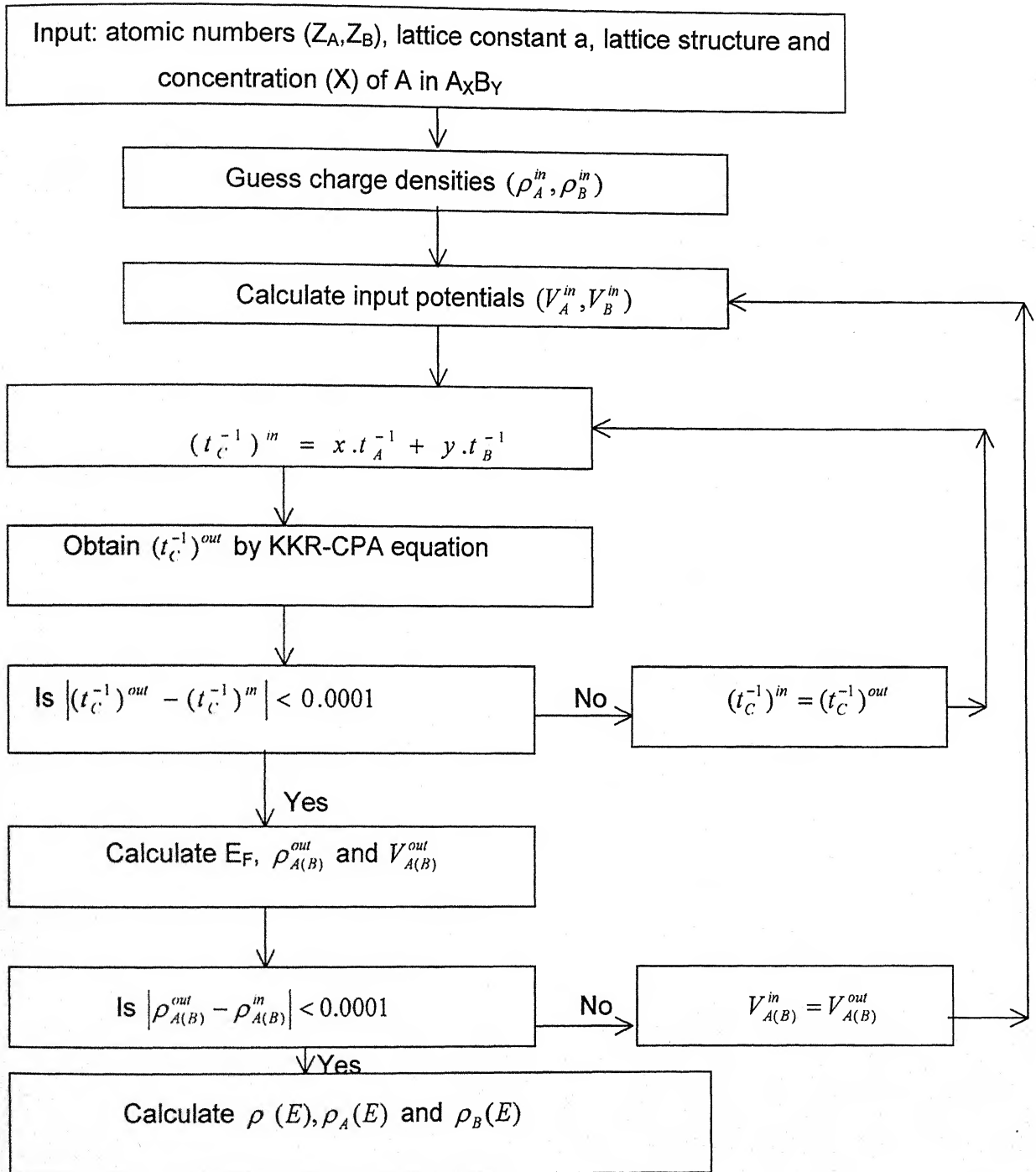


Chart-3.1

For the new charge densities, we have to calculate Fermi energy, as can be seen from equation (2.25). The Fermi energy is calculated using Lloyd formula for integrated density of states.

The Lloyd formula¹ is written as

$$N'(E) = N'_0(E) + \frac{2}{\pi} \text{Im} \left[x \cdot \ln \det |t_C^{-1} - t_B^{-1}| + y \cdot \ln \det |t_C^{-1} - t_A^{-1}| \right] - \frac{2}{\pi N} \text{Im} \sum_{\vec{K}} \ln \det |t_C^{-1} - B_{\vec{K}}| \quad (3.2)$$

where $N'(E)$ is the integrated density of states and $N'_0(E)$ is the free electron integrated density of states. Though this formula is easy to handle, it sometimes gives unphysical jumps, which can occur in \ln (logarithm) of a complex quantity, used in the formula. Kaprzyk and Bansil²⁰ have derived a generalized Lloyd formula, which does not give such unphysical jump and is given below:

$$N'(E) = (\text{Im}/\pi) \text{tr} \left[\frac{1}{N} \sum_{\vec{K}} \ln \left[G_0^{-1}(E, \vec{K}) + \beta^J - \beta^C \right]^{-1} - \ln(G_C) + x \cdot \ln \left[(\psi^A(r_m))^{-1} G_A \right] + y \cdot \ln \left[(\psi^B(r_m))^{-1} G_B \right] \right] \quad (3.3)$$

where

$$G_{A(B)} = \left[G_C^{-1} + \beta^C - \beta^{A(B)} \right]^{-1} \quad (3.4)$$

Here, the KKR-CPA Green's function G_C and the associated log-derivative β^C are the self-consistent solutions of the CPA equation (2.18)

$$x \cdot G_A + y \cdot G_B = G_C \quad (3.5)$$

where

$$G_c = \frac{1}{N} \sum_{\vec{K}} [G_0^{-1}(E, \vec{K}) + \beta^j - \beta^c]^{-1} \quad (3.6)$$

$$\beta_L^{A(B)}(E) = r^2 \frac{\partial}{\partial r} \ln Z_L^{A(B)}(E, r) \Big|_{r=r_m} \quad (3.7)$$

and β_L^j is the log-derivative for the spherical Bessel function. Note that $\psi_L^{A(B)}(r)$ and $Z_L^{A(B)}(r)$ have been already defined in equation (2.17).

Although equation (3.3) also contains the logarithm functions, but unphysical jumps of these functions cancel with each other. The integrated density of state at the Fermi energy gives the total number of valence electron in the alloy. Therefore, the Lloyd formula permits an evaluation of the Fermi energy without requiring an explicit computation of the density of states. We have used formula of Kaprzyk and Bansil, equation (3.3), to calculate the Fermi energy.

The calculation of charge densities from equation (2.25) using integration along real energy is very slow and time consuming. To speed up the calculations, the complex energy method^{27,28} has been used to calculate the charge densities and potentials. The \vec{K} -space integration is much faster in the complex plane because the integrand becomes smoother when the energy is complex.

To obtain full charge self-consistency it takes a large number of iterations to achieve convergence. Therefore, to facilitate both the CPA and charge self-consistency loops, we have used mixing schemes^{7,29}. In the CPA loop new t_c^{-1} is taken as

$$[(t_c^{-1})^m]_{ITCPA+1} = \alpha_{CPA} [(t_c^{-1})^m]_{ITCPA} + (1 - \alpha_{CPA}) [(t_c^{-1})^{out}]_{ITCPA} \quad (3.8)$$

where α_{CPA} is the mixing parameter for the CPA and ITCPA is the number of iterations. In the charge self-consistency loop, the new potential is taken as

$$[V_{A(B)}^m]_{ITCHARGE+1} = \alpha_{A(B)}^V [V_{A(B)}^m]_{ITCHARGE} + (1 - \alpha_{A(B)}^V) [V_{(B)}^{out}]_{ITCHARGE} \quad (3.9)$$

where $\alpha_{A(B)}^V$ is the mixing parameter for A(B) potential and ITCHARGE is the number of iteration in charge density loop. We have taken $\alpha_{A(B)}^V$ between 0.75 to 1.00 for all concentrations of Cr in the alloy. The CPA mixing $\alpha_{A(B)}^V$ is taken as 0.05.

The CPU time on Silicon-Graphics Indy-R4400 system for running single charge self-consistency loop is about 6 minutes. The required number of iterations for the convergence of the charge densities in the charge self-consistency loop is about 400 for all concentrations of Cr in the Cr-Al alloy. The final calculation of density of states and component density of states is done along the real energy axis and takes about another 15 minutes of CPU time on this machine.

Table 3.2 gives the Fermi energies (E_F) for various Cr-Al alloy composition and alloy density of states at the Fermi energy calculated within the charge self-consistent KKR-CPA.

Table- 3.2

Density of states (DOS) at Fermi energy (E_F) for Cr_xAl_y alloys

S.No.	X	E_F (Ry)	DOS at E_F (St/Ry.atom)
1.	1.0	0.78117	9.5378
2.	0.95	0.75992	9.4620
3.	0.85	0.74931	11.0413
4.	0.75	0.74194	11.6706

3.3 RESULTS AND DISCUSSION

We have applied the charge self-consistent KKR-CPA method to calculate the electronic structure of paramagnetic bcc Cr_xAl_y alloys. We have calculated the charge self-consistent potential, charge densities, component density of states and density of states of Cr_xAl_y alloys for concentrations $X=0.95, 0.85$ and 0.75 . We have presented component density of states, density of states and density of states at Fermi energy for above concentrations, in figure 3.1 to 3.10. These results can be used directly for calculating electronic structure (Fermi surface, band structure, conductivity, optical properties, transport properties etc.) of the alloys. We have also compared our calculated density of states with experimental measured X-Ray photo spectra (XPS) of Cr_xAl_y alloys²⁴ at concentration $X=0.95, 0.85$ and 0.75 .

Figure 3.1 shows the comparison of the average density of states calculated using the charge self-consistent KKR-CPA, with those of Cr-based rigid band model for $X=0.95$. We note that, although it is Cr-rich alloy, the Cr-based rigid band model does not work very well in this case. We notice that, there is no qualitative and quantitative difference between the two results. However there is a shift in the charge self-consistent KKR-CPA density of states towards the lower energy region with respect to Cr-based rigid band model density of states. This shifts of density of states is more at higher energies.

DENSITY OF STATES (STATES/RYDBERG-ATOM)

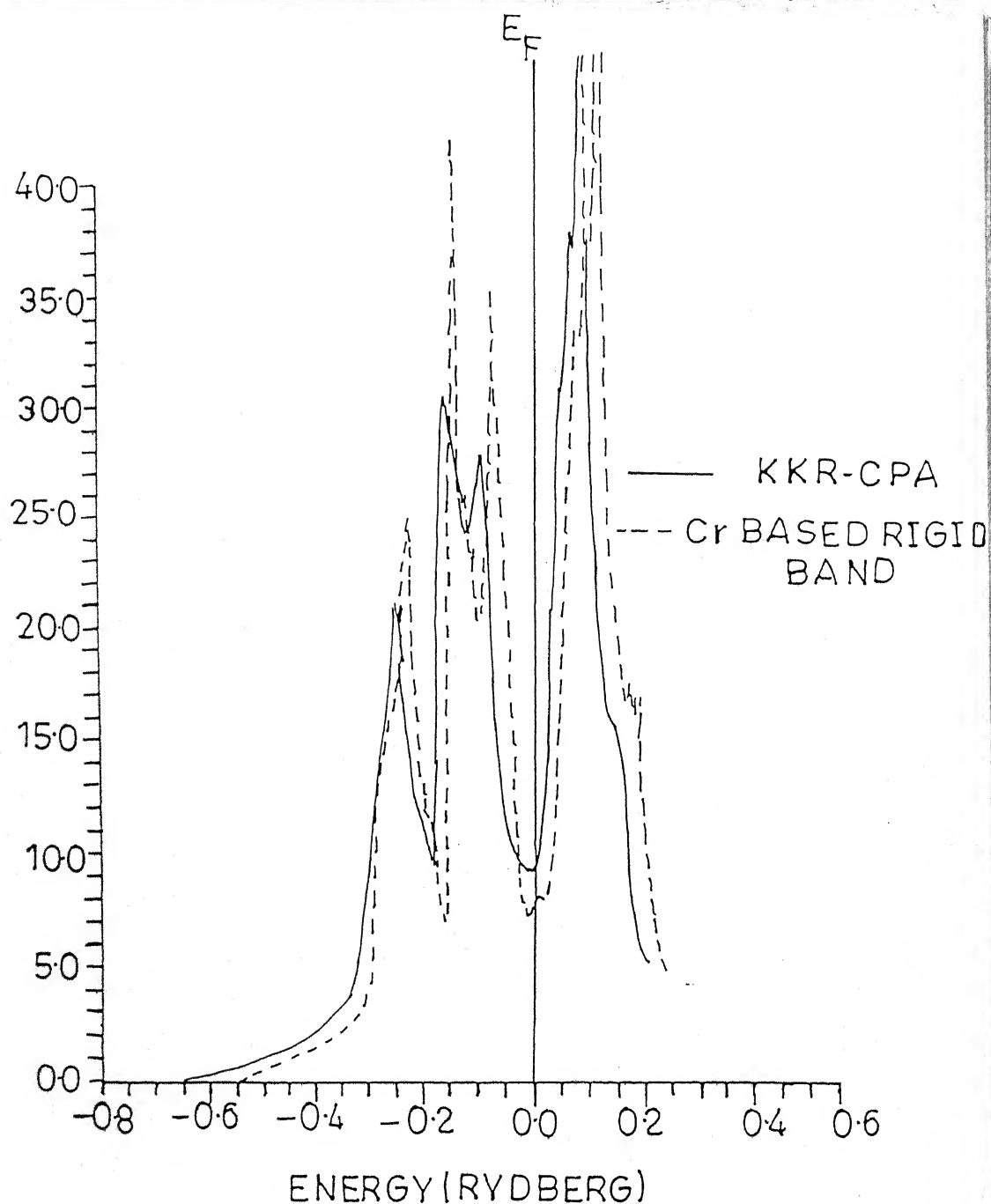


Figure 3.1. The average density of states by using charge self-consistent KKR-CPA method (solid curve) and density of states obtained by Cr-based rigid band model (broken curve) for $Cr_{0.95}Al_{0.05}$.

Figure 3.2 shows the comparison of the average density of states calculated using the charge self-consistent KKR-CPA, with those of Cr-based rigid band model for $X=0.85$. We observed that, although it is Cr-rich alloy, the Cr-based rigid band model does not work in this case. We notice that, there is a marked qualitative and quantitative difference between the two results.

Figure 3.3 shows the comparison of the average density of states calculated using the charge self-consistent KKR-CPA, with those of Cr-based rigid band model for concentration $X=0.75$. There is big qualitative and quantitative difference between the two results. We find that it is also Cr-rich alloy; but the Cr-based rigid band model totally fails in this case. On the basis of above results it is found that Cr-based rigid band model fails in the calculations of electronic structure of Cr-Al alloys.

In figures 3.4, 3.5 and 3.6, we present the component density of states of Cr and Al in Cr_xAl_y alloys for concentration $X=0.95$, 0.85 and 0.75 respectively. One can use these results in the analysis and calculations of electronic structure of these alloys. The component density of states can be compared with experimental results of soft X-Ray (emission and absorption) spectra. Therefore, these results will be very important for experimentalist.

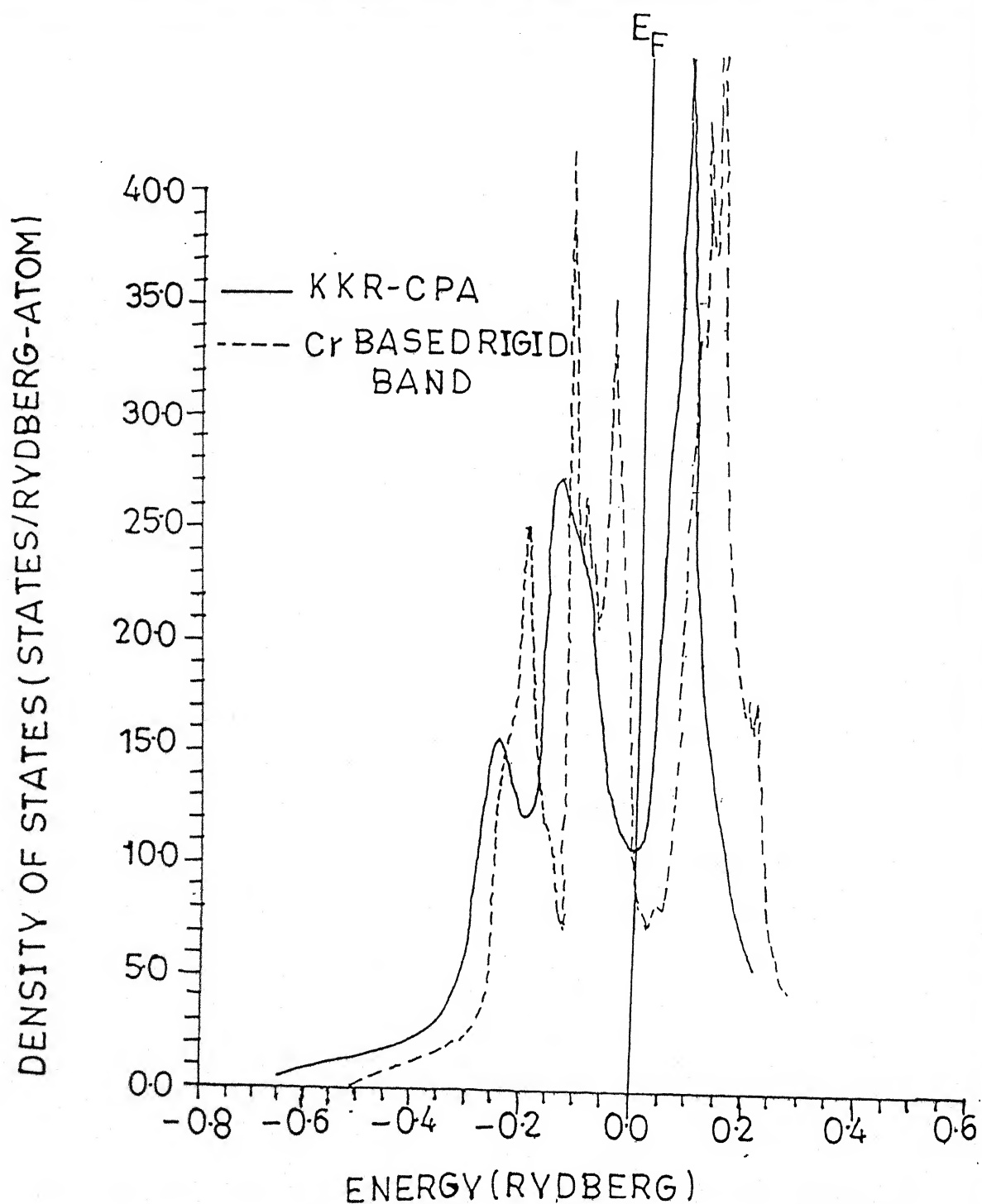


Figure 3.2. The average density of states by using charge self-consistent KKR-CPA method (solid curve) and density of states obtained by Cr-based rigid band model (broken curve) for $Cr_{0.85}Al_{0.15}$.

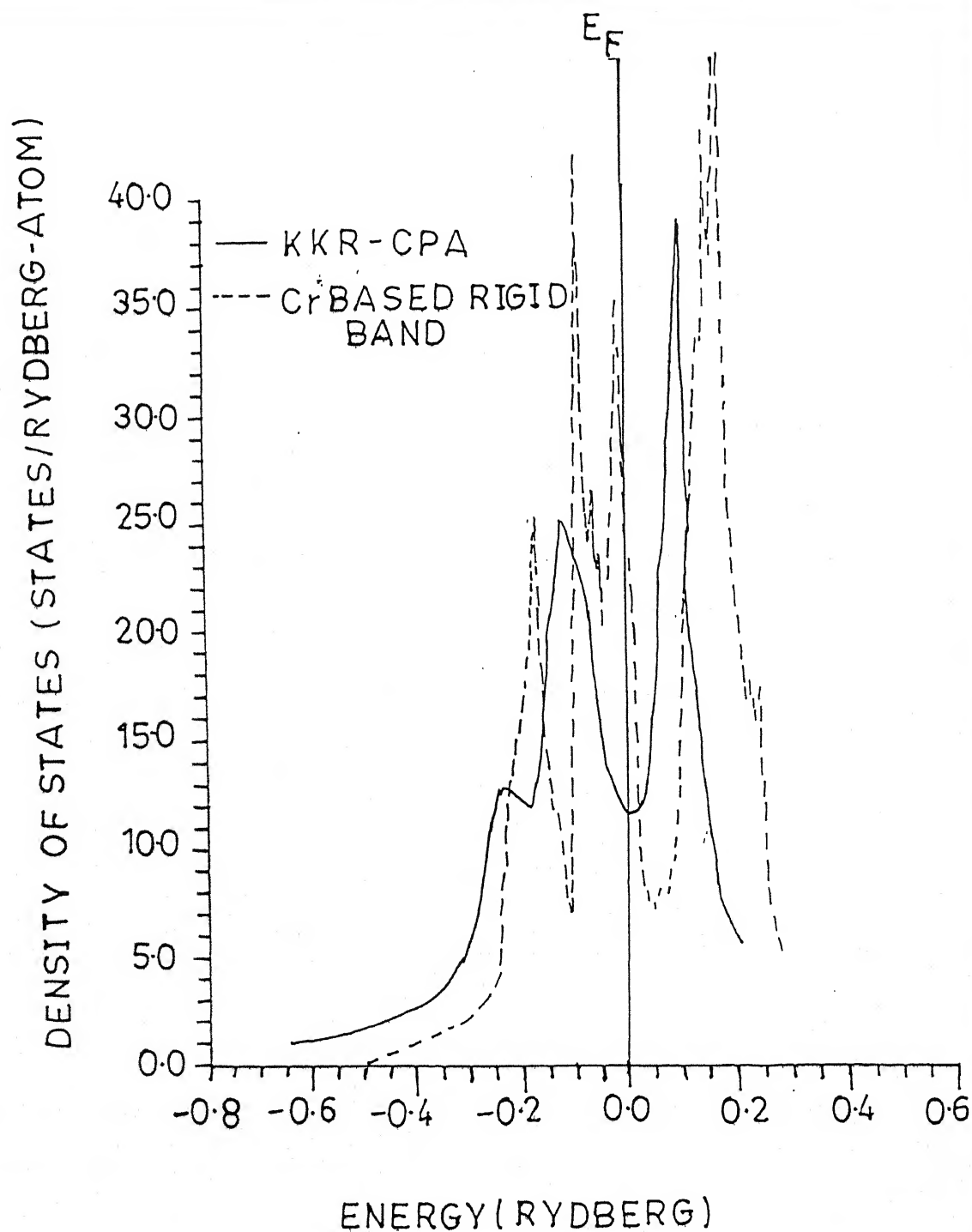


Figure 3.3. The average density of states by using charge self-consistent KKR-CPA method (solid curve) and density of states obtained by Cr-based rigid band model (broken curve) for $Cr_{0.75}Al_{0.25}$.

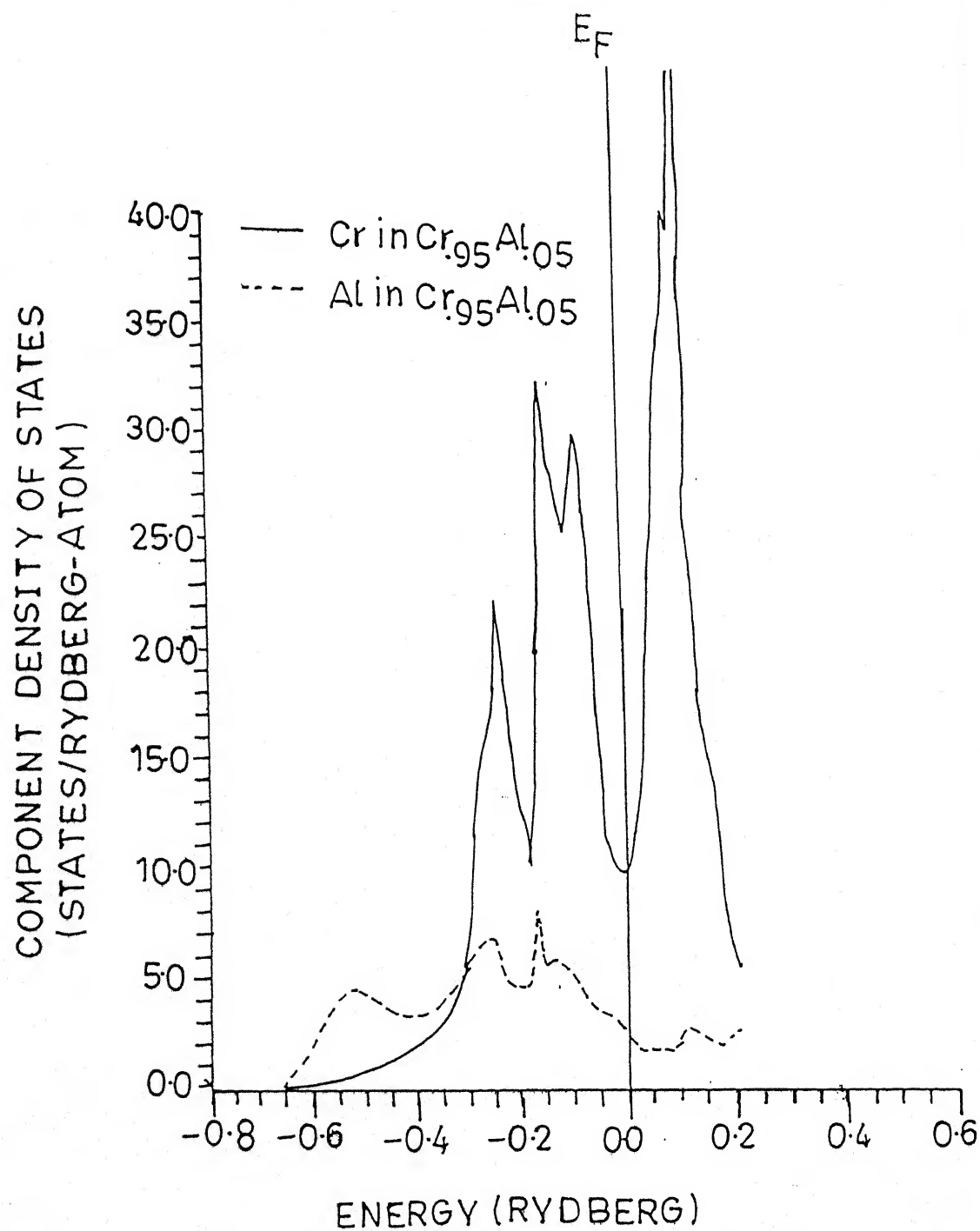


Figure 3.4. The component density of states of Cr (solid curve) and Al (broken curve) in $Cr_{0.95}Al_{0.05}$.

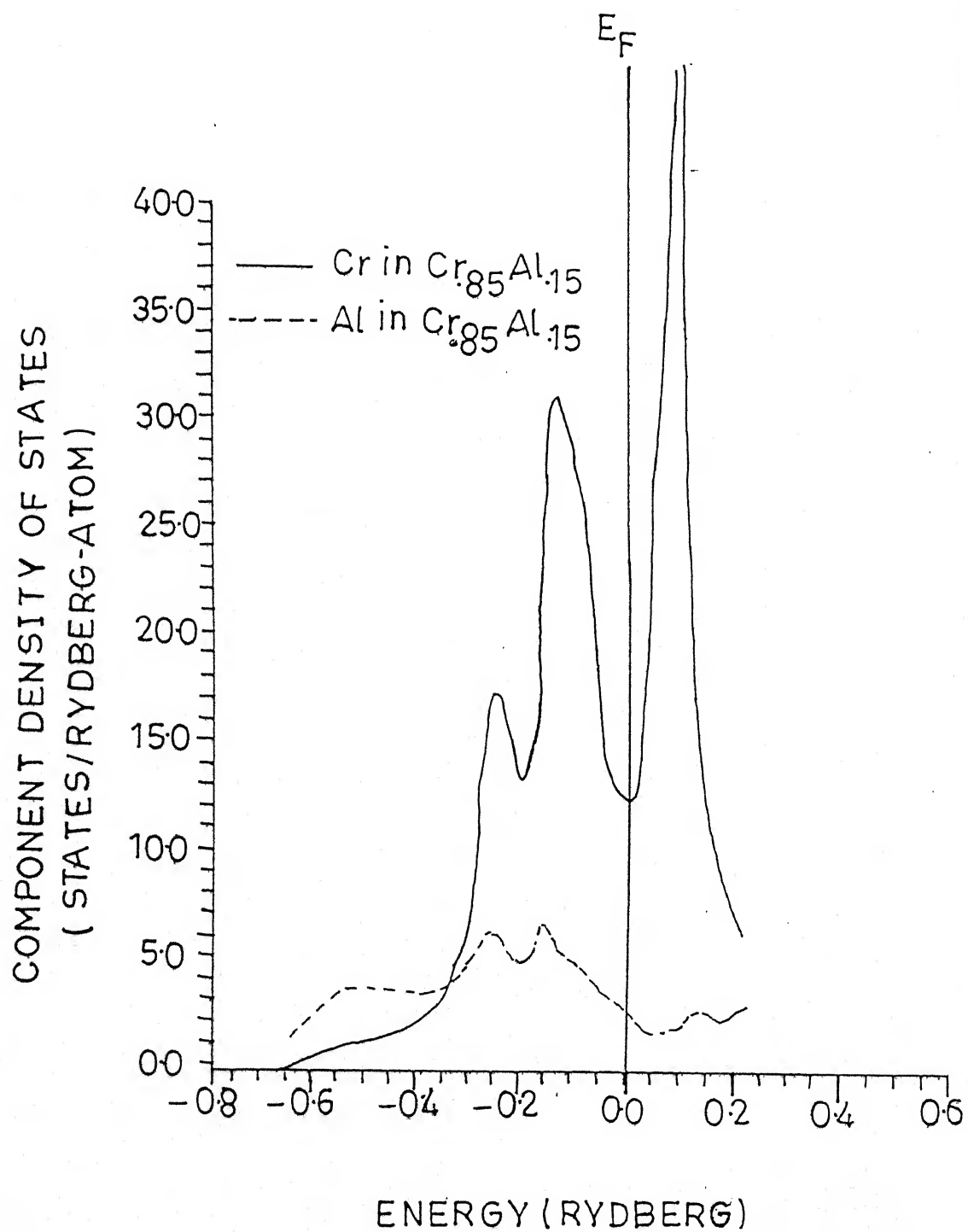


Figure 3.5. The component density of states of *Cr* (solid curve) and *Al* (broken curve) in $Cr_{0.85}Al_{0.15}$.

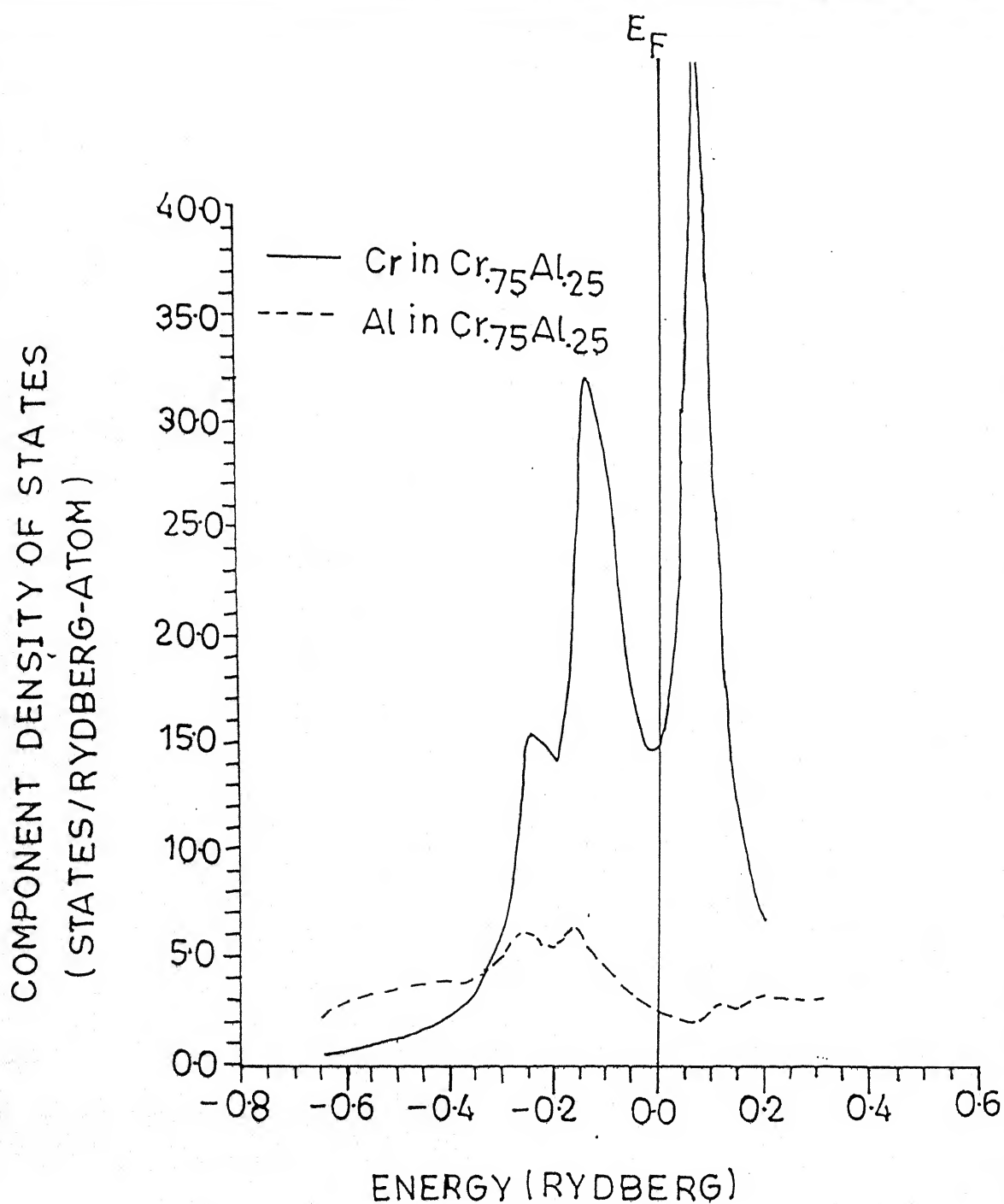


Figure 3.6. The component density of states of Cr (solid curve) and Al (broken curve) in $\text{Cr}_{0.75}\text{Al}_{0.25}$.

In figure 3.7, we show the comparison of the charge self-consistent KKR-CPA density of states (our theoretical results) with available results of X-Ray photo spectra (XPS)²⁴ for $Cr_{0.95}Al_{0.05}$ alloy. The structures (the position of peaks) in our theoretical results are well reflected in X-Ray photo spectra (XPS) results. The theoretical half-width of density of states (DOS) curve below Fermi energy is 2.20 Rydberg approximately. We find that our results are in good agreement with experimental results.

In figure 3.8, we show the comparison of the charge self-consistent KKR-CPA density of states (our theoretical results) with available results of X-Ray photo spectra (XPS)²⁴ for $Cr_{0.85}Al_{0.15}$ alloy. The structures in our theoretical results are very well reflected in X-Ray photo spectra (XPS) results. The theoretical half-width of density of states (DOS) curve below Fermi energy is 2.31 Rydberg approximately. It is noticed that the half-width of the band increases about 5% of the $Cr_{0.95}Al_{0.05}$ alloy, which is quite satisfactory with XPS experimental results. Thus we find that our theoretical results are in very good agreement with experimental results.

In figure 3.9, we show the comparison of the charge self-consistent KKR-CPA density of states (our theoretical results) with available results of X-Ray photo spectra (XPS)²⁴ for $Cr_{0.75}Al_{0.25}$ alloy. The structures in our theoretical results are in very good agreement with reflected X-Ray photo spectra (XPS) results. The theoretical half width of density of states (DOS) curve below Fermi energy is 2.20 Rydberg approximately. It is observed that the half width of the theoretical band decreases with respect to $Cr_{0.85}Al_{0.15}$

alloy. Thus we found that half width of the DOS band changes approximately 5% at 85 atomic percentage of Cr. It is less for 95 and 75 atomic percentage of Cr, as it was found in XPS results²⁴. Therefore, our results of calculated KKR-CPA density of states (DOS) are in very good agreement with XPS experimental results.

In figure 3.10 we show the DOS at Fermi energy (E_F) for Cr_xAl_y alloys as a function of Al concentration. We found that DOS at E_F increases with increase of Al concentration. It is noticed that there is sharp increase between 5 to 15 percentages of Al concentration. These results can be used for analysis of experimental results.

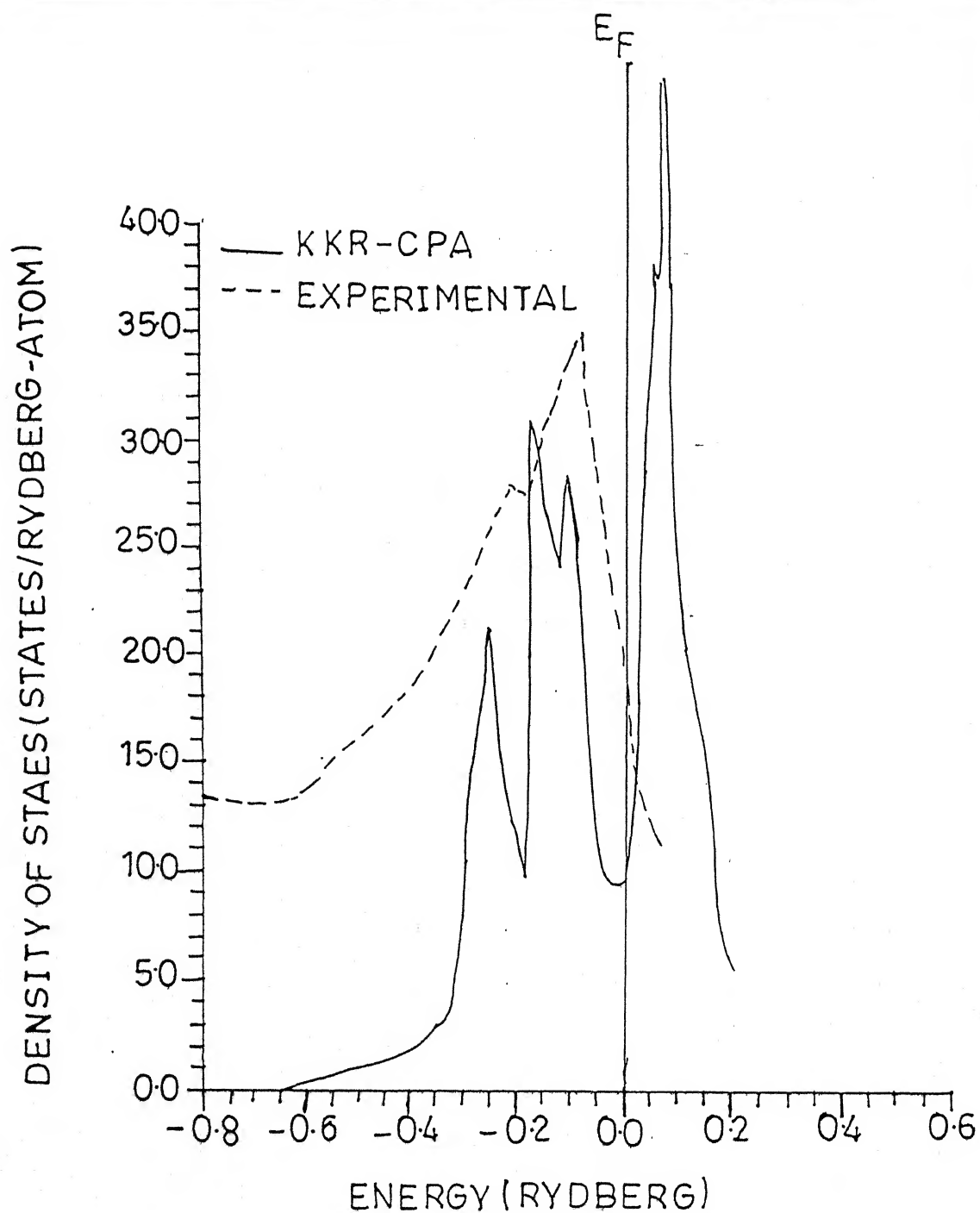


Figure 3.7. The average density of states by using charge self-consistent KKR-CPA. method (solid curve) and experimental X-ray photo spectra results (broken curve) for $Cr_{0.95}Al_{0.05}$.

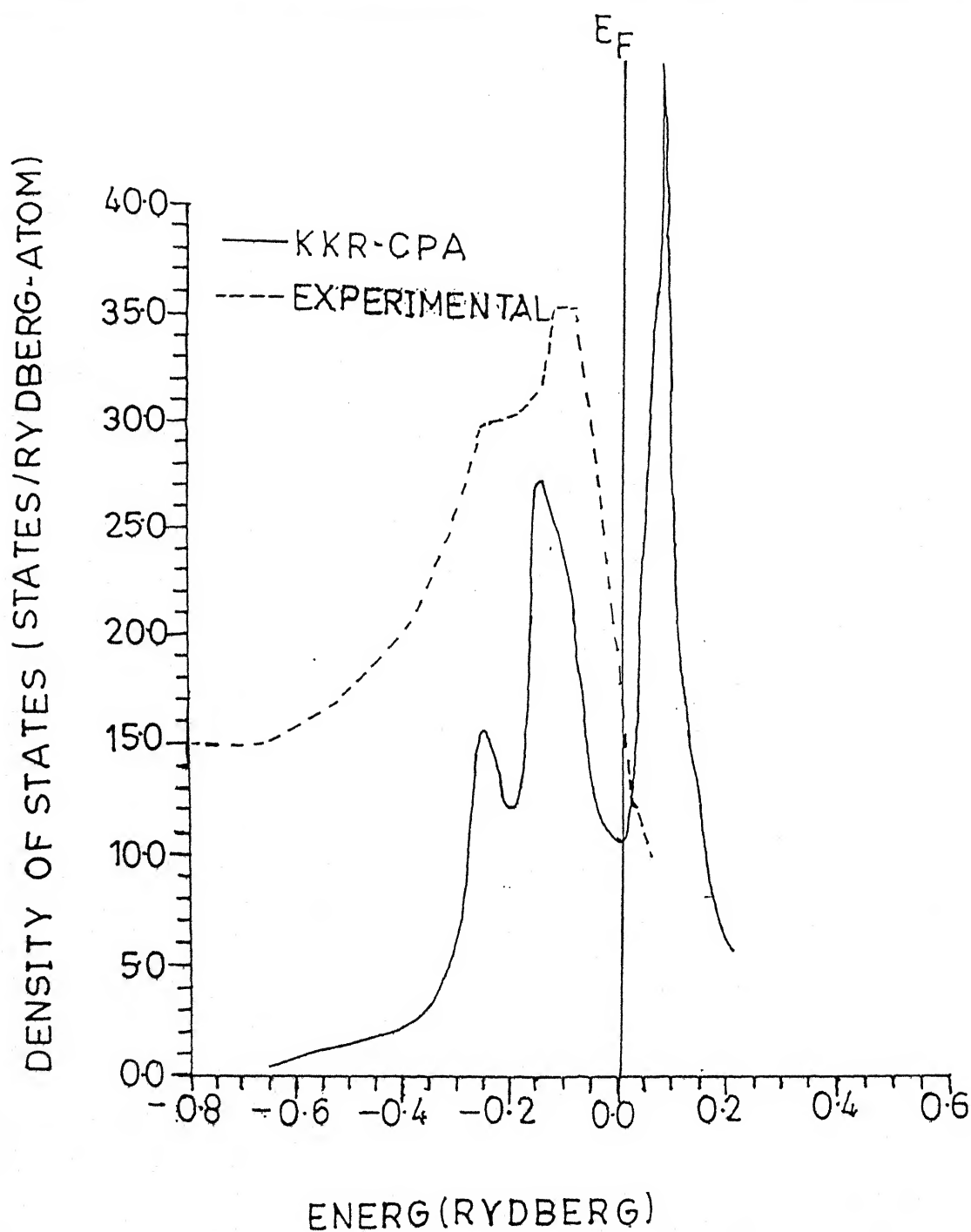


Figure 3.8. The average density of states by using charge self-consistent KKR-CPA method (solid curve) and experimental X-ray photo spectra results (broken curve) for $Cr_{0.85}Al_{0.15}$.

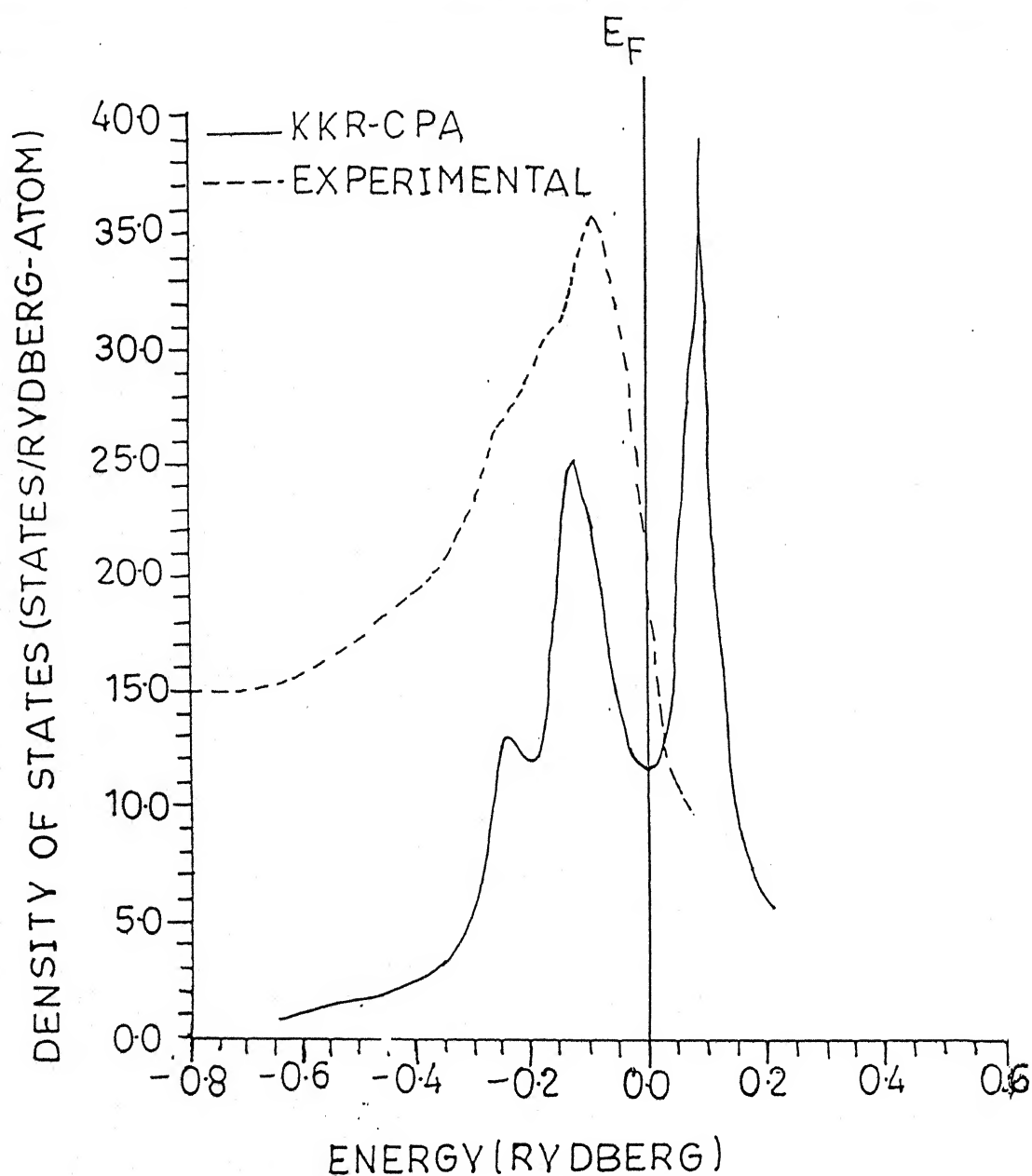


Figure 3.9. The average density of states by using charge self-consistent KKR-CPA method (solid curve) and experimental X-ray photo spectra results (broken curve) for $Cr_{0.75}Al_{0.25}$.

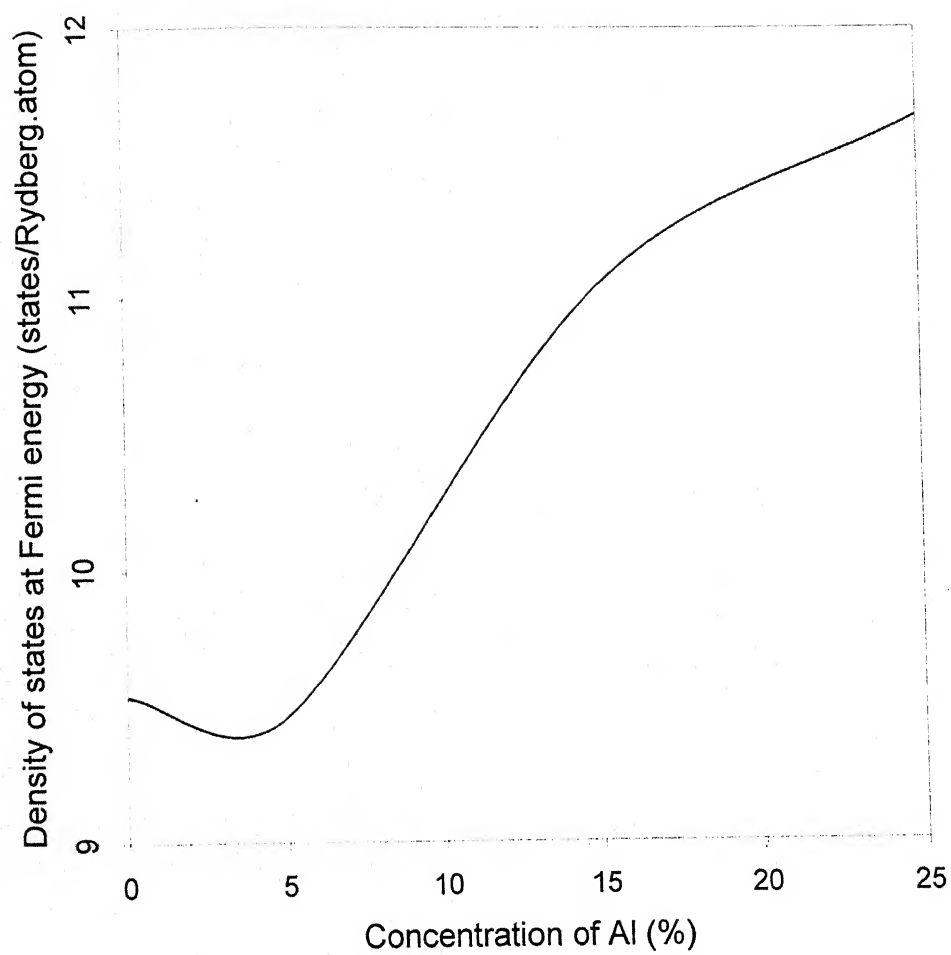


Figure 3.10, Density of states at Fermi energy Verses concentration of Al (%) in Cr_xAl_y alloys.

3.4 CONCLUSIONS:

We have applied the charge self-consistent KKR-CPA method to Cr_xAl_y disordered alloy system. We have calculated the self-consistent charge densities, self-consistent potentials, component density of states and density of states for concentrations $X=0.95, 0.85$ and 0.75 by using the charge self-consistent KKR-CPA method. It is found that charge-self consistent KKR-CPA density of states for different concentrations of alloy is in very good agreement with reflected X-ray photo spectra (XPS) results. It is found that half width of DOS band of these alloys increases approximately 5% at 85 atomic percentages of Cr with respect to 95 and 75 percent of Cr, which explains the change in shape and half width of experimental XPS results. It is also found that Cr-based rigid band model fails in the calculation of electronic structure of Cr-Al alloys.

CHAPTER- 4

APPLICATION OF KORRINGA-KOHN-ROSTOKER COHERENT-POTANTIAL-APPROXIMATION TO S-PHASE SHIFT DOUBLE- PEAK SEMICIRCULAR MODEL

4.1 INTRODUCTION

Because of the lengthy computation and complexity involved in the KKR-CPA method, it is difficult and time consuming to calculate the electronic structure of realistic systems. The density of states (DOS) is the basic quantity to understand the electronic structure of solids. The DOS of realistic system have many peaks (structures) when we plot it as a function of energy. We have proposed the double-peak semicircular model by which one can estimate about the realistic density of states without expending more time and computational efforts. The S-phase shift semicircular model has several advantages. (i) Because of semicircular modeling, the involved k -space integration, required to obtain the site-diagonal path operator is bypassed, thus reduces the computational efforts. (ii) The KKR-CPA calculation for single peak model has been tried out before Soven et al.³⁰, Rajput et al.³¹ and Yadav³². In the S-phase shift model we shall assume that the S-phase shift dominates and B , t and T all the matrices involve in the KKR-CPA method reduces in the scalar form in the angular momentum space. The CPA equation for this model can be solved transparently by reducing it in polynomial form and using the computational method.

4.2 THE S-PHASE SHIFT SEMICIRCULAR MODEL

For this model we have assumed that the phase shift has resonance behaviour and the cotangent of phase shift $C_{A(B)}$ is as

$$C_{A(B)} = \frac{E_{A(B)} - E}{\Gamma_{A(B)}} \quad (4.1)$$

where $E_{A(B)}$ is the resonant energy (band center) and $\Gamma_{A(B)}$ is half-width of resonance. Another approximation is that k-space structure function is assumed as

$$B_{\vec{k}} = \frac{B_{\vec{q}}}{\chi} - i \quad (4.2)$$

has no explicit dependence of energy (i.e. independent of energy) where $\chi = E^{1/2}$ and $B_{\vec{q}}$ is the Fourier transformation of real space structure function B_{nm} . The $B_{\vec{q}}(\chi)$ is as

$$B_{\vec{q}}(\chi) = \frac{1}{N} \sum_{nm} e^{i\vec{k} \cdot \vec{R}_{nm}} B_{nm}$$

$$B_{\vec{q}}(\chi) = \sum_{n \neq m}^N e^{i\vec{k} \cdot \vec{R}_{nm}} B_{nm} \quad (4.3)$$

In equation (4.3) by translational property one index m is fixed and we sum only on index n , then on the shell energy t-matrix element

$$\tau(\chi) = -(\chi)^{-1} e^{i\delta_L} \sin(\delta_L) \quad (4.4)$$

where δ_L is the phase shift.

From equation (4.4) we can write

$$\tau^{-1} = -\chi \cot \delta + i\chi$$

If we write $\cot(\delta) = C$, then

$$\tau^{-1} = -\chi C + i\chi \quad (4.5)$$

Now the explicit scalar form of path operator for the model has been derived as follows

$$\begin{aligned} T^{00} &= \frac{1}{N} \sum_{\bar{q}} \frac{1}{\tau^{-1} - B_{\bar{q}}} \\ T^{00} &= \frac{1}{N} \sum_{\bar{q}} \frac{1}{-\chi C + i\chi - B_{\bar{q}}} \\ T^{00} &= -\frac{1}{\chi} \sum_{\bar{q}} \frac{1}{N(C + \frac{B_{\bar{q}}}{\chi} - i)} \end{aligned}$$

with the help of equation (4.2)

$$T^{00} = -\frac{1}{\chi} \cdot \frac{1}{N} \sum_{\bar{k}} \frac{1}{C + B_{\bar{k}}} \quad (4.6)$$

We can write

$$T^{00} = -\frac{1}{\chi} \int \frac{1}{N} \sum_{\bar{k}} \frac{1}{C+b} \delta(b - B_{\bar{k}}) db \quad (4.7)$$

If we take the distribution of $B_{\bar{k}}$ as

$$f^0(b) = \frac{1}{N} \sum_{\bar{k}} \delta(b - B_{\bar{k}}) \quad (4.8)$$

From above equation we can see

$$\int_{-\infty}^{+\infty} f^0(b) db = 1$$

We will choose the distribution function $f^0(b)$ which must satisfy the above condition thus it can be written as

$$\begin{aligned} f^0(b) db &= \frac{2}{\pi} (1-b^2)^{1/2} && \text{When } |b| \leq 1 \\ &= 0 && \text{When } |b| > 1 \end{aligned} \quad (4.9)$$

By using equations (4.7), (4.8), (4.9), the path operator can be written as

$$\begin{aligned} T^{00} &= -\frac{1}{\chi} \int_{-1}^{+1} \frac{1}{C+b} f^0(b) db \\ T^{00} &= -\frac{1}{\chi} \int_{-1}^{+1} \frac{2(1-b^2)^{1/2}}{\pi(C+b)} db \end{aligned} \quad (4.10)$$

By substituting $b = \cos \theta$ it will reduce as

$$T^{00} = -\frac{1}{\pi \cdot \chi} \int_0^{2\pi} \frac{\sin^2 \theta}{(C + \cos \theta)} d\theta \quad (4.11)$$

Using complex analysis it can be written as

$$T^{00} = -\frac{1}{\pi \cdot \chi} \oint \frac{i(Z^2 - 1)^2}{2Z^2(Z^2 + 2CZ + 1)} dZ \quad (4.12)$$

or

$$T^{00} = -\frac{1}{\pi \cdot \chi} \frac{i}{2} \oint f(Z) dZ \quad (4.13)$$

where $f(Z) = \frac{(Z^2 - 1)}{2Z^2(Z^2 + 2CZ + 1)}$

The poles of integrands are $Z=0$ of order 2, other two poles $Z=Z_1$ and $Z=Z_2$ are the roots of equation $Z^2 + 2CZ + 1 = 0$, such that

$$Z_1 \cdot Z_2 = 1 \quad (4.14)$$

$$Z_1 + Z_2 = -2C \quad (4.15)$$

We can find Z_1 and Z_2 by solving equation (4.14) and (4.15) as

$$\left. \begin{aligned} Z_1 &= -C + (C^2 - 1)^{1/2} \\ Z_2 &= -C - (C^2 - 1)^{1/2} \end{aligned} \right\} \quad (4.16)$$

Now,

(a) The Residue at $Z=0$ of $f(Z)$

$$= \lim_{Z \rightarrow 0} \frac{d}{dZ} \left\{ \frac{(Z^2 - 1)^2}{Z^2 + 2CZ + 1} \right\}$$

$$= -2C \quad (4.17)$$

(b) The Residue at $Z=Z_1$ and $Z=Z_2$, if we take $+i\varepsilon$ imaginary part in the energy then

$$E = E + i\varepsilon \quad \text{for} \quad \varepsilon \rightarrow 0$$

and

$$C = \frac{E_A - E}{\Gamma_A}$$

which will be as

$$C = C - i\delta \quad \text{for} \quad \delta \rightarrow 0$$

Now from equation (4.14) if $|Z_1| > 1$ then $|Z_2| < 1$ and hence Z_1 will lie out side unit radius circle and we will evaluate the residue at $Z = Z_2$ as

$$= \lim_{Z \rightarrow Z_2} \frac{(Z - Z_2)(Z_2^2 - 1)^2}{Z_2^2(Z - Z_2)(Z_2 - Z_1)}$$

$$= (Z_2 - Z_1)$$

$$= -2(C^2 - 1)^{1/2} \quad (4.18)$$

hence path operator T^{00} will be

$$T^{00} = -\frac{1}{\pi \cdot \chi} \frac{i}{2} 2\pi i \quad \{\text{Residue at } Z = 0 + \text{Residue at } Z = Z_2\}$$

$$T^{00} = -\frac{2}{\chi} [C + (C^2 - 1)^{1/2}] \quad (4.19)$$

Path operator for effective CPA medium will be

$$T_{CP}^{00} = -\frac{2}{\chi} [C_{CP} + (C_{CP}^2 - 1)^{1/2}]$$

if we write $C = C_{CP}$, then

$$T^{00} = -\frac{2}{\chi} [C + (C^2 - 1)^{1/2}] \quad (4.20)$$

For CPA medium (+) sign may be (-) sign depending upon the modulus of Z_1 and Z_2 , then

$$\left. \begin{aligned} T^{00} &= -\frac{2}{\chi} [C + (C^2 - 1)^{1/2}] && \text{; if } |Z_1| > 1 \\ \text{or,} &&& \\ T^{00} &= -\frac{2}{\chi} [C - (C^2 - 1)^{1/2}] && \text{; if } |Z_1| < 1 \end{aligned} \right\} \quad (4.21)$$

If we define new variable g^{00} such that

$$T^{00} = -\frac{1}{\chi} g^{00} \quad (4.22)$$

then

$$g^{00} = 2[C + (C^2 - 1)^{1/2}] \quad (4.23)$$

Notice that the path operator T^{00} is Hergltoz and g^{00} is anti Hergltoz.

The DOS for S-phase shift semicircular model has been calculated by Lloyd's formula¹ as follows: As we are taking binary substitutional disordered alloy $A_X B_Y$, where X is the concentration of A type atoms in alloy and Y is the concentration of B type atoms in alloy. By using equation (4.1) the cotangent of phase shift for A and B atoms are

$$\left. \begin{aligned} C_A &= \frac{E_A - E}{\Gamma_A} \\ C_B &= \frac{E_B - E}{\Gamma_B} \end{aligned} \right\} \quad (4.24)$$

By using equations (4.5) we can write

$$\left. \begin{aligned} t_A^{-1} &= -\chi.C_A + i.\chi \\ t_B^{-1} &= -\chi.C_B + i.\chi \end{aligned} \right\} \quad (4.25)$$

The change in density of states

$$\delta\rho(E) = \rho_{cp}(E) - \rho_0(E) \quad (4.26)$$

where $\rho_0(E)$ = free electron density of states per atom, and

$\rho_{cp}(E)$ = coherent potential density of states per atom.

The change in density of states by Lloyd's formula¹ is given as

$$\delta\rho(E) = -\frac{1}{\pi} \text{Im} g \left[\left\langle T^{00} \frac{d}{dE} t_{cp}^{-1} \right\rangle - \frac{1}{N} \sum_{\bar{q}} \frac{1}{(t_{cp}^{-1} - B_{\bar{q}})} \frac{d}{dE} (B_{\bar{q}}) \right] \quad (4.27)$$

In above equation, the first term

$$\left\langle T^{00} \frac{d}{dE} t_{cp}^{-1} \right\rangle = T^{00} U^{eff} \quad (4.28)$$

where

$$U^{eff} = \bar{U} + \frac{t_{cp}^{-1} - \bar{t}^{-1}}{t_A^{-1} - t_B^{-1}} (U_A - U_B) \quad (4.29)$$

In equation (4.29)

$$U = \frac{d}{dE} (t^{-1})$$

and

$$\bar{U} = \frac{d}{dE} (\bar{t}^{-1})$$

therefore,

$$U_A = \frac{d}{dE} (t_A^{-1}) = \chi \cdot \frac{1}{\Gamma_A} - \frac{1}{2\chi} C_A + \frac{i}{2\chi}$$

$$U_B = \frac{d}{dE}(t_B^{-1}) = \chi \cdot \frac{1}{\Gamma_B} - \frac{1}{2\chi} C_B + \frac{i}{2\chi}$$

$$U_A - U_B = \chi \left[\frac{1}{\Gamma_A} - \frac{1}{\Gamma_B} \right] + \frac{1}{2\chi} [C_B - C_A] \quad (4.30)$$

$$\bar{U} = \frac{d}{dE}(\bar{t}^{-1}) = \frac{d}{dE}[\chi C_A + \chi C_B]$$

$$= \chi \left[\frac{X}{\Gamma_A} + \frac{Y}{\Gamma_B} \right] - \frac{1}{2\chi} [\chi C_A + \chi C_B] + \frac{i}{2\chi}$$

$$\bar{U} = \chi \left[\frac{X}{\Gamma_A} + \frac{Y}{\Gamma_B} \right] - \frac{\bar{C}}{2\chi} + \frac{i}{2\chi} \quad (4.31)$$

$$\bar{t}^{-1} - t^{-1} = -\chi [C - \bar{C}] \quad (4.32)$$

$$t_A^{-1} - t_B^{-1} = -\chi [C_A - C_B] \quad (4.33)$$

By using the equation (4.30), (4.31), (4.32) and (4.33) the explicit form of U^{eff} is

$$U^{\text{eff}} = \chi \left[\frac{X}{\Gamma_A} + \frac{Y}{\Gamma_B} \right] + \frac{(i - C)}{2\chi} + \frac{(C - \bar{C})}{(C_A - C_B)} \cdot \chi \left[\frac{1}{\Gamma_A} - \frac{1}{\Gamma_B} \right] \quad (4.34)$$

The change in density of states in equation (4.27) can be written in two parts as

$$\delta\rho(E) = -\frac{1}{\pi} \text{Im } g [\text{First part} + \text{Second part}] \quad (4.35)$$

where

$$\text{First part} = \left\langle T^{00} \frac{d}{dE} (t_{cp}^{-1}) \right\rangle$$

$$= T^{00} U^{eff}$$

By using equation (4.21) and (4.34), the first part can be written as:

First part

$$= -\frac{2}{\chi} [C + (C^2 - 1)^{1/2}] \chi \left[\left\{ \frac{X}{\Gamma_A} + \frac{Y}{\Gamma_B} \right\} \right] - \frac{C}{2\chi} + \frac{(C - \bar{C})}{(C_A - C_B)} \cdot \chi \left[\frac{1}{\Gamma_A} - \frac{1}{\Gamma_B} \right] - \frac{2i}{2\chi^2} [C + (C^2 - 1)^{1/2}] \quad (4.36)$$

Now,

$$\begin{aligned} \text{Second part} &= -\frac{1}{N} \sum_{\bar{q}} \frac{1}{(t_{cp}^{-1} - B_{\bar{q}})} \cdot \frac{d}{dE} (B_{\bar{q}}) \\ &= -\frac{1}{N} \sum_{\bar{q}} \frac{1}{(-\chi \cdot C + i \cdot \chi - B_{\bar{q}})} \cdot \frac{d}{dE} (B_{\bar{q}}) \\ &= \frac{1}{N} \sum_{\bar{q}} \frac{1}{(\chi \cdot C - i \cdot \chi + B_{\bar{q}})} \cdot \frac{d}{dE} (B_{\bar{q}}) \\ &= \frac{1}{N} \sum_{\bar{q}} f(B_{\bar{q}}) \end{aligned} \quad (4.37)$$

where

$$f(B_{\bar{q}}) = \frac{1}{\chi \cdot C - i \cdot \chi + B_{\bar{q}}} \cdot \frac{d}{dE}(B_{\bar{q}}) \quad (4.38)$$

With the help of equation (4.2) we can get the energy derivative of $B_{\bar{q}}$ as

$$\frac{d}{dE}(B_{\bar{q}}) = \frac{B_{\bar{k}} + i}{2 \cdot \chi}$$

By using above equation we can write

$$f(B_{\bar{q}}) = \frac{(B_{\bar{k}} + i)}{2 \cdot \chi^2 (C + B_{\bar{k}})} \quad (4.39)$$

Recall the equation (4.37)

$$\begin{aligned} \text{Second part} &= \frac{1}{N} \sum_{\bar{q}} f(B_{\bar{q}}) \\ &= \frac{1}{N} \sum_{\bar{k}} \frac{1}{2 \cdot \chi^2} \cdot \frac{(B_{\bar{k}} + i)}{(C + B_{\bar{k}})} \\ &= \frac{1}{N} \sum_{\bar{k}} \frac{1}{2 \cdot \chi^2} \cdot \frac{B_{\bar{k}}}{(C + B_{\bar{k}})} + \frac{1}{N} \sum_{\bar{k}} \frac{1}{2 \cdot \chi^2} \cdot \frac{i}{(C + B_{\bar{k}})} \\ &= \frac{1}{N} \sum_{\bar{k}} \int_{-1}^{+1} \frac{b \cdot \delta(b - B_{\bar{k}}) \cdot db}{2 \cdot \chi^2 (C + b)} + \frac{i}{N} \sum_{\bar{k}} \int_{-1}^{+1} \frac{\delta(b - B_{\bar{k}}) \cdot db}{2 \cdot \chi^2 (C + b)} \\ &= \frac{1}{2 \cdot \chi^2} \int_{-1}^{+1} \frac{f^0(b) b \cdot db}{(C + b)} + \frac{i}{2 \cdot \chi^2} \int_{-1}^{+1} \frac{f^0(b) db}{(C + b)} \end{aligned} \quad (4.40)$$

Now we can write second part as

$$\text{Second part} = \text{First integral} + \text{Second integral} \quad (4.41)$$

$$\text{where, First integral} = \frac{1}{2 \cdot \chi^2} \int_{-1}^{+1} \frac{f^0(b)b \cdot db}{(C+b)}$$

We choose the same distribution function $f^0(b)$ from equation (4.9) then first integral will be

$$= -\frac{1}{2 \cdot \chi^2} \int_{-1}^{+1} \frac{2(1-b^2)^{1/2}}{\pi(C+b)} b \cdot db$$

Putting $b = \cos \theta$, then

$$\text{First integral} = \frac{1}{\pi \cdot \chi^2} \int_0^\pi \frac{\sin^2 \theta \cdot \cos \theta \cdot d\theta}{(C + \cos \theta)}$$

$$= \frac{1}{2\pi \cdot \chi^2} \int_0^{2\pi} \frac{\sin^2 \theta \cdot \cos \theta \cdot d\theta}{(C + \cos \theta)} \quad \{\text{Since } f(2\pi - \theta) = f(\theta)\}$$

or

$$\text{First integral} = \frac{1}{2\pi \cdot \chi^2} I_1$$

$$\text{where} \quad I_1 = \int_0^{2\pi} \frac{\sin^2 \theta \cdot \cos \theta \cdot d\theta}{(C + \cos \theta)}$$

Using complex analysis it can be written as

$$I_1 = \frac{i}{4} \oint \frac{(Z^2 - 1)^2 (Z^2 + 1)}{Z^3 (Z^2 + 2CZ + 1)}$$

$$= \frac{i}{4} \oint f(Z) dZ$$

where

$$f(Z) = \frac{(Z^2 - 1)^2 (Z^2 + 1)}{Z^3 (Z^2 + 2CZ + 1)}$$

The poles of integrands are $Z = 0$ of order 3. Other two poles are $Z = Z_1$ and $Z = Z_2$ which are roots of $Z^2 + 2CZ + 1$

Now,

(a) Residue at $Z = 0$ of order 3

$$\begin{aligned} &= \text{Limit}_{Z \rightarrow 0} \frac{1}{2!} \frac{d^2}{dZ^2} \left[\frac{(Z^2 - 1)^2 (Z^2 + 1)}{(Z^2 + 2CZ + 1)} \right] \\ &= 4C^2 - 2 \end{aligned}$$

(b) Residue at $Z = Z_2$

$$\begin{aligned} &= \text{Limit}_{Z \rightarrow Z_2} \left[\frac{(Z - Z_2)(Z^2 - 1)^2 (Z^2 + 1)}{Z^3 (Z - Z_2)(Z - Z_1)} \right] \\ &= (Z_2 - Z_1)(Z_1 + Z_2) \\ &= -2(C^2 - 1)^{1/2}(-2C) \\ &= 4C(C^2 - 1)^{1/2} \end{aligned}$$

Therefore,

$$I_1 = \frac{i}{4} 2\pi i \quad (\text{Residue at } Z = 0 + \text{Residue at } Z = Z_2)$$

$$= -\frac{\pi}{2} [4C^2 - 2 + 4C(C^2 - 1)^{1/2}]$$

$$I_1 = -\pi [2C^2 - 1 + 2C(C^2 - 1)^{1/2}]$$

By substituting the value of I_1 , we get

$$\text{First integral} = -\frac{1}{2.\chi^2} [2C^2 - 1 + 2C(C^2 - 1)^{1/2}] \quad (4.42)$$

Now second integral of equation (4.40) will be as

$$\begin{aligned} \text{Second integral} &= \frac{i}{2.\chi^2} \int_{-1}^{+1} \frac{f^0(b).db}{(C+b)} \\ &= -\frac{i}{2.\chi} \left[-\frac{1}{\chi} \int_{-1}^{+1} \frac{f^0(b).db}{(C+b)} \right] \\ &= -\frac{i}{2.\chi^2} I_2 \end{aligned}$$

I_2 , has already been calculated in equation (4.10). Therefore, second integral is as

$$\text{Second integral} = \frac{i}{2.\chi^2} . 2 [C + (C^2 - 1)^{1/2}] \quad (4.43)$$

By putting the value of first integral (4.42) and second integral (4.43) in equation (4.41), we get the second part as

Second part
$$= -\frac{1}{2\chi^2} [2C^2 - 1 + 2C(C^2 - 1)^{1/2}] + \frac{i}{2\chi^2} \cdot 2[C + (C^2 - 1)^{1/2}] \quad (4.44)$$

The explicit form of $\delta\rho(E)$ can be shown by combining equations (4.36) and (4.44) in equation (4.35).

The change in density of states

$$\delta\rho(E) = \frac{1}{\pi} \text{Im} g \left[2(C + (C^2 - 1)^{1/2}) \left\{ \left(\frac{X}{\Gamma_A} + \frac{Y}{\Gamma_B} \right) + \left(\frac{(C - \bar{C})}{(C_A - C_B)} \right) \left(\frac{1}{\Gamma_A} - \frac{1}{\Gamma_B} \right) \right\} \right] \quad (4.45)$$

The change in density of state can be written by using equation (4.23) as

$$\delta\rho(E) = \frac{1}{\pi} \text{Im} g \left[g^{00} \left\{ \left(\frac{X}{\Gamma_A} + \frac{Y}{\Gamma_B} \right) + \left(\frac{(C - \bar{C})}{(C_A - C_B)} \right) \left(\frac{1}{\Gamma_A} - \frac{1}{\Gamma_B} \right) \right\} \right] \quad (4.46)$$

4.3 DOUBLE-PEAK SEMICIRCULAR MODEL

For this model we will assume (like s-phase-shift semicircular model) that the phase shift has resonance behaviour and the cotangent of phase shift $C_{A(B)}$ is as

$$C_{A(B)} = \frac{E_{A(B)} - E}{\Gamma_{A(B)}}$$

where $E_{A(B)}$ is the resonant energy (band center) and $\Gamma_{A(B)}$ is half-width of resonance. Another similar approximation is that k-space structure function is assumed as

$$B_{\vec{k}} = \frac{B_{\vec{q}}}{\chi} - i$$

has no explicit dependence of energy (i.e. independent of energy) where $\chi = E^{1/2}$ and $B_{\vec{q}}$ is the Fourier transformation of real space structure function B_{nm} as given in equation (4.3).

Now for double peak semicircular model, the explicit form of path operator will be similar to s-phase shift semicircular model as

$$T^{00} = -\frac{1}{\chi} \int \frac{1}{N} \sum_{\vec{k}} \frac{1}{C+b} \delta(b - B_{\vec{k}}) db \quad (4.47)$$

in which the distribution of $B_{\vec{k}}$ is

$$f^0(b) = \frac{1}{N} \sum_{\vec{k}} \delta(b - B_{\vec{k}}) \quad (4.48)$$

and

$$\int_{-\infty}^{+\infty} f^0(b) db = 1 \quad (4.49)$$

Therefore, for double peak semicircular model we choose the distribution function $f^0(b)$, which must satisfy the above condition. Thus it can be written as

$$\left. \begin{aligned} f^0(b) &= \frac{1}{\pi} \{1 - (1+b)^2\}^{1/2} && \text{when } -2 \leq b \leq 0 \\ &= \frac{1}{\pi} \{1 - (1-b)^2\}^{1/2} && \text{when } 0 \leq b \leq 2 \\ &= 0 && \text{when } |b| > 2 \end{aligned} \right\} \quad (4.50)$$

Then from equation (4.47), (4.48) and (4.50)

$$\begin{aligned} T^{00} &= -\frac{1}{\chi} \int_{-2}^{+2} \frac{f^0(b)}{C+b} db \\ &= -\frac{1}{\chi} \int_{-2}^0 \frac{1}{\pi} \cdot \frac{\{1 - (1+b)^2\}^{1/2}}{C+b} db - \frac{1}{\chi} \int_0^{+2} \frac{1}{\pi} \cdot \frac{\{1 - (1-b)^2\}^{1/2}}{C+b} db \end{aligned} \quad (4.51)$$

Let the first term of equation (4.51) of T^{00} will be as

$$\text{First term of } T^{00} = -\frac{1}{\chi} \int_{-2}^0 \frac{1}{\pi} \cdot \frac{\{1 - (1+b)^2\}^{1/2}}{C+b} db \quad (4.52)$$

Putting $(1+b) = X \Rightarrow db = dX$

$$= -\frac{1}{\chi} \int_{-1}^{+1} \frac{1}{\pi} \cdot \frac{\{1-X^2\}^{1/2}}{C+X-1} dX$$

Now let $C' = C - 1$

$$= -\frac{1}{\chi} \int_{-1}^{+1} \frac{1}{\pi} \cdot \frac{\{1-X^2\}^{1/2}}{C'+X} dX$$

Now substituting $X = \cos \theta \Rightarrow dX = -\sin \theta d\theta$

$$\text{First term of } T^{00} = -\frac{1}{\chi \pi} \int_0^\pi \frac{(1-\cos^2 \theta)^{1/2}}{C'+\cos \theta} \sin \theta d\theta$$

$$= -\frac{1}{\chi \pi} \int_0^\pi \frac{\sin^2 \theta}{C'+\cos \theta} d\theta$$

$$= -\frac{1}{2 \cdot \chi \pi} \int_0^{2\pi} \frac{\sin^2 \theta}{C'+\cos \theta} d\theta \quad \{ \text{Since } f(2\pi - \theta) = f(\theta) \}$$

$$\text{Now put } Z = e^{i\theta} \Rightarrow dZ = iZ d\theta \Rightarrow d\theta = \frac{dZ}{iZ} \quad (4.53)$$

$$= -\frac{1}{2 \cdot \chi \pi} \int_C \frac{\left[\frac{(Z - \frac{1}{Z})}{2i} \right]^2}{\left[C' + \frac{1}{2} \left(Z + \frac{1}{Z} \right) \right]} \cdot \frac{dZ}{iZ}$$

$$= \frac{1}{4 \cdot \chi \pi i} \int_C \frac{\left[\frac{(Z^2 - 1)}{Z^2} \right]^2}{(Z^2 + 2C'Z + 1)} dZ$$

$$= -\frac{i}{4\chi\pi} \oint \frac{(Z^2-1)^2}{Z^2(Z^2+2C'Z+1)} dZ = \oint f(Z) dZ \quad (4.54)$$

where

$$f(Z) = \frac{-i}{4\chi\pi} \cdot \frac{(Z^2-1)^2}{Z^2(Z^2+2C'Z+1)}$$

or

$$f(Z) = \frac{-i}{4\chi\pi} \frac{(Z^2-1)^2}{Z^2(Z-\alpha)(Z-\beta)}$$

The singularities of $f(Z)$ are given by

$$Z^2[Z^2+2C'Z+1]=0$$

$$\text{i.e. } Z^2(Z-\alpha)(Z-\beta)=0 \quad (4.55)$$

This yields

$$Z=0 \text{ (a pole of order 2)}$$

$$Z=\alpha \text{ (a pole of order 1)}$$

$$Z=\beta \text{ (a pole of order 1)}$$

we have

$$\alpha + \beta = -2C'; \alpha\beta = 1 \text{ \& } \alpha - \beta = \pm 2\sqrt{C'^2-1} \quad (4.56)$$

$$\text{therefore, } \alpha = -C' + \sqrt{C'^2-1} \quad ; \quad \beta = -C' - \sqrt{C'^2-1}$$

(i) Residue of $f(Z)$ at $Z=\alpha$ will be as

$$\text{Res } f(Z) = \lim_{Z \rightarrow \alpha} (Z-\alpha)f(Z)$$

$$\begin{aligned}
&= \lim_{Z \rightarrow \alpha} (Z - \alpha) \cdot \frac{-i}{4 \cdot \chi \cdot \pi} \cdot \frac{(Z^2 - 1)^{1/2}}{Z^2 (Z - \alpha)(Z - \beta)} \\
&= \frac{-i}{4 \cdot \chi \cdot \pi} \cdot \frac{(\alpha^2 - 1)^2}{\alpha^2 (\alpha - \beta)} \quad \{\text{Since } \alpha \cdot \beta = 1\} \\
&= \frac{-i}{4 \cdot \chi \cdot \pi} \cdot \frac{(\alpha^2 - 1/\alpha)^2}{(\alpha - \beta)} \\
&= \frac{-i}{4 \cdot \chi \cdot \pi} (\alpha - \beta) = \frac{-i}{4 \cdot \chi \cdot \pi} \cdot 2\sqrt{C^2 - 1} \\
\text{Res}_{Z=\alpha} f(Z) &= \frac{-i}{2 \cdot \chi \cdot \pi} \cdot \sqrt{C^2 - 1} \tag{4.57a}
\end{aligned}$$

Similarly, residue of $f(Z)$ at $Z=\beta$ will be as

$$\text{Res}_{Z=\beta} f(Z) = \frac{+i}{2 \cdot \chi \cdot \pi} \cdot \sqrt{C^2 - 1} \tag{4.57b}$$

(ii) Residue at $Z = 0$

$$\begin{aligned}
\text{Res}_{Z=0} f(Z) &= \lim_{Z \rightarrow 0} \frac{1}{(2-1)!} \cdot \frac{d}{dZ} [(Z-0)^2 f(Z)] \\
&= \lim_{Z \rightarrow 0} \frac{d}{dZ} \left[Z^2 \cdot \frac{-i}{4 \cdot \chi \cdot \pi} \cdot \frac{(Z^2 - 1)^2}{Z^2 (Z^2 + 2C^2 Z + 1)} \right]
\end{aligned}$$

$$= \lim_{Z \rightarrow 0} \frac{-i}{4\chi\pi} \left[\frac{2(Z^2 - 1) \cdot 2Z(Z^2 + 2C'Z + 1) - (Z^2 - 1)^2 \cdot (2Z + 2C')}{(Z^2 + 2C'Z + 1)^2} \right]$$

$$= \frac{-i}{4\chi\pi} \cdot \frac{-2C'}{1} = \frac{iC'}{2\chi\pi}$$

$$\text{Res}_{Z=0} f(Z) = \frac{iC'}{2\chi\pi} \quad (4.58)$$

Hence by Cauchy Residue theorem

$$\oint f(Z) dZ = 2\pi i \cdot [\text{sum of residues inside unit circle}]$$

$$= 2\pi i \left[\frac{i}{2\chi\pi} \sqrt{C'^2 - 1} + \frac{iC'}{2\chi\pi} \right]$$

$$\left. \begin{aligned} \oint f(Z) dZ &= \frac{1}{\chi} \left[-C' - \sqrt{C'^2 - 1} \right] ; & \text{if } \left| -(C-1) + \sqrt{(C-1)^2 - 1} \right| < 1 \\ \text{or} \\ \oint f(Z) dZ &= \frac{1}{\chi} \left[-C' + \sqrt{C'^2 - 1} \right] ; & \text{if } \left| -(C-1) + \sqrt{(C-1)^2 - 1} \right| > 1 \end{aligned} \right\} \quad (4.59)$$

Thus, the first term of T^{00} will be as

$$\begin{aligned} \Rightarrow \frac{-1}{\chi} \int_{-\pi}^0 \frac{\{1 - (1+b)^2\}^{1/2}}{C+b} db &= \frac{1}{\chi} \left[-C' \mp \sqrt{C'^2 - 1} \right] \\ \text{First term of } T^{00} &= \frac{1}{\chi} \left[-(C-1) \mp \sqrt{(C-1)^2 - 1} \right] \end{aligned} \quad (4.60)$$

where \mp sign depend on the conditions of equation (4.59)

Now we take the second term of equation (4.51) of T^{00} will be as

$$\Rightarrow \text{Second term of } T^{00} = -\frac{1}{\chi} \int_0^{+2} \frac{1}{\pi} \cdot \frac{\{1-(1-b)^2\}^{1/2}}{C+b} db$$

putting $(1-b)=X \Rightarrow db = -dX$ and let $C' = C+1$

$$\Rightarrow = -\frac{1}{\chi} \int_{-1}^{+1} \frac{1}{\pi} \cdot \frac{\{1-X^2\}^{1/2}}{C'-X} dX$$

substituting $X = \cos \theta \Rightarrow dX = -\sin \theta \cdot d\theta$

$$= -\frac{1}{\chi \pi} \int_{\pi}^0 \frac{\sin^2 \theta}{C' - \cos \theta} \cdot d\theta = \frac{1}{\chi \pi} \int_0^{\pi} \frac{\sin^2 \theta}{C' - \cos \theta} \cdot d\theta$$

$$= -\frac{1}{2 \cdot \chi \pi} \int_0^{2\pi} \frac{\sin^2 \theta}{C' - \cos \theta} \cdot d\theta \quad (4.61)$$

$$\text{putting } Z = e^{i\theta} \Rightarrow dZ = iZ \cdot d\theta \quad (4.62)$$

$$\Rightarrow = -\frac{1}{2 \cdot \chi \pi} \oint \frac{[(Z - 1/Z)/2i]^2}{[C' - 1/2 \cdot (Z + 1/Z)]} \cdot \frac{dZ}{iZ}$$

$$= -\frac{1}{4 \cdot \chi \pi i} \oint \frac{(Z^2 - 1)^2}{Z^2 (Z^2 - 2C'Z + 1)} \cdot dZ \quad (4.63)$$

Let

$$f(Z) = \frac{i}{4\chi\pi} \cdot \frac{(Z^2 - 1)^2}{Z^2(Z^2 - 2C'Z + 1)}$$

$$= \frac{i}{4\chi\pi} \frac{(Z^2 - 1)^2}{Z^2(Z - \alpha)(Z - \beta)} \quad (4.64)$$

The singularities of $f(Z)$ are given by

$$Z^2[Z^2 - 2C'Z + 1] = 0$$

$$\text{i.e. } Z^2(Z - \alpha)(Z - \beta) = 0$$

we have

$$\alpha + \beta = -2C'; \quad \alpha\beta = 1 \quad \& \quad \alpha - \beta = \pm 2\sqrt{C'^2 - 1}$$

$$\alpha = C' + \sqrt{C'^2 - 1} \quad ; \quad \beta = C' - \sqrt{C'^2 - 1}$$

Only one pole among (α, β) will lie inside the contour of unit circle due to conditions $\alpha\beta = 1$.

Thus the poles lying inside the contour C are

(i) A simple pole at $Z = \alpha$ or at $Z = \beta$

(ii) A double pole at $Z = 0$

(i) Residue of $f(Z)$ at $Z = \alpha$

$$\text{Res}_{Z=\alpha} f(Z) = \lim_{Z \rightarrow \alpha} (Z - \alpha) f(Z)$$

$$= \lim_{Z \rightarrow \alpha} (Z - \alpha) \cdot \frac{i}{4\chi\pi} \cdot \frac{(Z^2 - 1)^2}{Z^2(Z - \alpha)(Z - \beta)}$$

$$= \frac{i}{4.\chi.\pi} \cdot \frac{(\alpha^2 - 1)^2}{\alpha^2(\alpha - \beta)} \quad \{\text{Since } \alpha.\beta = 1\}$$

$$= \frac{i}{4.\chi.\pi} \cdot \frac{(\alpha^2 - 1/\alpha)^2}{(\alpha - \beta)}$$

$$= \frac{i}{4.\chi.\pi} (\alpha - \beta) = \frac{i}{4.\chi.\pi} . 2\sqrt{C'^2 - 1}$$

$$\text{Res}_{Z=a} f(Z) = \frac{i}{2.\chi.\pi} \cdot \sqrt{C'^2 - 1}$$

or,

$$\text{Res}_{Z=a} f(Z) = \frac{i}{2.\chi.\pi} \cdot \sqrt{C'^2 - 1}$$

(4.65)

now,

(ii) Residue at $Z = 0$

$$\text{Res}_{Z=0} f(Z) = \lim_{Z \rightarrow 0} \frac{1}{(2-1)!} \cdot \frac{d}{dZ} [(Z-0)^2 f(Z)]$$

$$= \lim_{Z \rightarrow 0} \frac{d}{dZ} \left[Z^2 \cdot \frac{i}{4.\chi.\pi} \cdot \frac{(Z^2 - 1)^2}{Z^2(Z^2 - 2C'Z + 1)} \right]$$

$$= \lim_{Z \rightarrow 0} \frac{i}{4.\chi.\pi} \left[\frac{2(Z^2 - 1).2Z(Z^2 - 2C'Z + 1) - (Z^2 - 1)^2.(2Z - 2C')}{(Z^2 - 2C'Z + 1)^2} \right]$$

$$= \frac{i}{4.\chi.\pi} \cdot \frac{2C'}{1} = \frac{iC'}{2.\chi.\pi}$$

$$\text{Res}_{Z=0} f(Z) = \frac{iC'}{2\chi\pi} \quad (4.66)$$

hence by Cauchy Residue theorem

$$\begin{aligned} \oint f(Z) dZ &= 2\pi i \cdot [\text{Sum of Residues}] \\ &= 2\pi i \cdot \left[\frac{i}{2\chi\pi} \sqrt{C'^2 - 1} + \frac{iC'}{2\chi\pi} \right] \\ \oint f(Z) dZ &= -\frac{1}{\chi} \left[C' \mp \sqrt{C'^2 - 1} \right] \end{aligned}$$

Second term of $T^{00} =$

$$\left. \begin{aligned} \oint f(Z) dZ &= -\frac{1}{\chi} \left[(C+1) + \sqrt{(C+1)^2 - 1} \right] ; \text{ if } \left| -(C+1) + \sqrt{(C+1)^2 - 1} \right| < 1 \\ \text{or,} \\ \oint f(Z) dZ &= -\frac{1}{\chi} \left[(C+1) - \sqrt{(C+1)^2 - 1} \right] ; \text{ if } \left| -(C+1) + \sqrt{(C+1)^2 - 1} \right| > 1 \end{aligned} \right\} \quad (4.67)$$

Now using equation (4.60) and (4.67), combining first and Second term of T^{00}

$$T^{00} = -\frac{1}{\chi} \left[(C-1) \mp \sqrt{(C-1)^2 - 1} + (C+1) \mp \sqrt{(C+1)^2 - 1} \right] \quad (4.68)$$

If we define new variable g^{DP} such that

$$\Rightarrow T^{00} = -\frac{1}{\chi} \cdot g^{DP} \quad (4.69)$$

$$\text{Then } \Rightarrow g^{DP} = \left[(C-1) \mp \sqrt{(C-1)^2 - 1} + (C+1) \mp \sqrt{(C+1)^2 - 1} \right] \quad (4.70)$$

Notice that the path operator T^{00} is Hergltz and g^{DP} is anti Hergltz.

4.4 DENSITY OF STATES:

The change in density of states for S-phase shift double-peak semi circular model is also calculated by Lloyd's formula¹ as given in equation (4.27), which is recalled:

$$\delta\rho(E) = -\frac{1}{\pi} \text{Im } g \left[\left\langle T^{00} \frac{d}{dE} t_{cp}^{-1} \right\rangle - \frac{1}{N} \sum_{\bar{q}} \frac{1}{(t_{cp}^{-1} - B_{\bar{q}})} \frac{d}{dE} (B_{\bar{q}}) \right] \quad (4.71)$$

In above equation let the first term

$$\left\langle T^{00} \frac{d}{dE} t_{cp}^{-1} \right\rangle = T^{00} U^{eff} \quad (4.72)$$

where

$$U^{eff} = \chi \left[\frac{X}{\Gamma_A} + \frac{Y}{\Gamma_B} \right] + \frac{(i-C)}{2\chi} + \frac{(C-\bar{C})}{(C_A-C_B)} \cdot \chi \left[\frac{1}{\Gamma_A} - \frac{1}{\Gamma_B} \right] \quad (4.73)$$

and T^{00} for double peak semicircular model is given by equation (4.68) as

$$= -\frac{1}{\chi} \left[(C-1) \mp \sqrt{(C-1)^2 - 1} + (C+1) \mp \sqrt{(C+1)^2 - 1} \right] \quad (4.74)$$

The change in density of states in equation (4.71) can be written in two parts as

$$\delta\rho(E) = -\frac{1}{\pi} \text{Im } g [\text{First part} + \text{Second part}] \quad (4.75)$$

where,

$$\begin{aligned} \text{First part} = & \left[-\frac{1}{\chi} \left\{ (C-1) \mp \sqrt{(C-1)^2 - 1} + (C+1) \mp \sqrt{(C+1)^2 - 1} \right\} \right. \\ & \left. * \left\{ \chi \left(\frac{X}{\Gamma_A} + \frac{Y}{\Gamma_B} \right) + \frac{(i-C)}{2\chi} + \frac{(C-\bar{C})}{(C_A - C_B)} \cdot \chi \left(\frac{1}{\Gamma_A} - \frac{1}{\Gamma_B} \right) \right\} \right] \end{aligned} \quad (4.76)$$

The second part of equation (4.71) on R.H.S.

$$\begin{aligned} \text{Second part} &= -\frac{1}{N} \sum_{\bar{q}} \frac{1}{(t_{cp}^{-1} - B_{\bar{q}})} \cdot \frac{d}{dE}(B_{\bar{q}}) \\ &= -\frac{1}{N} \sum_{\bar{q}} \frac{1}{(-\chi.C + i.\chi - B_{\bar{q}})} \cdot \frac{d}{dE}(B_{\bar{q}}) \\ &= \frac{1}{N} \sum_{\bar{q}} \frac{1}{(\chi.C - i.\chi + B_{\bar{q}})} \cdot \frac{d}{dE}(B_{\bar{q}}) \\ &= \frac{1}{N} \sum_{\bar{q}} f(B_{\bar{q}}) \end{aligned} \quad (4.77)$$

where,

$$f(B_{\bar{q}}) = \frac{1}{\chi.C - i.\chi + B_{\bar{q}}} \cdot \frac{d}{dE}(B_{\bar{q}}) \quad (4.78)$$

With the help of equation (4.2) we can calculate the energy derivative of $B_{\bar{q}}$ as

$$\frac{d}{dE}(B_{\bar{q}}) = \frac{B_{\bar{q}} + i}{2.\chi}$$

By using above equation we can write

$$f(B_{\bar{q}}) = \frac{(B_{\bar{k}} + i)}{2.\chi^2(C + B_{\bar{k}})} \quad (4.79)$$

Now, by using equation (4.77)

$$\begin{aligned} \text{Second part} &= \frac{1}{N} \sum_{\bar{q}} f(B_{\bar{q}}) \\ &= \frac{1}{N} \sum_{\bar{k}} \frac{1}{2.\chi^2} \cdot \frac{(B_{\bar{k}} + i)}{(C + B_{\bar{k}})} \\ &= \frac{1}{N} \sum_{\bar{k}} \frac{1}{2.\chi^2} \cdot \frac{B_{\bar{k}}}{(C + B_{\bar{k}})} + \frac{1}{N} \sum_{\bar{k}} \frac{1}{2.\chi^2} \cdot \frac{i}{(C + B_{\bar{k}})} \\ &= \frac{1}{N} \sum_{\bar{k}} \int_{-\infty}^{+\infty} \frac{b.\delta(b - B_{\bar{k}}).db}{2.\chi^2(C + b)} + \frac{i}{N} \sum_{\bar{k}} \int_{-\infty}^{+\infty} \frac{\delta(b - B_{\bar{k}}).db}{2.\chi^2(C + b)} \\ &= \frac{1}{2.\chi^2} \int_{-\infty}^{+\infty} \frac{f^0(b)b.db}{(C + b)} + \frac{i}{2.\chi^2} \int_{-\infty}^{+\infty} \frac{f^0(b).db}{(C + b)} \end{aligned} \quad (4.80a)$$

We can write second part as:

$$\text{Second part} = \frac{1}{2.\chi^2} \cdot [\text{First integral (I}_1\text{)}] + \frac{1}{2.\chi^2} \cdot i \cdot [\text{Second integral (I}_2\text{)}] \quad (4.80b)$$

$$\text{where, first integral (I}_1\text{)} = \int_{-\infty}^{+\infty} \frac{f^0(b)b.db}{(C + b)}$$

We choose the value of $f^0(b)$ from equation (4.50) then first integral will be

$$\int_{-2}^{+2} \frac{f^0(b)}{C + b} \cdot b.db = \frac{1}{\pi} \int_{-2}^0 \frac{\{1 - (1+b)^2\}^{1/2}}{C + b} \cdot b.db + \frac{1}{\pi} \int_0^{+2} \frac{\{1 - (1-b)^2\}^{1/2}}{C + b} \cdot b.db \quad (4.81)$$

Let the first term of above equation (4.81)

$$\text{First term of } I_1 = \frac{1}{\pi} \int_{-2}^0 \frac{\{1 - (1+b)^2\}^{1/2}}{C+b} \cdot b \cdot db$$

putting $(1+b) = X \Rightarrow db = dX$

$$= \frac{1}{\pi} \int_{-1}^{+1} \frac{\{1 - X^2\}^{1/2} \{X - 1\}}{C + X - 1} dX$$

$$= \frac{1}{\pi} \int_{-1}^{+1} \frac{\{1 - X^2\}^{1/2} X}{C + X - 1} dX - \frac{1}{\pi} \int_{-1}^{+1} \frac{\{1 - X^2\}^{1/2}}{C + X - 1} dX$$

now let $C' = C - 1$

$$= \frac{1}{\pi} \int_{-1}^{+1} \frac{\{1 - X^2\}^{1/2} X}{C' + X} dX - \frac{1}{\pi} \int_{-1}^{+1} \frac{\{1 - X^2\}^{1/2}}{C' + X} dX$$

using equation (4.60)

$$\text{First term of } I_1 = \frac{1}{\pi} \int_{-1}^{+1} \frac{\{1 - X^2\}^{1/2} X}{C' + X} dX - \left[(C-1) \mp \sqrt{(C-1)^2 - 1} \right] \quad (4.82)$$

Now taking the first part of first term of I_1 on R.H.S. of equation (4.82).

$$\text{First part of first term of } I_1 = \frac{1}{\pi} \int_{-1}^{+1} \frac{\{1 - X^2\}^{1/2} X}{C' + X} dX$$

Now substituting $X = \cos \theta \Rightarrow dX = -\sin \theta . d\theta$

$$= \frac{1}{\pi} \int_0^{\pi} \frac{(1 - \cos^2 \theta)^{1/2} . \cos \theta}{C' + \cos \theta} \sin \theta . d\theta$$

$$= \frac{1}{\pi} \int_0^{\pi} \frac{\sin^2 \theta . \cos \theta}{C' + \cos \theta} . d\theta$$

$$= \frac{1}{2\pi} \int_0^{2\pi} \frac{\sin^2 \theta . \cos \theta}{C' + \cos \theta} . d\theta \quad \{ \text{Since } f(2\pi - \theta) = f(\theta) \}$$

$$\text{Now putting } Z = e^{i\theta} \Rightarrow dZ = iZ . d\theta \Rightarrow d\theta = \frac{dZ}{iZ}$$

$$= \frac{1}{2\pi} \int_C \frac{\left[\frac{(Z - \frac{1}{Z})}{2i} \right]^2 \left[\frac{(Z + \frac{1}{Z})}{2} \right]}{\left[C' + \frac{1}{2} \left(Z + \frac{1}{Z} \right) \right]} . \frac{dZ}{iZ}$$

$$= \frac{i}{8\pi} \oint \frac{(Z^2 - 1)^2 . (Z^2 + 1)}{Z^3 (Z^2 + 2C'Z + 1)} . dZ = \frac{i}{8\pi} \oint f(Z) dZ \quad (4.83)$$

where,

$$f(Z) = \frac{(Z^2 - 1)^2 . (Z^2 + 1)}{Z^3 (Z^2 + 2C'Z + 1)} \quad (4.84)$$

$$= \frac{(Z^2 - 1)^2 . (Z^2 + 1)}{Z^3 (Z - \alpha)(Z - \beta)}$$

The poles of integrands are $Z = 0$ of order 3, other two poles are $Z = \alpha$ and $Z = \beta$, which are the roots of $Z^2 + 2C'Z + 1$.

(a) Residue at $Z = 0$

$$\text{Res}_{Z=0} f(Z) = \lim_{Z \rightarrow 0} \frac{1}{(3-1)!} \cdot \frac{d^2}{dZ^2} [(Z-0)^3 f(Z)]$$

$$= \lim_{Z \rightarrow 0} \frac{1}{2!} \cdot \frac{d^2}{dZ^2} \left[Z^3 \cdot \frac{(Z^2 - 1)^2 \cdot (Z^2 + 1)}{Z^3 (Z^2 + 2C'Z + 1)} \right]$$

on solving we get

$$\text{Res}_{Z=0} f(Z) = 4C'^2 - 2 \quad (4.85)$$

(b) Residue at $Z = \alpha$

$$\text{Res}_{Z=\alpha} f(Z) = \lim_{Z \rightarrow \alpha} (Z - \alpha) f(Z)$$

$$= \lim_{Z \rightarrow \alpha} (Z - \alpha) \cdot \frac{(Z^2 - 1)^2 \cdot (Z^2 + 1)}{Z^3 (Z - \alpha)(Z - \beta)}$$

$$= \lim_{Z \rightarrow \alpha} \frac{(Z^2 - 1)^2 \cdot (Z^2 + 1)}{Z^3 (Z^2 - Z\beta)}$$

$$= \frac{(\alpha^2 - 1)^2 \cdot (\alpha^2 + 1)}{\alpha^3 (\alpha^2 - \alpha\beta)}$$

{Since $\alpha\beta = 1$ }

$$\begin{aligned}
&= \frac{(\alpha^2 - 1)^2 \cdot (\alpha^2 + 1)}{\alpha^2 (\alpha^2 - 1)} \\
&= \frac{(\alpha^2 - 1) \cdot (\alpha^2 + 1)}{\alpha^2} = (\alpha - 1/\alpha)^2 \cdot (\alpha + 1/\alpha) \\
&= (\alpha - \beta) \cdot (\alpha + \beta) \tag{4.86}
\end{aligned}$$

Using equation (4.56)

$$\left. \begin{aligned}
\text{Res}_{Z=\alpha} f(Z) &= \left(-2\sqrt{C'^2 - 1} \right) (-2C') = 4C' \sqrt{C'^2 - 1} \\
\text{or,} \\
\text{Res}_{Z=\beta} f(Z) &= -4C' \sqrt{C'^2 - 1}
\end{aligned} \right\} \tag{4.87}$$

Using Cauchy Residue theorem

First part of first term of $I_1 = \oint f(Z) dZ = 2\pi i \cdot [\text{sum of residues}]$

$$= 2\pi i \left[4C'^2 - 2 \mp 4C' \sqrt{C'^2 - 1} \right] = 4\pi i \left[2C'^2 - 1 \mp 2C' \sqrt{C'^2 - 1} \right] \tag{4.88}$$

From equation (4.82), (4.83) and (4.88) we have

$$\begin{aligned}
\text{First part of first term of } I_1 &= \frac{1}{\pi} \int_{-1}^{+1} \frac{(1 - X^2)^{1/2} \cdot X}{C' + X} \cdot dX = \frac{i}{8\pi} \cdot 4\pi i \left[2C'^2 - 1 \mp 2C' \sqrt{C'^2 - 1} \right] \\
\text{or,} \\
\frac{1}{\pi} \int_{-1}^{+1} \frac{(1 - X^2)^{1/2} \cdot X}{C' + X} \cdot dX &= -\frac{1}{2} \left[2(C - 1)^2 - 1 \mp 2(C - 1) \sqrt{(C - 1)^2 - 1} \right] \\
&\tag{4.89}
\end{aligned}$$

Therefore, the first part of first integral (I_1), of equation (4.81)

$$\frac{1}{\pi} \int_{-2}^0 \frac{(1-(1+b)^2)^{1/2}}{C+b} \cdot b \cdot db = -\frac{1}{2} \left[2(C-1)^2 - 1 \mp 2(C-1) \sqrt{(C-1)^2 - 1} \right] - \left[(C-1) \mp \sqrt{(C-1)^2 - 1} \right] \quad (4.90)$$

Now, second part of first integral (I_1), of equation (4.81).

$$\text{Second part of } I_1 = \frac{1}{\pi} \int_0^2 \frac{\{1-(1-b)^2\}^{1/2}}{C+b} \cdot b \cdot db$$

$$\text{putting } 1-b = -X \Rightarrow db = dX$$

$$= \frac{1}{\pi} \int_{-1}^{+1} \frac{\{1-X^2\}^{1/2}}{C+1+X} \cdot (1+X) \cdot dX$$

$$= \frac{1}{\pi} \int_{-1}^{+1} \frac{\{1-X^2\}^{1/2}}{C+1+X} \cdot X \cdot dX + \frac{1}{\pi} \int_{-1}^{+1} \frac{\{1-X^2\}^{1/2}}{C+1+X} dX$$

using equation (4.67)

$$\text{Second part of } I_1 = \frac{1}{\pi} \int_{-1}^{+1} \frac{\{1-X^2\}^{1/2}}{(C+1)+X} \cdot X \cdot dX + \left\{ (C+1) \mp \sqrt{(C+1)^2 - 1} \right\} \quad (4.91)$$

Now using equation (4.89), second part of first integral (I_1).

$$\frac{1}{\pi} \int_0^{+2} \frac{\{1 - (1-b)^2\}^{1/2}}{C+b} .b.db = -\frac{1}{2} \left[2(C+1)^2 - 1 \mp 2(C+1)\sqrt{(C+1)^2 - 1} \right] + \left\{ (C+1) \mp \sqrt{(C+1)^2 - 1} \right\} \quad (4.92)$$

Using equation (4.90) & (4.92), the first integral of equation (4.80) will be as

$$I_1 = \int_{-2}^{+2} \frac{f^0(b)}{C+b} .b.db = -\frac{1}{2} \left[2(C+1)^2 - 1 \mp 2(C+1)\sqrt{(C+1)^2 - 1} \right] + \left\{ (C+1) \mp \sqrt{(C+1)^2 - 1} \right\} \\ - \frac{1}{2} \left[2(C-1)^2 - 1 \mp 2(C-1)\sqrt{(C-1)^2 - 1} \right] - \left\{ (C-1) \mp \sqrt{(C-1)^2 - 1} \right\}$$

After simplification we have,

$$\int_{-2}^{+2} \frac{f^0(b)}{C+b} .b.db = 1 - 2C^2 - C \left[\sqrt{(C+1)^2 - 1} \right] - C \left[\sqrt{(C-1)^2 - 1} \right] \quad (4.93)$$

The second integral (I_2) is already solved in equation (4.51) and given in equation (4.69) and (4.70) as:

$$I_2 = \left[(C-1) \mp \sqrt{(C-1)^2 - 1} \right] + (C+1) \mp \sqrt{(C+1)^2 - 1}$$

Therefore, after combining I_1 and I_2 in equation (4.80b) we get

$$\text{The second part of equation (4.71)} = \frac{1}{2.\chi^2} \int \frac{f^0(b)}{C+b} .b.db + \frac{i}{2.\chi^2} \int \frac{f^0(b)}{C+b} .db \\ = -\frac{1}{2.\chi^2} \left[2C^2 - 1 + C \left\{ \sqrt{(C+1)^2 - 1} \right\} + C \left\{ \sqrt{(C-1)^2 - 1} \right\} \right] \\ + \frac{i}{2.\chi^2} \left[(C-1) + \sqrt{(C-1)^2 - 1} \right] + (C+1) + \sqrt{(C+1)^2 - 1} \quad (4.94)$$

Therefore, the change in density of states from equation (4.71) after substituting the First part and Second part from equation (4.76) and (4.94) respectively.

$$\delta\rho(E) = -\frac{1}{\pi} \text{Im } g \left[\left\{ -\frac{1}{\chi} \left((C-1) + \sqrt{(C-1)^2 - 1} + (C+1) + \sqrt{(C+1)^2 - 1} \right) \right\} * \left\{ \chi \left(\frac{X}{\Gamma_A} + \frac{Y}{\Gamma_B} \right) + \left(\frac{i-C}{2\chi} \right) + \left(\frac{C-\bar{C}}{C_A - C_B} \right) \cdot \chi \left(\frac{1}{\Gamma_A} - \frac{1}{\Gamma_B} \right) \right\} - \frac{1}{2\chi^2} \left\{ 2C^2 - 1 + C\sqrt{(C+1)^2 - 1} + C\sqrt{(C-1)^2 - 1} \right\} + \frac{i}{2\chi^2} \left\{ (C-1) + \sqrt{(C-1)^2 - 1} + (C+1) + \sqrt{(C+1)^2 - 1} \right\} \right]$$

We have defined $g^{DP} = \left((C-1) + \sqrt{(C-1)^2 - 1} + (C+1) + \sqrt{(C+1)^2 - 1} \right)$ in equation (4.70), therefore,

$$\begin{aligned} \delta\rho(E) = & -\frac{1}{\pi} \text{Im } g \left[\left\{ -\frac{1}{\chi} (g^{DP}) \right\} * \left\{ \chi \left(\frac{X}{\Gamma_A} + \frac{Y}{\Gamma_B} \right) - \frac{1}{\chi} (g^{DP}) \cdot \left(\frac{i}{2\chi} \right) + \left(\frac{C}{2\chi^2} \right) \cdot (g^{DP}) \right. \right. \\ & - \frac{1}{\chi} (g^{DP}) \cdot \left(\frac{C-\bar{C}}{C_A - C_B} \right) \cdot \chi \left(\frac{1}{\Gamma_A} - \frac{1}{\Gamma_B} \right) \left. \right\} - \frac{1}{2E} 2C^2 + \frac{1}{2E} - \frac{C}{2E} \sqrt{(C+1)^2 - 1} \\ & - \frac{C}{2E} \sqrt{(C-1)^2 - 1} + \frac{i}{2\chi^2} (g^{DP}) \quad ; \quad \{ \text{Since } \chi^2 = E \} \end{aligned}$$

On solving above equation after neglecting the real part (1/2E), we get the change in density of states for double peak semicircular model as

$$\delta\rho(E) = \frac{1}{\pi} \text{Im } g \left[g^{DP} \left\{ \left(\frac{X}{\Gamma_A} + \frac{Y}{\Gamma_B} \right) + \left(\frac{C-\bar{C}}{C_A - C_B} \right) \left(\frac{1}{\Gamma_A} - \frac{1}{\Gamma_B} \right) \right\} \right] \quad (4.95)$$

4.5 THE CPA EQUATION AND COMPUTATIONAL DETAILS:

From equation (2.23) for S-phase shift double peak semicircular model

$$t_c^{-1} = [X.t_A^{-1} + Y.t_B^{-1} + (t_c^{-1} - t_A^{-1})T^{00}(t_c^{-1} - t_B^{-1})]$$

where,

$$\left. \begin{aligned} t_c^{-1} &= -\chi.C + i.\chi \\ t_A^{-1} &= -\chi.C_A + i.\chi \\ t_B^{-1} &= -\chi.C_B + i.\chi \end{aligned} \right\} \quad (4.96)$$

$$\Rightarrow -\chi.C + i.\chi = -\chi[X.C_A - i.X + Y.C_B - i.Y] + [-\chi.C + i.\chi + \chi.C_A - i.\chi] * T^{00} * [-\chi.C + i.\chi + \chi.C_B - i.\chi]$$

$$\Rightarrow -\chi.C + i.\chi = -\chi[X.C_A + Y.C_B - i.(X + Y)] + \chi^2 [C - C_A] * T^{00} * [C - C_B]$$

$$\Rightarrow -C + i = -[X.C_A + Y.C_B - i] + \chi [C - C_A] * T^{00} * [C - C_B]$$

since $X+Y=1$

$$\Rightarrow -C = -[X.C_A + Y.C_B] + \chi [C - C_A] * T^{00} * [C - C_B]$$

$$\Rightarrow C = [X.C_A + Y.C_B] - \chi [C - C_A] * T^{00} * [C - C_B] \quad (4.97)$$

Using equation (4.69) we have $T^{00} = -\frac{1}{\chi}.g^{DP}$

Then the CPA equation for this model will be as

$$\Rightarrow C = [X.C_A + Y.C_B] + [C - C_A] * g^{DP} * [C - C_B] \quad (4.98)$$

where,

$$g^{DP} = \left[(C-1) \mp \sqrt{(C-1)^2 - 1} + (C+1) \mp \sqrt{(C+1)^2 - 1} \right]$$

here \mp sign depends on the conditions.

Therefore, the change in density of states by Lloyds formula will be as

$$\delta\rho(E) = \frac{1}{\pi} \text{Im} g \left\{ \left[(C-1) \mp \sqrt{(C-1)^2 - 1} + (C+1) \mp \sqrt{(C+1)^2 - 1} \right] * \right. \\ \left. \left[\left(\frac{X}{\Gamma_A} + \frac{Y}{\Gamma_B} \right) + \left(\frac{(C-\bar{C})}{(C_A - C_B)} \right) \left(\frac{1}{\Gamma_A} - \frac{1}{\Gamma_B} \right) \right] \right\} \quad (4.99)$$

Now for programming we prepare the algorithm first,

STEP 1: We declare the cotangent of phase shift for A and B type of atoms (i.e. C_A & C_B respectively), energy (E), resonance half width for A and B type of atom (i.e. Γ_A and Γ_B respectively), band centres of A and B (i.e. E_A & E_B) and change in density of states (δ DOS).

STEP 2: Input concentration of A (i.e. X), energy (E), resonance half width (i.e. Γ_A and Γ_B) and band centres (i.e. E_A & E_B).

STEP 3: Calculate C_A , C_B and \bar{C} from following formulas

$$C_A = \frac{(E_A - E)}{\Gamma_A}$$

$$C_B = \frac{(E_B - E)}{\Gamma_B}$$

$$\bar{C} = X.C_A + Y.C_B$$

STEP 4: Start the CPA loop.

STEP 5: Calculate g^{DP} .

STEP 6: Calculate $[(C - \bar{C}) - [C - C_A] * g^{DP} * [C - C_B]]$ (i.e. FCO) and its first derivative (i.e. FDCO).

STEP 7: Calculate effective (C) by Newton-Raphson's method.

$$C_{eff} = C - \frac{FCO}{FDCO}$$

STEP 8: Repeat the step 3 to 7 till convergence; then calculate the change in density of states (i.e. δDOS) and store energy (E) Vs change in DOS (δDOS).

STEP 9: Increase the energy and repeat step 2 to step 8 for same concentration, band centres and resonance half width but for different energies.

C Programme to calculate the DOS

COMPLEX CEFF,CA,CB,CBAR,C,FC0,FDC0,G00,EXPR1,EXPR2

COMPLEX G001,G002,A1,A2,B1,B2

OPEN (UNIT=30,FILE='OUT1.CDR')

CEFF=CMPLX(0.0,0.0)

X=0.8

Y=1.0-X

E=-4.03+CMPLX(0.0,0.00)

NE=0

SUM=0.0

DE=0.03

50 E=E+DE

NE=NE+1

EA=-2.0

EB=2.0

GA=1.0

GB=2.0

CA=(EA-E)/GA

CB=(EB-E)/GB

CBAR=X*CA+Y*CB

C=CBAR+CMPLX(0.0,0.0000000001)

IF (DOS .GE. 0.00000001) C=CEFF

DO 100 I=1,1000

A1=C-1.0

B1=CSQRT(C*C-2.0*C)

A2=C+1.0

B2=CSQRT(C*C+2.0*C)

```

IF (CABS(-(C-1.0)+CSQRT(C*C-2.0*C)) .GT. 1.0) G001=A1+B1
IF (CABS(-(C-1.0)+CSQRT(C*C-2.0*C)) .LT. 1.0) B1=-B1
IF (CABS(-(C+1.0)+CSQRT(C*C+2.0*C)) .GT. 1.0) G002=A2-B2
IF (CABS(-(C+1.0)+CSQRT(C*C+2.0*C)) .LT. 1.0) B2=-B2
G001=A1+B1
G002=A2+B2
G00=G001+G002
FC0=C-CBAR-((C-CA)*(C-CB)*G00)
FDC0=1.0+(CA+CB-2.0*C)*G00
1+(C*(CA+CB))*(2.0+(A1/B1)+(A2/B2))
1-(C*C)*(2.0+(A1/B1)+(A2/B2))
1-(CA*CB)*(2.0+(A1/B1)+(A2/B2))
CEFF=C-(FC0/FDC0)
IF (CABS(CEFF-C) .LT. 0.0001) GO TO 101
C=CEFF
100 CONTINUE
101 EXPR1=(X/GA)+(Y/GB)+((C-CBAR)/(CA-CB))*((GB-GA)/(GA*GB))
EXPR2=EXPR1*G00
DOS=AIMAG(EXPR2)/3.14159
DOS=ABS(DOS)
SUM=SUM+DOS*DE
WRITE (30,*) 'E,DOS,I,SUM', E,DOS,I,SUM
IF (REAL(E) .LT. 6.0) GO TO 50
STOP
END

```

4.6 RESULTS AND DISCUSSION:

We have calculated the change in density of states (δDOS) with respect to free electron density of states for $A_X B_Y$ alloys of resonance half widths $\Gamma_A = 1, \Gamma_B = 1$ and 2 , band centers at $E_A = -2$ and $E_B = 2$ for different concentrations.

Figure 4.1 shows the change in DOS of pure B constituent (i.e. $X=0.0$ concentration) for unit half width $\Gamma_B = 1$ and band centre $E_B = 2$. We see that double peaks are forming according to the model at the position of $E_B \pm \Gamma_B$. Similarly Figure 4.9 shows the change in DOS of pure A (i.e. $X=1$ concentration) for unit half width $\Gamma_A = 1$ and band centre $E_A = -2$. Again we see that double peaks are forming according to the model.

Figure 4.2 shows the change in DOS of alloy for constituent metals band centres $E_A = -2$ and $E_B = 2$, resonance half width $\Gamma_A = \Gamma_B = 1$ and low concentration $X=0.1$. The double peaks in δDOS are observed around 1 and 3 , which are at the combinations of band centre and half width of B i.e. $(E_B \pm \Gamma_B)$. Thus these peaks are arising due to majority of B types of atoms in alloy. One single small peak is observed near $E_A = -2$, which is near the band centre of A. This peak is arising due to energy levels of low concentrations of A types of atoms in alloy. Thus we found that all structures in δDOS are arising near band centre and combination of band centres and half widths of constituent metals.

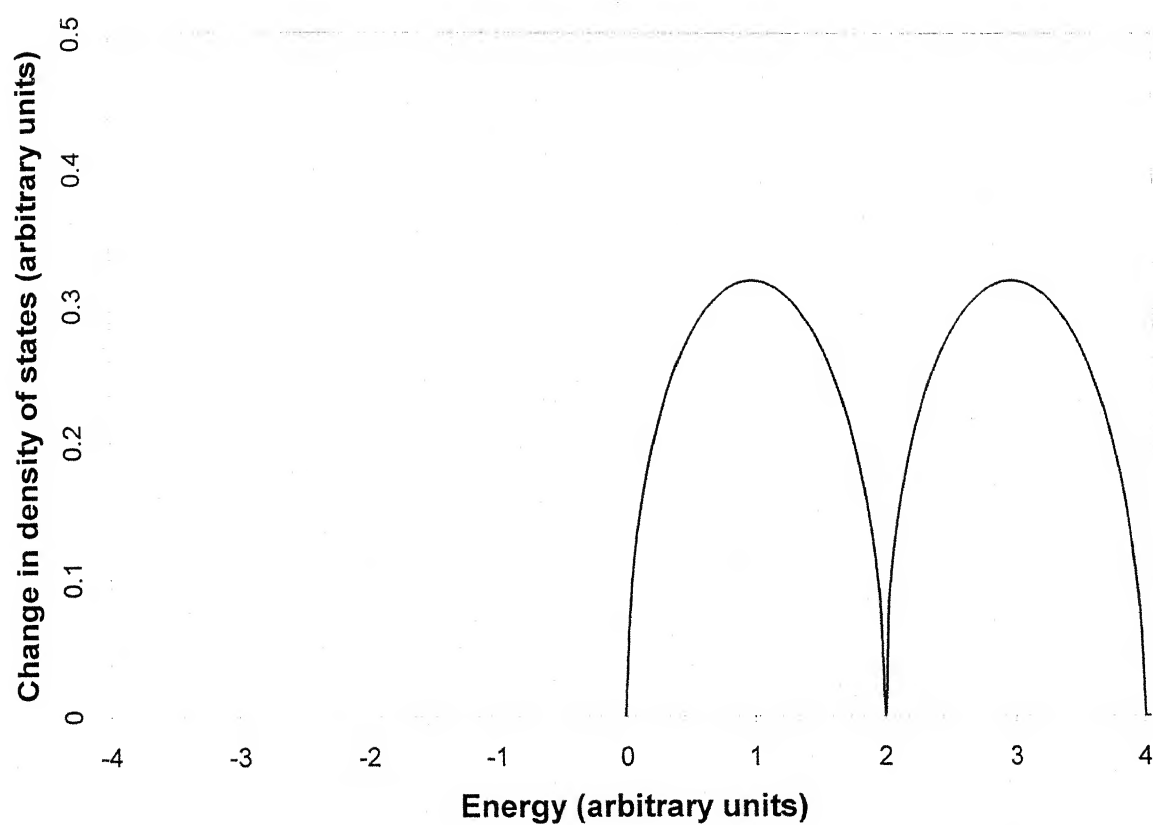


Figure 4.1, Change in density of state for $\Gamma_A=1.0, \Gamma_B=1.0, E_A=-2.0$ and $E_B=2.0$ for concentration $X=0.0$

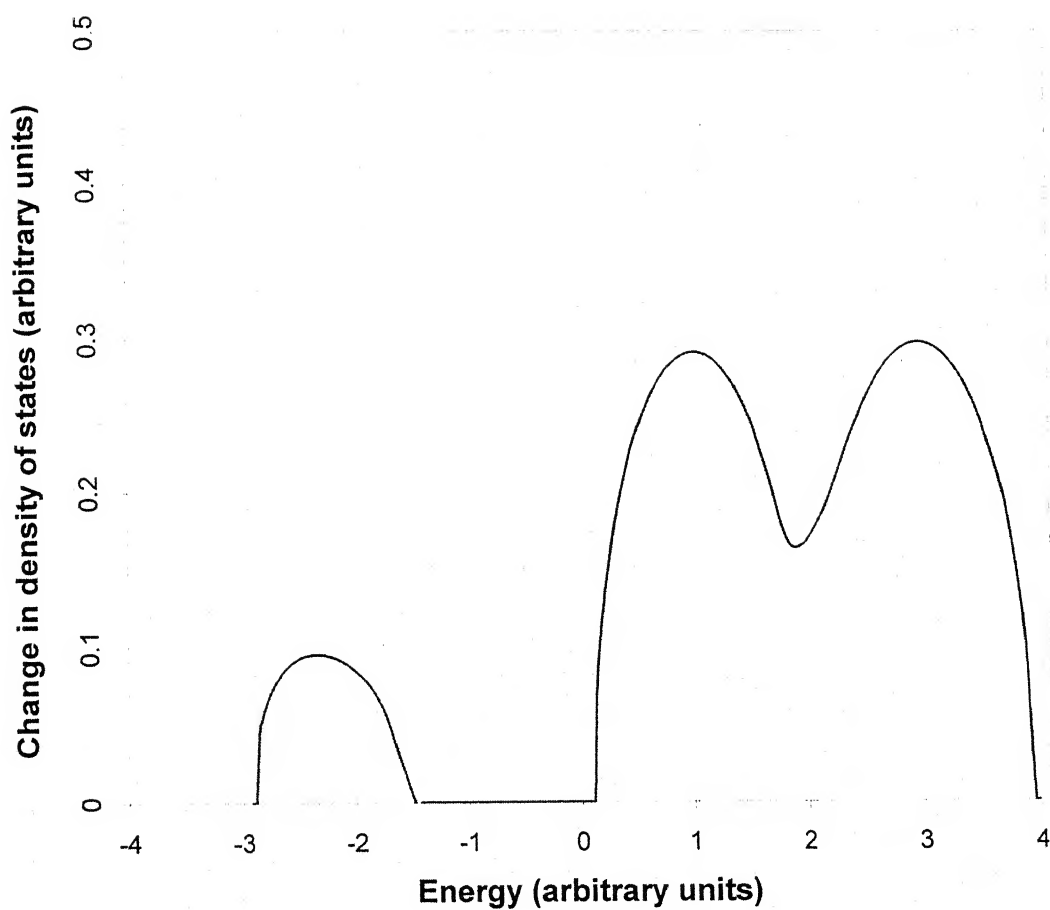


Figure 4.2, Change in density of states for $\Gamma_A=1.0, \Gamma_B=1.0, E_A=-2.0$ and $E_B=2.0$ for concentration $X=0.1$

Figure 4.3 shows change in DOS for same band centres and same resonance half width as in figure 4.2 but different concentration $X=0.2$. We see that bigger peaks (double peaks) are near $E=1$ and 3 , which are combination of band centres and half width of B. Thus these are arising due to majority of B types of atoms in the alloy. One single little flat small peak is around $E= -2$, which arises due to energy levels of minor (20%) concentration of atoms in alloy. Again we found that all structures in δDOS are arising near band centres and combination of band centres and half width of constituent metals.

Figure 4.4 shows change in DOS for same band centres and same resonance half width as in figure 4.2 but different concentration $X=0.3$. We see that major band shows double peaks behavior at $E=1$ and 3 , due to 70% majority of B types of atoms in alloy. For this concentration, single peak shows more flattening nature due to 30% concentration of A type of atoms in alloy and indicate that it will change in double peak after more increase in concentration.

Figure 4.5 shows change in DOS for same band centres and same resonance half width as in figure 4.2 but concentration $X=0.35$. We see that majority band show double peak behavior at $E=1$ and 3 , due to 65% majority concentration of B types of atoms in the alloy. Minority band shows two shoulders near $E= -3$ and -1 , which are combinations of band centres and resonance half width of A type of atoms (i.e. $E_A \pm \Gamma_A$), thus we found that all

structures in δDOS are near combination of band centres and resonance half width.

Figure 4.6 shows change in DOS for same band centres and same resonance half width as in figure 4.2 but $X=0.4$. Now we see that both (majority and minority) band shows double peak behavior. The structures in minority band are near $E = -3$ and -1 , which are combination of band centres and resonance half width of A metal ($E_A \pm \Gamma_A$). Similarly the structures in majority band are near combination of band centres and resonance half width of B metal. Thus we can say that structures of double peak behavior in minority band is clear for more than $X=0.35$ (or 35% of A type of atoms in alloy).

Figure 4.7 shows change in DOS for same band centres and same resonance half width as in figure 4.2 but for high concentrations $X=0.5$ ($Y=0.5$). In first band, we see that the double peak at energies $E = -3$ and -1 , which are combination of band centres and resonance half width of A type metal ($E_A \pm \Gamma_A$). Similarly in second band we see that the structures at $E=1$ and 3 , which are combination ($E_B \pm \Gamma_B$). Thus, we found that all structures in δDOS are arising near combination of band centres and resonance half width of constituent metals.

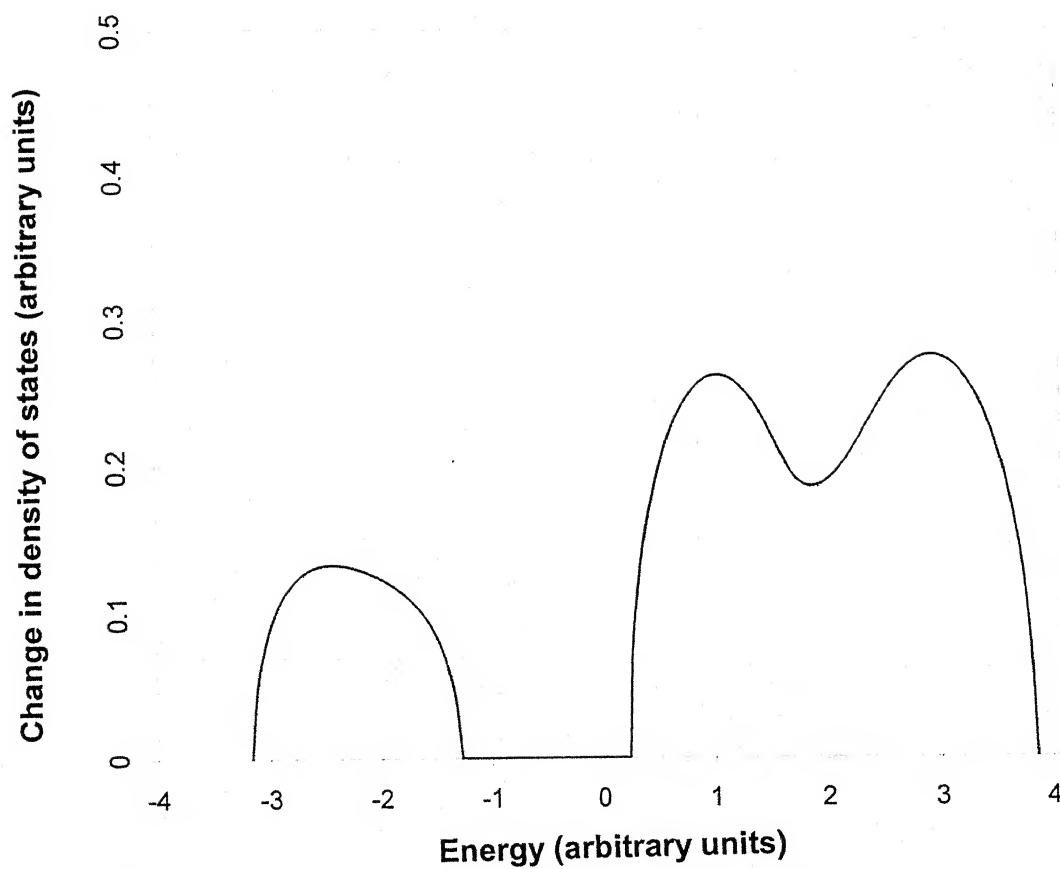


Figure 4.3, Change in density of states for $\Gamma_A=1.0, \Gamma_B=1.0, E_A=-2.0$ and $E_B=2.0$ for concentration $X=0.20$

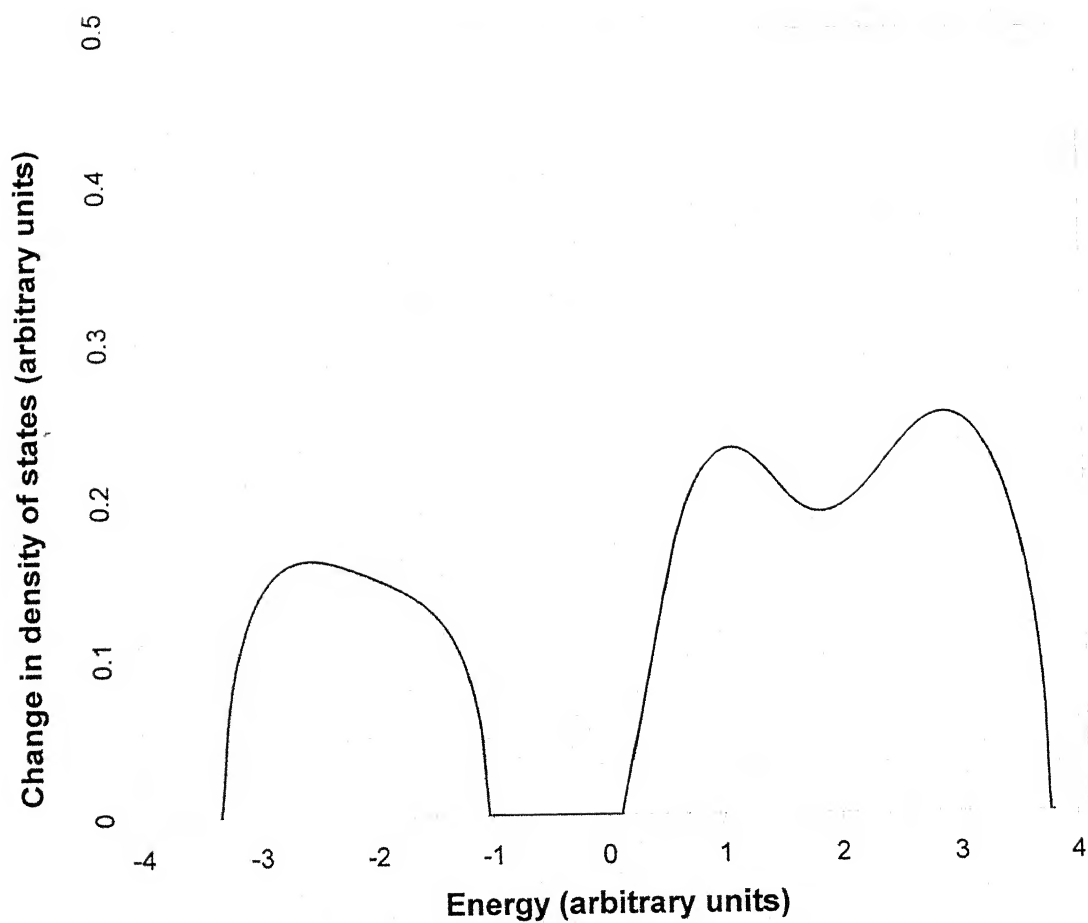


Figure 4.4, Change in density of states for $\Gamma_A=1.0, \Gamma_B=1.0, E_A=-2.0$ and $E_B=2.0$ for concentration $X=0.30$

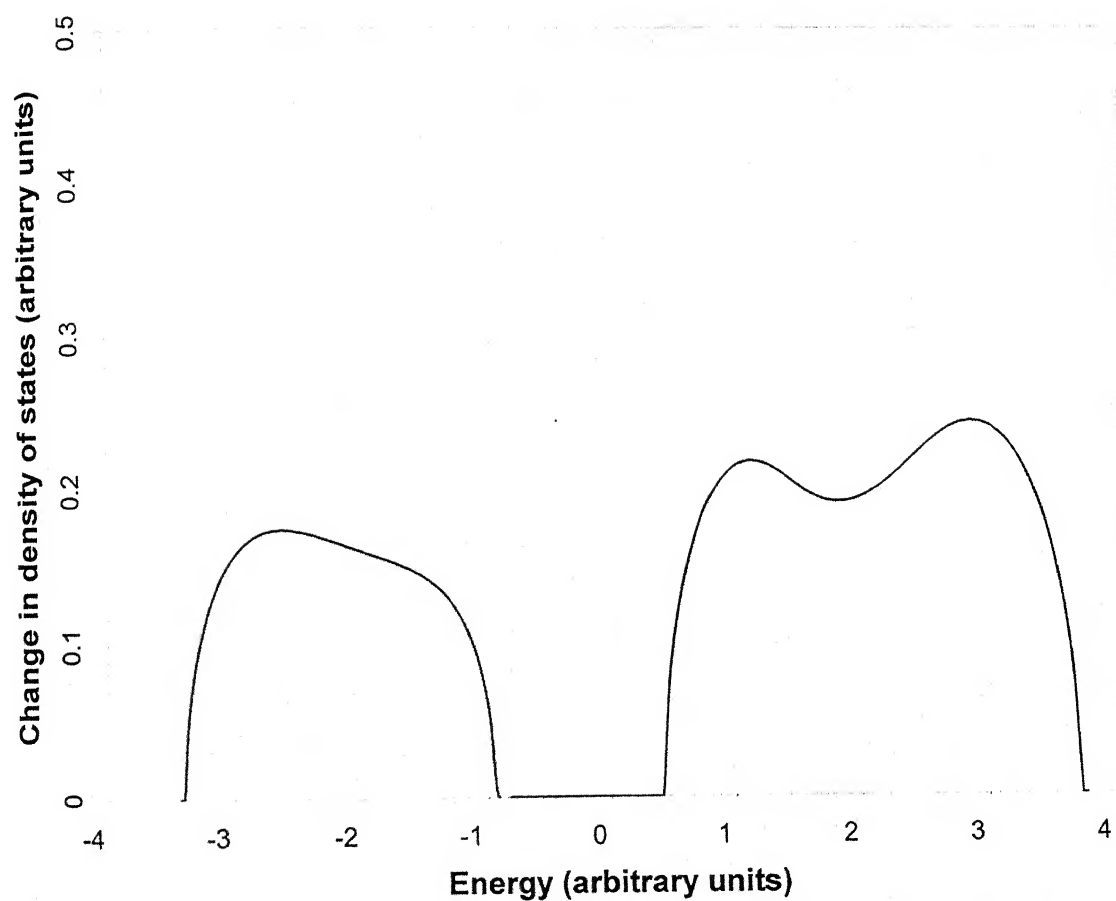


Figure 4.5, Change in density of states for $\Gamma_A=1.0, \Gamma_B=1.0, E_A=-2.0$ and $E_B=2.0$ for concentration $X=0.35$

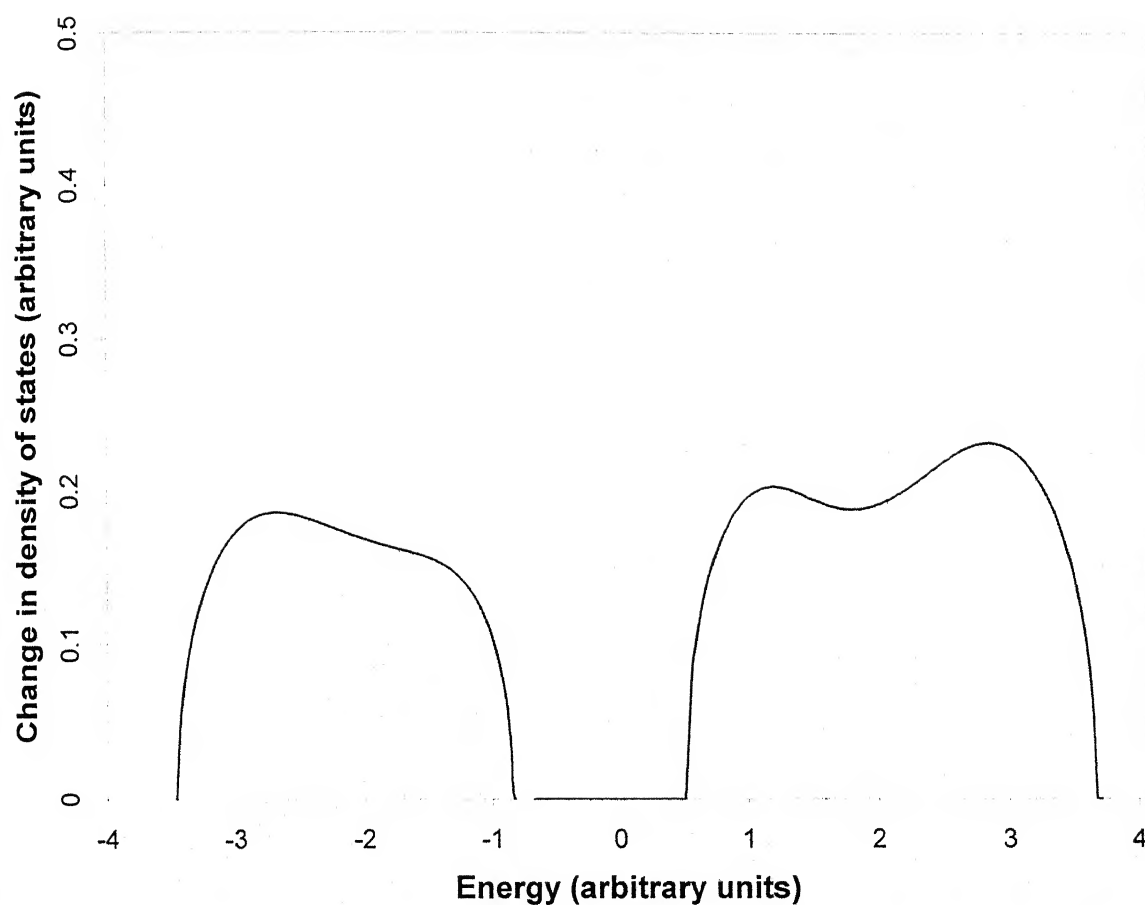


Figure 4.6, Change in density of states for $\Gamma_A=1.0, \Gamma_B=1.0, E_A=-2.0$ and $E_B=2.0$ for concentration $X=0.40$

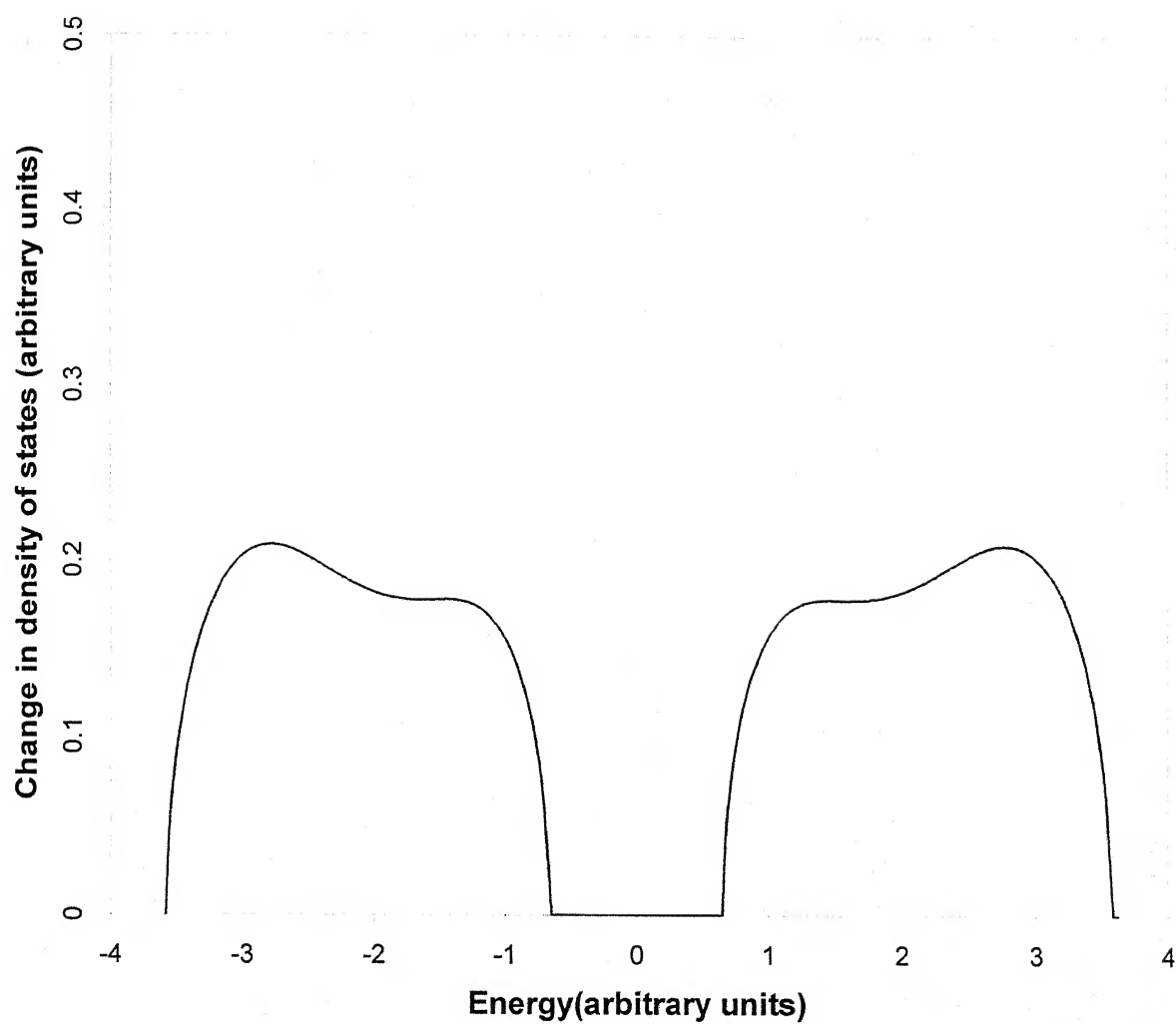


Figure 4.7, Change in density of states for $\Gamma_A=1.0, \Gamma_B=1.0, E_A=-2.0$ and $E_B=2.0$ for concentration $X=0.50$

Figure 4.8 shows change in DOS for same band centres and resonance half width as in figure 4.2 but $X=0.9$ (i.e. low concentration 10% of B type of atoms in alloy). We see that majority band shows structure near $E = -3$ and -1 , which are due to A type of atoms in alloy while minority band shows single small peak near $E=2$, which is due to energy levels of B type of atoms in alloy.

Figures 4.10 to 4.15 show the change in DOS for $E_A=-2$, $E_B=2$, $\Gamma_A=1$ (same as in figure 2) but for double resonance half width $\Gamma_B=2$ and different concentrations $X=0.0, 0.1, 0.4, 0.5, 0.9$ and 1.0 .

Figure 4.10 shows the change in DOS of pure B metals (i.e. $X=0.0$) for double half width $\Gamma_B=2$ and band centres $E_B=2$, we see that double peak are at $E=0$ and 4 , which are combination of band centres and resonance half width ($E_B \pm \Gamma_B$). Similarly Figure 4.15 shows the change in DOS of pure A metals (i.e. $X=1$) for unit half width Γ_A and band centres $E_A=-2$. Again we see that double peaks are forming at $E=-3$ and -1 , which are combination of band centres and resonance half width of A metal ($E_A \pm \Gamma_A$).

Figure 4.11 shows the change in DOS for band centres $E_A=-2$ and $E_B=2$ resonance half width $\Gamma_A=1$, $\Gamma_B=2$ and low concentration ($X=0.10$). We see that majority band shows the double peaks at $E=0$ and 4 , which are combination of band centres and resonance half width of B. Thus these peaks are arising due to majority of B type of atoms in alloy. We see one

single peak between $E = -3$ and -2 , which is arising due to energy levels of minority of A type of atoms.

Figure 4.12 shows the change in DOS of alloy for same parameters as in figure 4.11 but for different concentration $X=0.4$. We see that majority band shows structures at combination of band centres and half width of B type of atoms in alloy. Minority band shows two structures near $E = -3$ and -1 , which are again combination of band centres and half width of A types of atoms.

Figure 4.13 shows the change in DOS of alloy for same parameters as in figure 4.11 but for high concentration $X=Y=0.5$. We see that both band show clear double peak behavior at the combination of band centres and resonance half width of constituent atoms.

Figure 4.14 shows the change in DOS of alloy for same parameters as in figure 4.11 but for different concentration $X=0.9$. Now we see that first band shows peaks at $E_A = -3$ and -1 , which are combination of band centres and resonance half width of A ($E_A \pm \Gamma_A$). Another small band shows small flat peak between $E=1$ and 4 , which is coming due to energy levels of B type of atoms near its band centres $E_B=2$.

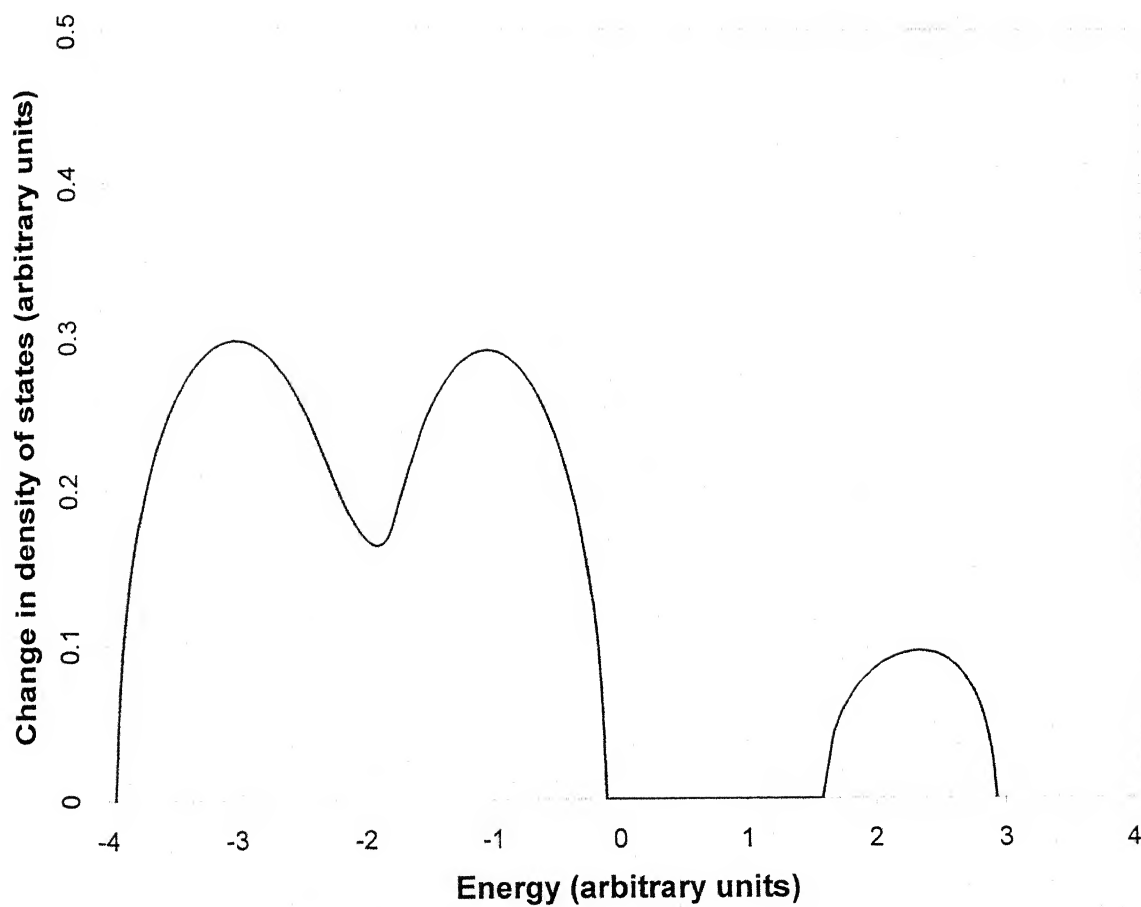


Figure 4.8, Change in density of states for $\Gamma_A=1.0, \Gamma_B=1.0, E_A=-2.0$ and $E_B=2.0$ for concentration $X=0.90$

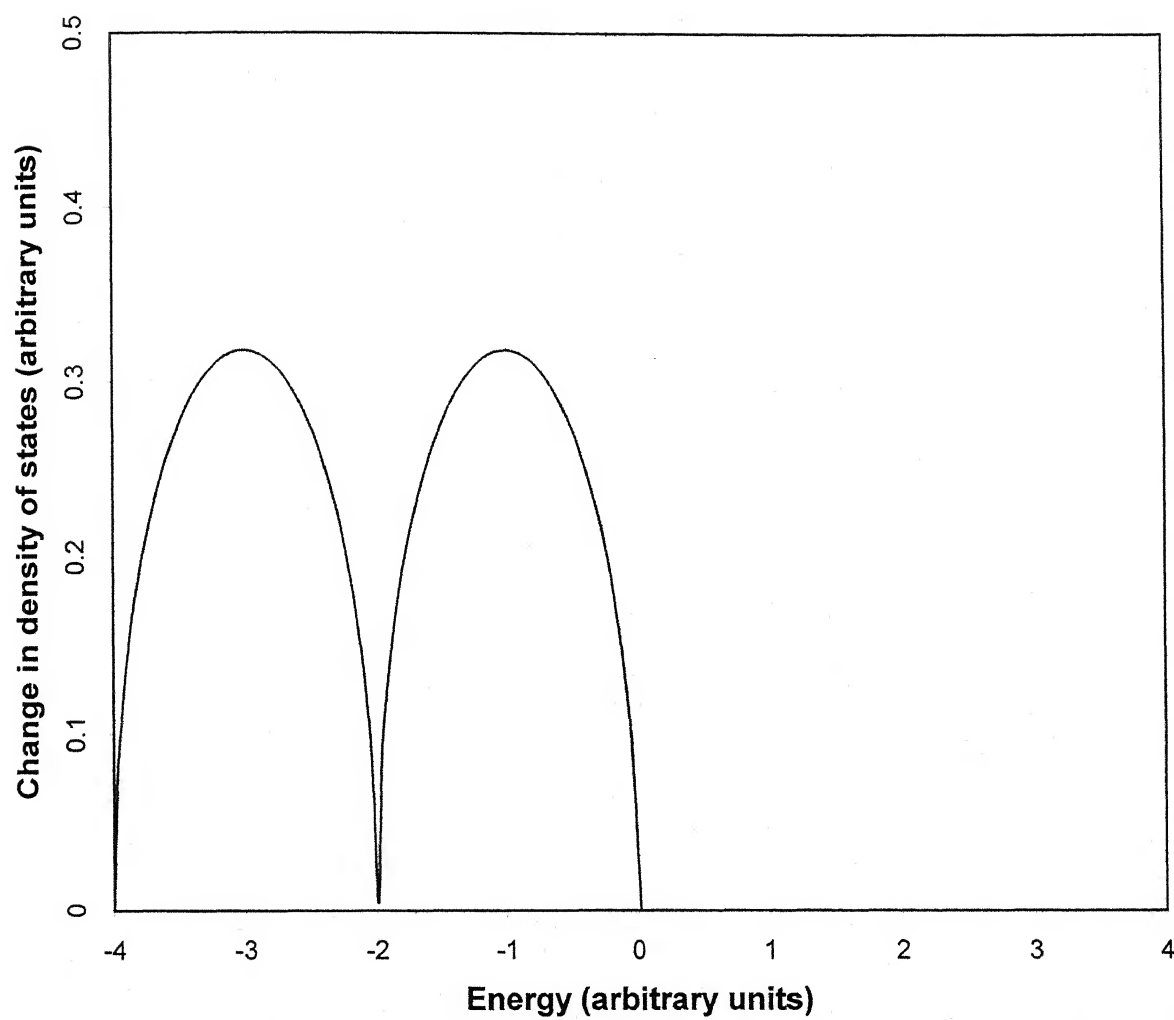


Figure 4.9, Change in density of state for $\Gamma_A=1.0, \Gamma_B=1.0, E_A=-2.0$ and $E_B=2.0$ for concentration $X=1.0$

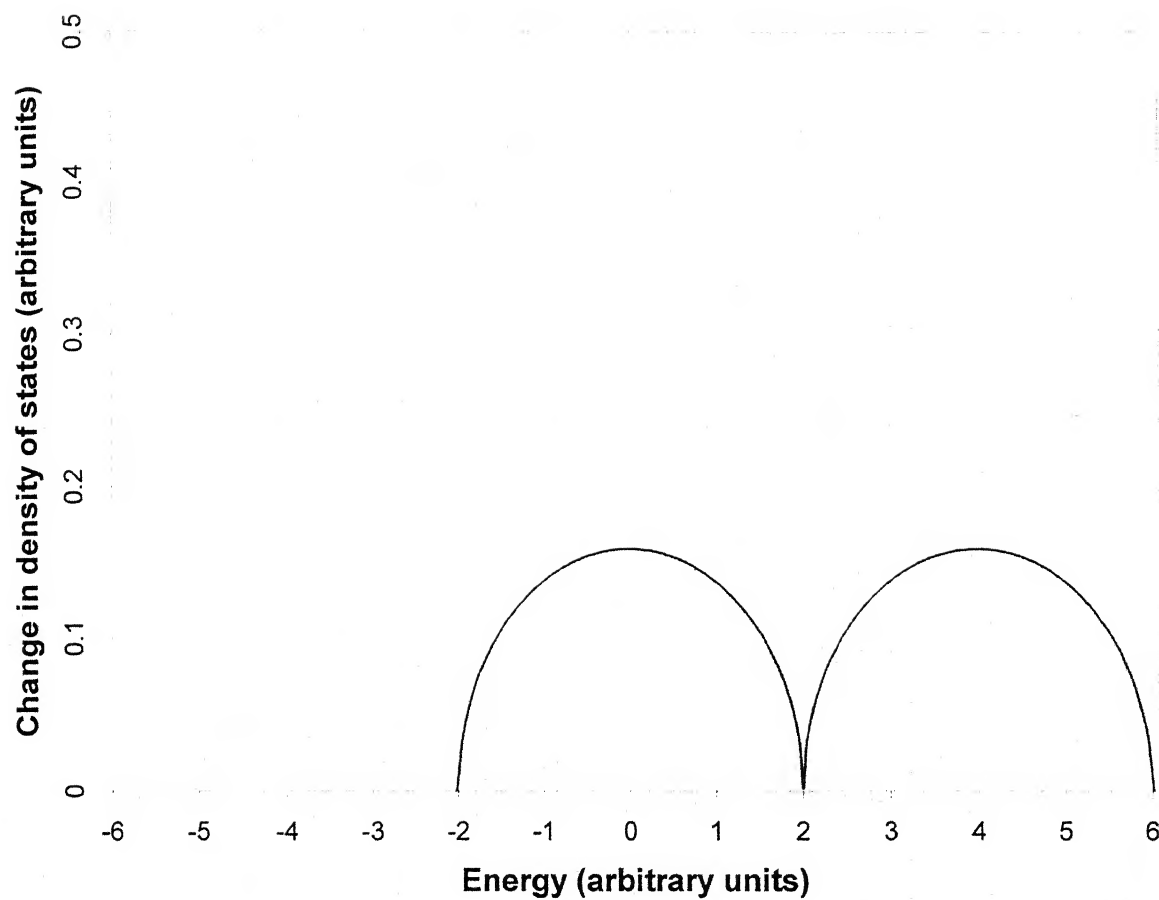


Figure 4.10, Change in density of state for $\Gamma_A=1.0, \Gamma_B=2.0, E_A=-2.0$ and $E_B=2.0$ for concentration $X=0.0$

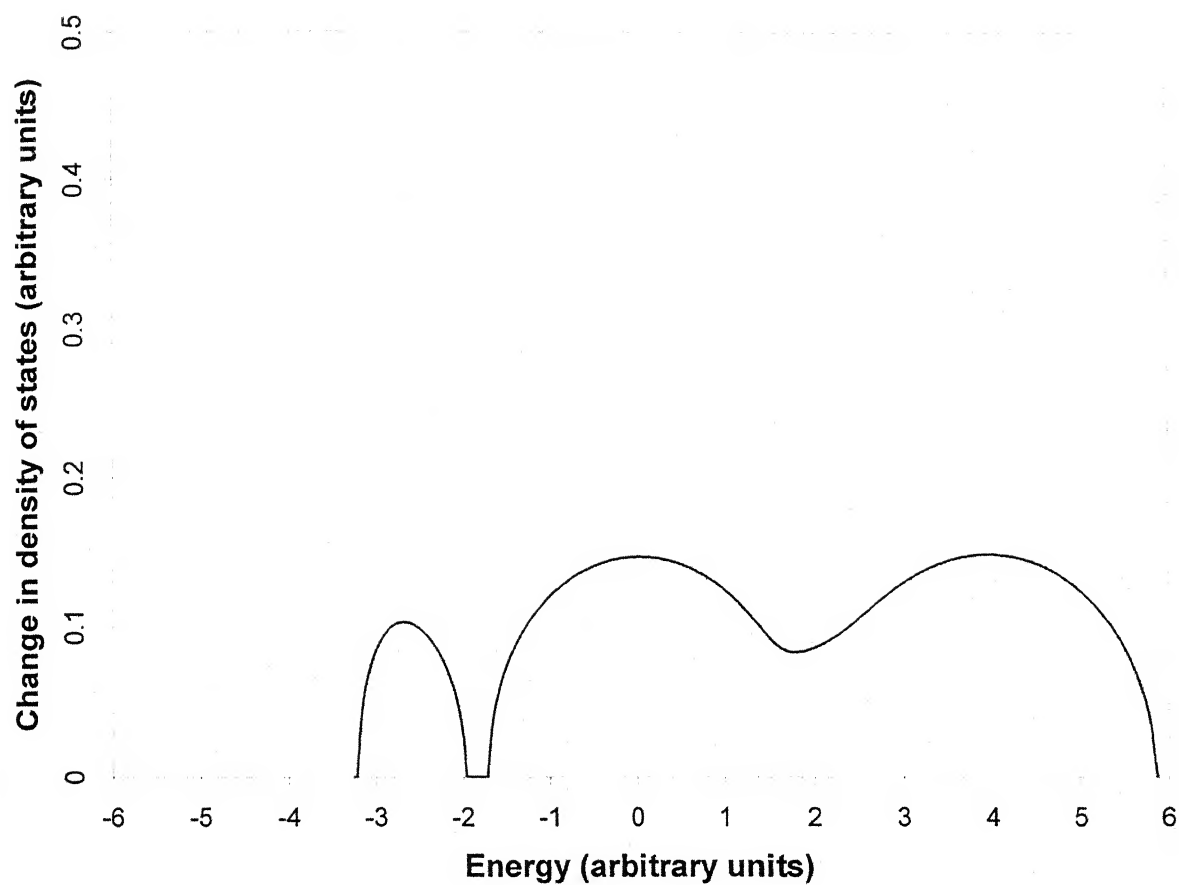


Figure 4.11, Change in density of state for $\Gamma_A=1.0, \Gamma_B=2.0, E_A=-2.0$ and $E_B=2.0$ for concentration $X=0.10$

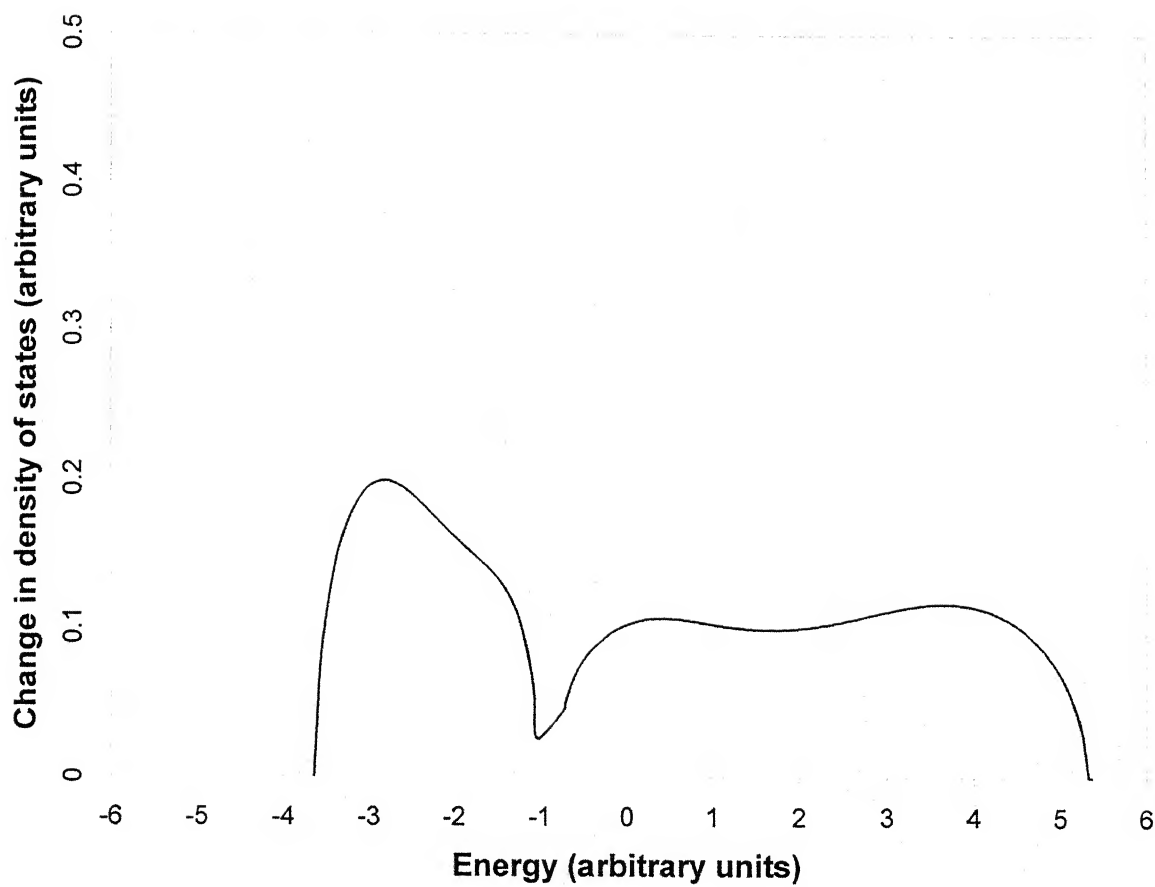


Figure 4.12, Change in density of state for $\Gamma_A=1.0, \Gamma_B=2.0, E_A=-2.0$ and $E_B=2.0$ for concentration $X=0.40$

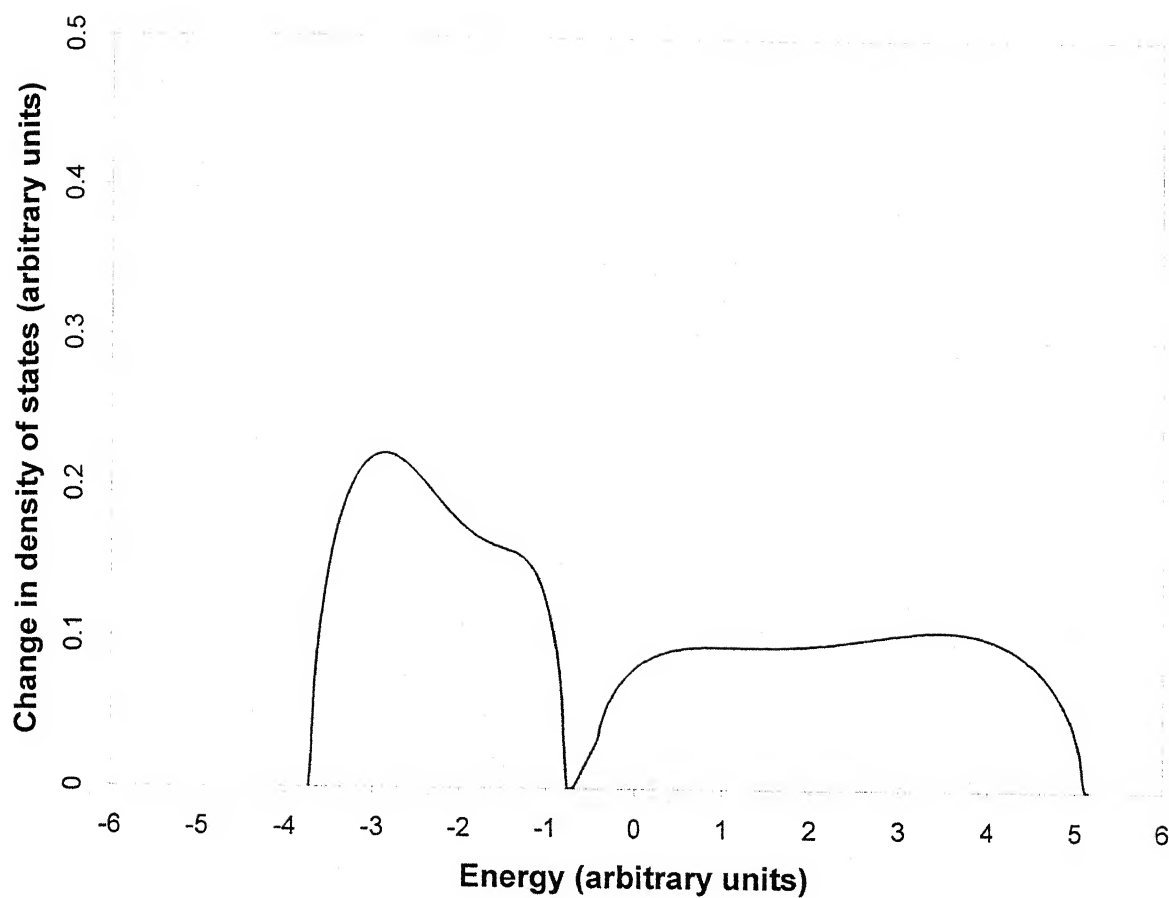


Figure 4.13, Change in density of state for $\Gamma_A=1.0$, $\Gamma_B=2.0$, $E_A=-2.0$ and $E_B=2.0$ for concentration $X=0.50$

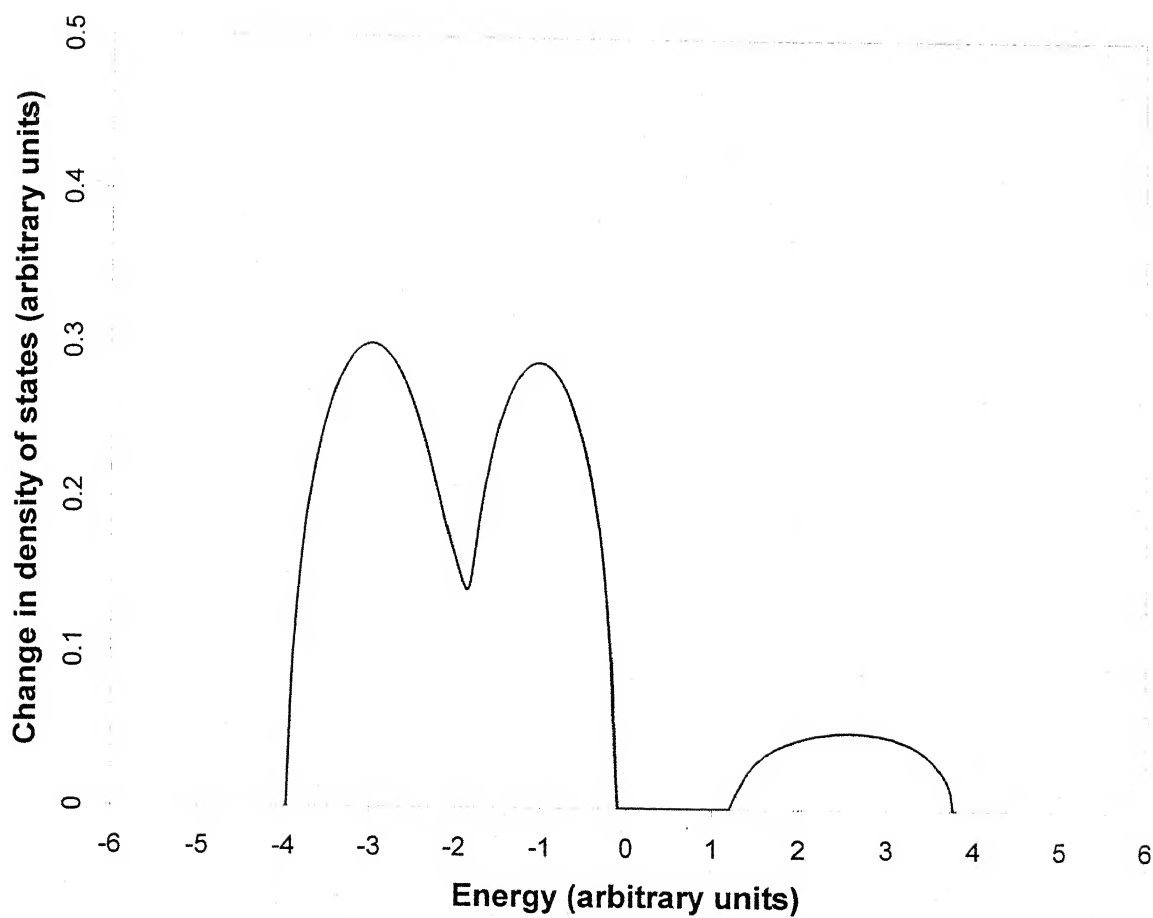


Figure 4.14, Change in density of state for $\Gamma_A=1.0, \Gamma_B=2.0, E_A=-2.0$ and $E_B=2.0$ for concentration $X=0.90$

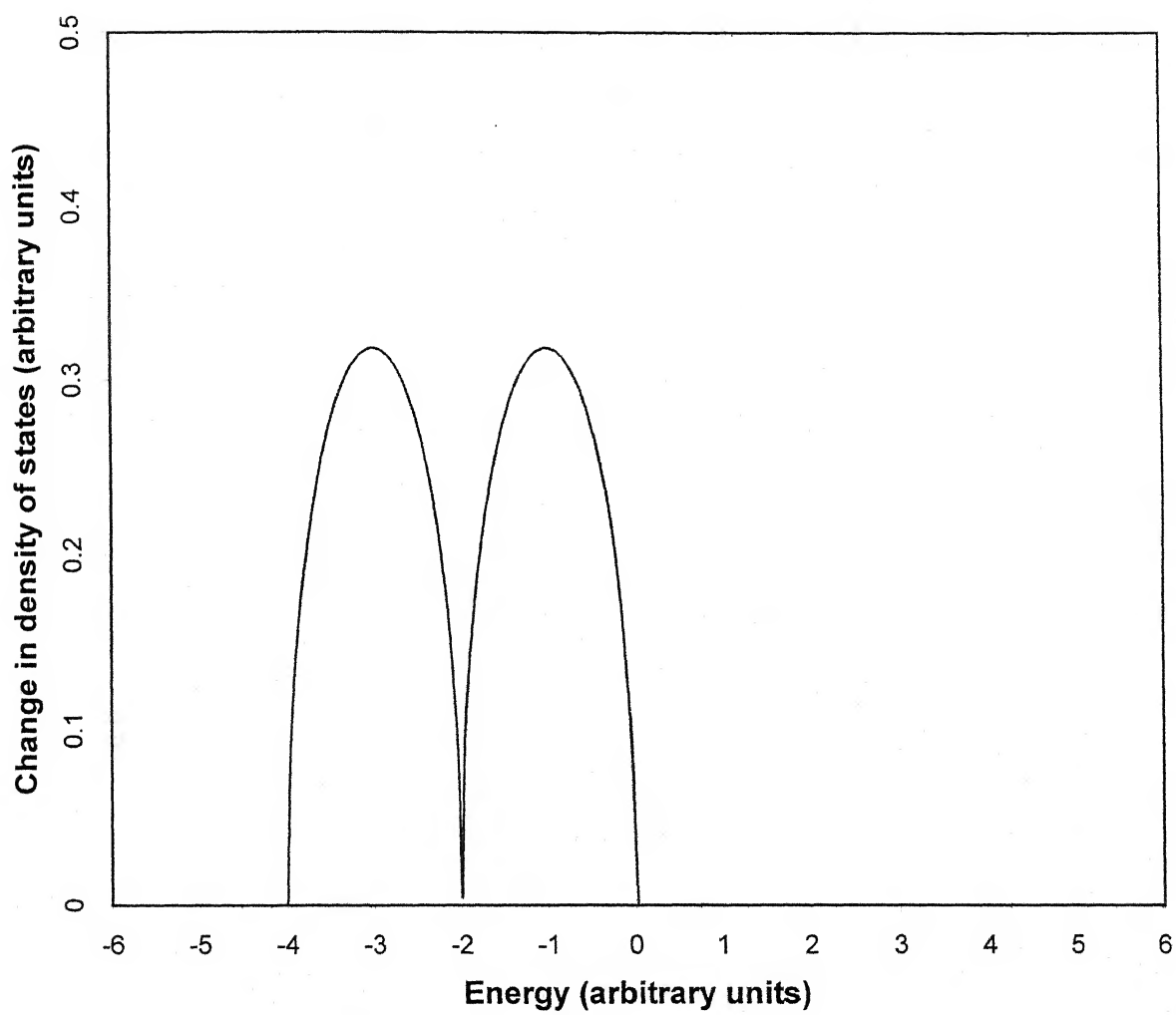


Figure 4.15, Change in density of state for $\Gamma_A=1.0, \Gamma_B=2.0, E_A=-2.0$ and $E_B=2.0$ for concentration $X=1.0$

4.7 CONCLUSIONS:

We have applied KKR-CPA formulation to S-phase shift double-peak semicircular model. We have also derived the explicit analytical form of change in density of states (δ DOS) for double peak semicircular model without using step function as in earlier work Yadav³², in which it was assumed that energy derivatives of step functions was zero. It has been found that structures in δ DOS are depending on the combination of band centres and bandwidth of constituent atoms. This model can be easily applied in the estimation of density of states of alloys in very beginning without much computational effort.

CHAPTER-5
SUMMARY AND CONCLUSIONS

In this thesis, we have discussed and described the applications of charge self-consistent KKR-CPA method for calculation of electronic structure of disordered alloys using muffin-tin potentials. The charge self-consistent KKR-CPA was applied to Cr-Al alloy, which is important bcc alloy system. We have calculated self-consistent charge densities, component density of states and density of states of Cr_xAl_y alloy for concentrations $X=0.95, 0.85$ and 0.75 . It is found that charge-self consistent KKR-CPA density of states for different concentrations of alloy is in very good agreement with reflected X-ray photo spectra (XPS) results. It is found that half width of DOS band of these alloys increases approximate 5% at 85 atomic percentages of Cr with respect to 95 and 75 percent of Cr, which explains the change in shape and half width of experimental XPS results. It is also found that Cr-based rigid band model fails in the calculation of electronic structure of Cr-Al alloys.

We have applied KKR-CPA formulation to s-phase shift double peak semicircular model. We have also derived the explicit analytical form of change of DOS (δ DOS) for double peak semicircular model. It has been found that structures in δ DOS depending on the combination of band centres and bandwidth of the constituent atoms. This model can be applied in the estimation of density of states of alloy in very beginning without much computational effort.

The KKR-CPA calculations can be improved by going beyond the single-site approximation and using the KKR-CPA, which has been formulated by Mookergee et al³³, Gray et al³⁴, Razee et al³⁵ and Rajput et

al³⁶. In this formulation they have used the augmented space formalism, which guarantees the herglotz properties of the averaged Green's function.

The KKR-CPA calculation can be improved in many other ways. One should improve upon the local density approximation, which we had used in our calculation. At present many researchers are engaged in this direction and have suggested various approximation such as gradient correction, GW approximation, weighted density (WD) approximation and self-interaction corrected (SIC) approximation etc³⁷. We feel that such approximations should be first tried and thoroughly tasted on simple systems and pure metals before these could be applied to disordered alloys. Stauton et al³⁸ has formulated the relativistic version of KKR-CPA theory and can be used to improve our KKR-CPA results. However, such corrections in case of Cr-Al alloys are supposed to be quite small. The other direction in which the theory for disordered alloys can be improved is by going beyond the muffin-tin approximation. The KKR-CPA band theory for pure metals has been generalized to non-muffin-tin potentials by Brown and Ciftan³⁹, Gonis⁴⁰ and Faulkner⁴¹. However, their methods have convergence problems as discussed by Gonis and Faulkner. To our knowledge the KKR-CPA theory has not been formulated for non-muffin-tin potentials so far and is still an open problem.

REFERENCES:

1. H. Ehrenreich and L.M. Schwartz, Solid State Physics 31, (1976).
2. J.S. Faulkner in Progress in Materials Science, ed. By T. Massalski (Pergamon, New York, 1982) vol. 27; J.S. Faulkner and G.M. Stocks, Phys. Rev. B21, 3222 (1980).
3. A. Bansil, Electronic Band Structure and its Applications, ed. M. Yussouff, (Springer-Verlag, Berlin, 1987), p 273; R.Prasad, Method of Electronic Structure Calculations, ed. O.R. Anderson, V. Kumar and A. Mookerjee (Singapore: World-Scientific) p 211; Indian J. pure Appl. Phys. 29, 255 (1991).
4. L. Nordhem, Ann. Phys. (Leipzig) 9, 607 and 641 (1931); F. Bassani and D. Brust, Phys. Rev. 131, 1524 (1963); H. Amar, K.H. Johnson, and C.B. Sommer's, Phys. Rev., 153 655 (1967); M.M. Pant and S. K. Joshi, Phys. Rev., 184, 635 (1969).
5. N.F. Mott and H. Jones, The theory of the properties of metals and alloys (Clarendon, Oxford, 1936); J. Friedel, Nuovo cimento suppl. 7, 287 (1958).
6. T.L. Loucks, Augmented Plane Wave Method, (Benjamin, New York, 1967).
7. V.L. Moruzzi, J.F. Janak and A.R. Williams, Calculated Electronic Properties of Metals (Pergamon, New York, 1978).
8. A. Bansil, L.M. Schwartz and H. Ehrenreich, Phys. Rev. B12, 2893 (1975).
9. A. Bansil, H. Ehrenreich , L.M. Schwartz and R.E. Watson Phys. Rev. B9, 445 (1974).

10. H. Asonen, M. Lindroos, M. Pessa, R. Prasad, R.S. Rao and A. Bansil, Phys. Rev. B25, 7075 (1982).
11. R. Prasad and A. Bansil, Phys. Rev. Letters, 48, 113 (1982).
12. R.S. Rao, A. Bansil, H. Asinen and M. Pessa, Phys. Rev. B29, 1713 (1984).
13. R. Prasad, S. C. Papadopoulos and A. Bansil, Phys. Rev. B23 2607 (1981).
14. R. Prasad, R. S. Rao and A. Bansil, in Excitations in Disordered System, ed. M. P. Thorpe (Plenum, New York, 1982).
15. P. Hohenberg and W. Kohn, Phys. Rev. 136, B 864 (1964). S. Lundqvist and N.H. March, Theory of the Inhomogeneous Electron Gas, (Plenum, New York, 1983). ; J. Callaway and N. H. March, Solid State Physics, 38, 135 (1984).
16. U. von Barth and L. Hedin, J. Phys. C: Solid state Phys. 5, 1629 (1972).
17. O. Gunnarsson and B. L. Lundqvist, Phys. Rev. B13, 4274 (1976).
18. S. H. Vosko and L. Wilk, Phys. Rev. B 22, 3812 (1980); S. H. Vosko, L. Wilk and M. Nusair, Can. J. Phys. 58, 1200 (1980).
19. $[B_q(\chi)]_{LL'} = A_{LL'} + i\chi\delta_{LL'}$, Where $A_{LL'}$ is the well-known structure function of band theory.
20. S. Kaprzyk and A. Bansil, Phys. Rev. B42, 7358, (1990). A. Bansil and S. Kaprzyk, Phys. Rev. B43, 10335, (1991).
21. H. Winter and G.M. Stocks, Phys. Rev. B27, 882 (1983). G. Ries and H. Winter, J. Phys. F: Met. Phys. 9, 1589 (1979).
22. S.S. Rajput, R. Prasad, R.M. Singru, S. Kaprzyk and A. Bansil, J.Phys. Condensed-Matter 8 2929 (1996). S.S. Rajput, R. Prasad, R.M. Singru,

- W. Triftshauser, A. Eckert, G. Kogel, S. Kaprzyk and A. Bansil, J.Phys. Condensed-Matter 5, 6419 (1993).
23. Handbook of Lattice Spacings and Structures of Metals and alloys, ed. W.B. Pearson (Pergmon press, 1958).
 24. K. Lawniczak - Jablonska, E. Minni, J. Pelka, E. Suoninen and J. Avleytner, Physica, Stat. Solid (b), 123, 627 (1984).
 25. R. Prasad and A. Bansil, Phys. Rev. B21, 496 (1980).
 26. S. Kaprzyk and P.E. Mijnarends J. Phys. C: Solid State Phys, 19, 1283 (1986).
 27. D.D. Johnson, F.J. Pinski and G.M. Stocks, Phys, Rev. B30, 5508 (1984).
 28. R. Zeller, J. Dentz and P.A. Dederichs, Solid State Commun, 44, 993 (1982).
 29. H. Akai and P.H. Dederichs, J. Phys. C: Solid State Phys. 18, 2455 (1985).
 30. P. Soven, Phys. Rev. B2, 4715 (1970).
 31. S.S. Rajput, S.S.A. Razee, R. Prasad and A. Mookerjee, J. Phys: Condens Matter 2, 2653 (1990).
 32. V.S. Yadav Ph.D. thesis B.U Jhansi, India, (1999).
 33. A. Mookerjee, J. Phys. C: Solid State Phys. 6, L205, 1340 (1973).
 34. L.J. Gray and T. Kaplan, Phys. Rev. B14, 3462 (1976); L.J. Gray and T Kaplan, J. Phys. C: Solid State Physics 9, L303, L483 (1976).
 35. S.S.A. Razee, S.S. Rajput, R. Prasad and A. Mookerjee, Phys. Rev. B42, 9391 (1990).
 36. S.S. Rajput Ph.D. thesis I.I.T. Kanpur, India, (1991).

37. R.W. Godby, M. Schluter and L. J. Sham, Phys. Rev. B37, 10159 (1988); R.W. Godby and R. J. Needs, Phys. Rev. Letters, 62, 1169 (1989); R.O. Jones and O. Gunnarsson, Rev. of Modern Phys 61, 689 (1989).
38. J. Staunton, B.L. Gyorffy and P. Weinberger, J. Phys. F: Met. Phys. 10, 2665 (1980).
39. R.G. Brown and M. Ciftan, Phys. Rev. B27, 4564 (1983); R.G. Brown and M. Ciftan, Phys. Rev. B33, 7937 (1986).
40. A. Gonis, Phys. Rev. B33, 5914 (1986).
41. J. S. Faulkner, Phys. Rev. B34, 5931 (1986); J. S. Faulkner, Phys. Rev. B32, 1339 (1985).